

MASS. INST. OF TECHNOLOGY
WITHDRAWN
JUN 21 1966
FROM
LIBRARIES
MIT LIBRARIES

OPTICAL RADAR STUDIES OF STRATOSPHERIC AEROSOLS

by

Gerald W. Grams

**B. S., Mankato State College
(1960)**

MASS. INST. TECH.
WITHDRAWN
LIBRARIES
FROM
MIT LIBRARIES

**SUBMITTED IN PARTIAL FULFILLMENT
OF THE REQUIREMENTS FOR THE
DEGREE OF DOCTOR OF
PHILOSOPHY**

at the

MASSACHUSETTS INSTITUTE OF TECHNOLOGY

May, 1966

Signature of Author.....
Department of Meteorology, May 31, 1966

Certified by.....

Accepted by.....
Chairman, Departmental Committee on Graduate Students

OPTICAL RADAR STUDIES OF STRATOSPHERIC AEROSOLS

by

Gerald W. Grams

Submitted to the Department of Meteorology
on May 31, 1966 in partial fulfillment
of the requirement for the degree
of Doctor of Philosophy

ABSTRACT

Observations of stratospheric aerosols have been made with an optical radar at Lexington, Massachusetts during a two year study. Some observations were also conducted at College, Alaska in the summer 1964, simultaneously with studies of noctilucent clouds. Vertical profiles of aerosol concentration were obtained by comparing the optical radar echoes with the expected return from a molecular atmosphere; the observed signal from 25-30 km altitude was used to calibrate the instrument.

The observations show that the aerosol layer near 20 km exhibited little temporal variability. The observed return from the layer was approximately 1.9 times the return from a molecular atmosphere; the daily rms fluctuation of this scattering ratio was about 0.3 and hourly fluctuations were smaller.

The data have compared with various meteorological parameters associated with conditions in the lower stratosphere. A significant negative correlation between fluctuations of dust and ozone measurements has been found.

Thesis Supervisor: Giorgio Fiocco
Title: Assistant Professor of Geophysics

ACKNOWLEDGEMENTS

The author gratefully acknowledges the encouragement, support, and helpful advice of Professor Giorgio Fiocco. Numerous discussions with Professor Reginald E. Newell are also greatly appreciated.

He is indebted to Wayne S. Hering and Thomas R. Borden, Jr. for making their ozone data available before publication and for discussions concerning these data. He is also thankful for valuable discussions and advice from Professor E. N. Lorenz, Professor R. M. Goody, Dr. H. L. Kasnitz, and Mr. G. M. Shannon, Jr.

The author appreciates the competent assistance of many individuals at the Massachusetts Institute of Technology—Mr. J. B. Thompson, Miss Isabelle Kole, and Mrs. Charlotte Newman, in particular. The author's wife, Rita Grams, has typed the manuscript and provided moral support.

Numerical calculations were performed in part at the Massachusetts Institute of Technology Computation Center. The research reported in this thesis was carried out at the Research Laboratory of Electronics and was supported by a grant from the National Aeronautics and Space Administration.

TABLE OF CONTENTS

	Page
Chapter 1. INTRODUCTION	1
Chapter 2. INSTRUMENTATION	13
Chapter 3. DETECTION OF AEROSOL LAYERS WITH OPTICAL RADAR	21
3.1 The optical radar equation	21
3.2 Back-scattering from atmospheric constituents	23
3.3 Quantitative estimates of atmospheric scattering parameters	31
Chapter 4. DATA REDUCTION AND ANALYSIS	41
Chapter 5. OBSERVATIONS OF STRATOSPHERIC AEROSOLS	58
Chapter 6. CONCLUSIONS	106
Appendix	110
References	114

LIST OF FIGURES

		Page
Figure 1.	Vertical distribution of stratospheric particles collected by inertial impactors, according to Chagnon and Junge. Tropospheric measurements of other investigators are included for comparison. (After Chagnon and Junge, 1961.)	2
Figure 2.	Photograph showing some of the characteristics of the stratospheric aerosol layer as observed during twilight from the Soviet spaceship "Vostok 6" on 17 June 1963 (after Rosenberg and Nikolaeva-Tereshkova, 1965)	7
Figure 3.	Schematic diagram of the apparatus.	14
Figure 4.	Photograph of the apparatus.	17
Figure 5.	Radar cross-section σ_m for spherical particles with refractive index 1.5 as a function of the Mie size parameter $\alpha = \frac{\pi r}{\lambda}$ where r is the radius of the scattering particle and λ is the wavelength of the incident radiation. The calculated values are normalized to the geometric cross-section of the particle.	30
Figure 6.	Number of dust particles required to backscatter the same amount of light as the molecular return from the lower stratosphere at the ruby wavelength. The dust particles are assumed to be Mie scatterers with refractive index 1.5 with sizes prescribed by a distribution function $dN = 2.1 \times 10^{15} d \log r$; the lower cut-off for the size distribution function is assumed to be 0.275μ . The molecular number density has been obtained from the U. S. Standard Atmosphere, 1962.	37
Figure 7.	Correction constants for Fig. 6 for different size distribution functions characterized by the slope ν and cut-off radius r_c .	38
Figure 8.	Sample data record showing five consecutive optical radar returns. An altitude scale is included at the bottom of the figure; enhanced echoes near 16 km are evident in the tracing.	42

	Page
Figure 9. Root-mean-square fluctuations of the photoelectron flux as a function of the average photoelectron flux observed for various 1/2 km altitude intervals. Relative units.	46
Figure 10. Estimated rms fluctuations of the average optical radar return for 1/2 km altitude intervals in the lower stratosphere as a function of the number of individual traces used to determine the average return. The fluctuations are expressed as a percent of the average signal for each altitude interval.	48
Figure 11. Graphical description of the effect of a systematic fluctuation of the digitized optical radar signal. Curve <u>a</u> : idealized optical radar echo; curve <u>b</u> : theoretical return from a molecular atmosphere; curve <u>c</u> : scattering ratios σ/σ_R derived from curves <u>a</u> and <u>b</u> . Curves <u>a</u> ⁺ and <u>a</u> ⁻ illustrate the effect of adding or subtracting, respectively, a constant signal level from curve <u>a</u> ; curves <u>c</u> ⁺ and <u>c</u> ⁻ are the consequent scattering ratio profiles.	55
Figure 12. Optical radar observations for 14 February 1964. Curve <u>a</u> : observed intensity of echoes from a vertically pointing optical radar. Curve <u>b</u> : expected intensity of echoes from a purely molecular atmosphere. Curve <u>c</u> : ratio of curve <u>a</u> to curve <u>b</u> , interpreted as the ratio of observed to molecular cross-sections.	59
Figure 13. Ten consecutive hourly profiles obtained on 11-12 March 1965 showing scattering ratios σ/σ_R for 1/2 km altitude intervals at the indicated observation times.	62
Figure 14. Graphical summary of optical radar data showing nightly average scattering ratios σ/σ_R for 1 km intervals in the lower stratosphere. Part 1.	65
Figure 15. Graphical summary of optical radar data. Part 2.	66
Figure 16. Graphical summary of optical radar data. Part 3.	67

	Page
Figure 17. Relation between the height of the center of mass of the aerosol layer and the height of the tropopause.	71
Figure 18. Daily variation of the observed scattering ratio σ/σ_R at 16 km altitude during the optical radar study.	73
Figure 19. Relation between the observed scattering ratio σ/σ_R at 16 km altitude and the northward component of wind velocity v at 100 mb.	76
Figure 20. Relation between the observed scattering ratio σ/σ_R at 16 km altitude and the wind direction at 100 mb.	77
Figure 21. Autocorrelation coefficients for dust observations near the center of mass of the aerosol layer.	79
Figure 22. Daily variation of the total amount of ozone in a vertical atmospheric column reduced to standard temperature and pressure.	82
Figure 23. Correlation coefficients for measurements of the ozone and dust content of the lower stratosphere as a function of altitude for several different time lags between the observations.	84
Figure 24. Correlation coefficients for total ozone measurements and the dust content of the lower stratosphere as a function of the time lag between the observations and the altitude of the dust measurements.	88
Figure 25. Relation between the observed scattering ratio σ/σ_R at 16 km altitude and the total amount of ozone in the atmosphere.	89
Figure 26. Correlation coefficients for deviations from the monthly mean of total ozone measurements and the dust content of the lower stratosphere as a function of the time lag between the observations and the altitude of the dust measurements.	91
Figure 27. Relation between the observed scattering ratio σ/σ_R at 16 km altitude and deviations	

	Page
from the monthly mean of the total amount of ozone in the atmosphere.	93
Figure 28. Autocorrelation coefficients for stratospheric ozone observations near the center of mass of the aerosol layer.	95
Figure 29. Autocorrelation coefficients for the total amount of ozone in a vertical atmospheric column.	96

LIST OF TABLES

	Page
Table 1. General characteristics of various optical radar systems used during the study.	20

APPENDIX

Table A1. Numerical summary of optical radar data. Part 1.	111
Table A2. Numerical summary of optical radar data. Part 2.	112
Table A3. Numerical summary of optical radar data. Part 3.	113

1. INTRODUCTION

The presence of a layer of particulate material in the lower stratosphere was deduced many years ago from observations of the purple light (Gruner and Kleinert, 1927; Gruner, 1942). This phenomenon is a purplish glow that appears in the western sky during twilight at about 40° solar depression. The observed temporal and spatial development of the purple light during the course of the twilight can be qualitatively explained by the optical effects of a layer of dust above the tropopause.

The existence of such a layer has been verified with particle sampling equipment carried on high-altitude balloons (Junge, Chagnon, and Manson, 1961; Chagnon and Junge, 1961). Vertical profiles of particle concentration obtained with an inertial impactor designed to collect particles larger than about 0.1 micron radius persistently exhibited a broad maximum in particle concentration at about 20 km altitude (see Fig. 1, taken from Chagnon and Junge, 1961). Supplementary data collected by impactors on U-2 aircraft at 20 km (Friend et al, 1961; Junge and Manson, 1961) showed that particle concentrations between 60°S and 70°N exhibited no systematic latitudinal variation and that the aerosol layer was indeed a world-wide feature of the lower stratosphere.

Chemical analysis of the particles collected by the impactors indicated that the majority of the particles were

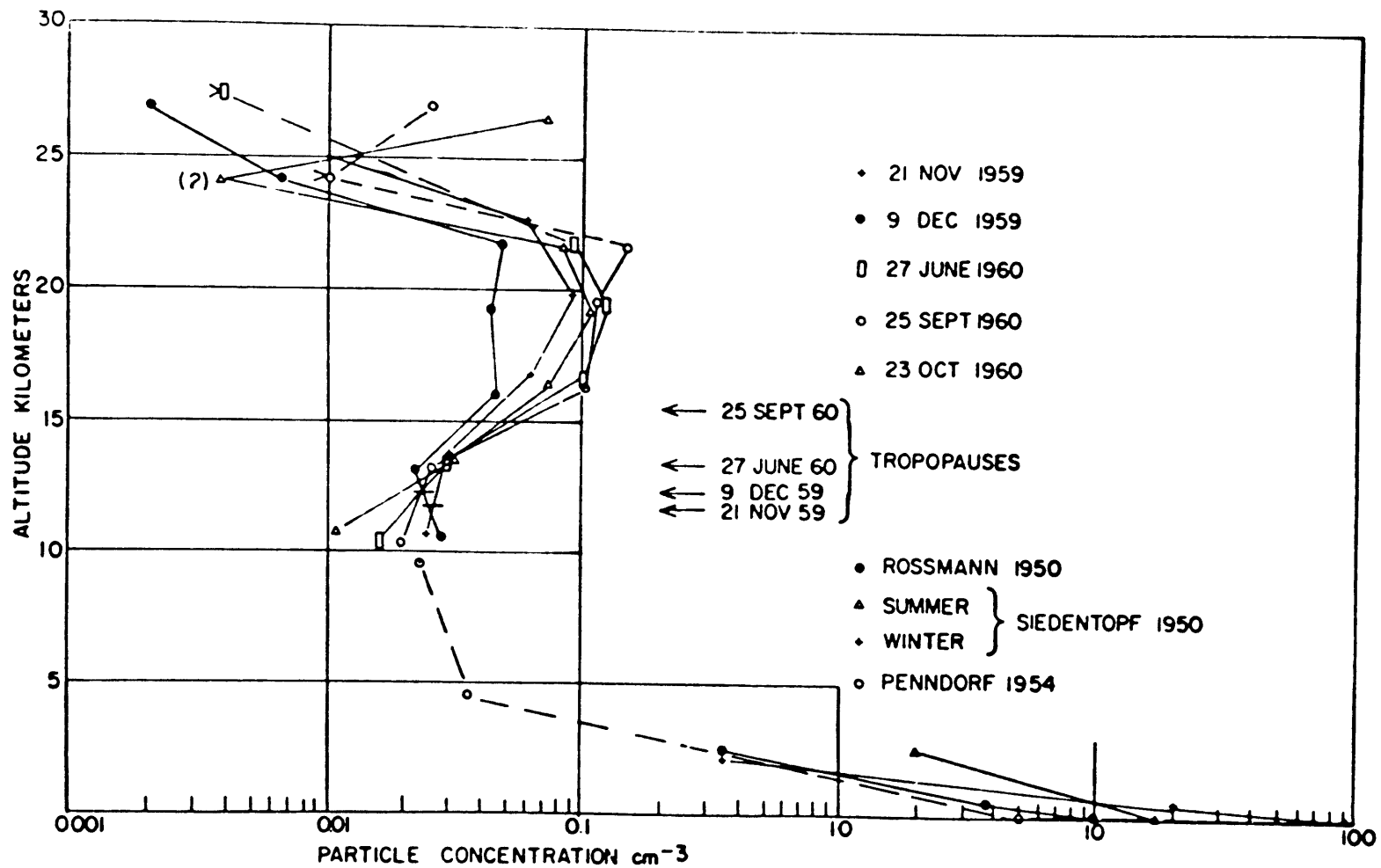


Fig. 1. Vertical distribution of stratospheric particles collected by inertial impactors, according to Chagnon and Junge. Tropospheric measurements of other investigators are included for comparison. (After Chagnon and Junge, 1961.)

composed of sulfates (Junge, Chagnon, and Manson, 1961). This result was confirmed by electron diffraction studies of U-2 samples; Friend et al (1961) found that more than 90% of the mass of the impacted particles was composed of crystalline ammonium sulfate or, on occasion, ammonium persulfate. The chemical composition of the particles and the observed shape of the concentration profiles led Junge to propose that the particles were formed in situ by oxidation of traces of gaseous sulfur compounds (hydrogen sulfide and sulfur dioxide) that had entered the stratosphere by vertical mixing processes; these sulfur-bearing gases were known to exist in the troposphere in sufficient amounts to maintain a steady state between formation of the sulfate particles and their removal by sedimentation and eddy diffusion.

Thus the direct sampling measurements demonstrated the existence of an omnipresent layer of particles in the lower stratosphere that are probably being continually formed by chemical reactions within the layer itself. The presence of the aerosol layer had been substantiated by other investigators since Gruner's detailed study of the purple light. For example, Bigg (1956) performed photometric observations of the rate of change of the intensity of twilight and related rapid variations of this parameter to the interaction of the edge of the earth's shadow with regions of dust particles in the atmosphere. These measurements have detected the presence of appreciable amounts of dust in the

15 to 20 km region and thereby support the results of the particle collections although the concept of a well-defined illumination discontinuity at the shadow boundary has been criticized, particularly by Megrelishvili (1958).

Perhaps the most sophisticated twilight observations that have been reported are those of Volz and Goody (1962) who measured the absolute intensity of the twilight at a fixed angle of elevation to derive quantitative information on the turbidity (dust content) of the upper atmosphere. On the basis of a carefully constructed theoretical model which incorporated the effects of scattering by the molecular and aerosol components of the atmosphere and absorption by atmospheric ozone, dust profiles were derived by comparing the observed twilight intensity with the expected intensity from the model atmosphere. Even though these results provide data that are smooth over at least 10 km altitude, the turbidity profiles usually displayed a broad maximum between 15 and 30 km in accordance with a stratospheric dust layer.

Observations obtained by other techniques have also corroborated the existence of the layer and, in some cases, provided additional details about it. An observation of the vertical distribution of diffuse radiation from the daytime sky measured by rocket photometry (Rössler, 1963) showed a radiation maximum at about 25 km which could be attributed to aerosol scattering. This rocket sounding, obtained in the Sahara, substantiates the measurement

reported by Chagnon and Junge (1961) which indicated that the concentration maximum may be located at higher levels in tropical regions.

The aureole photometry of Newkirk and Eddy (1964) also demonstrated the presence of the layer. The angular and spectral distribution of sunlight scattered in the stratosphere measured by a balloon-borne coronagraph was analyzed to provide information on the particulate material above the instrument and, by differentiation, on local aerosol parameters. The dust concentrations observed on two different flights of the instrument were consistent with the direct sampling results. Evidence was also obtained during this study that the dust "layer" may contain thin laminae with concentrations exceeding smoothed values by at least an order of magnitude. Such stratifications were also detected, at times, by the twilight observations of Bigg (1964).

On occasion thin dust layers in the lower stratosphere can be observed visually and photographically when viewed in the horizontal direction from aircraft or balloons (see, for example, Jacobs, 1954; Bull and James, 1956; Ross, 1958); these observations, however, could usually be associated with preceding volcanic eruptions and may not be a natural feature of the stratospheric aerosol distribution.

Searchlights have been used to detect the presence of scattering layers in the atmosphere (Rosenberg, 1960;

Elterman and Campbell, 1964). In this technique a searchlight beam directed into the atmosphere is scanned photometrically to measure altitude variations of the light scattered by atmospheric constituents. These observations have also shown strong aerosol scattering near 20 km. Recent research in the Soviet Union (Rosenberg, Sandomirsky, and Poldmaa, 1966) using twilight photometry and measurements from aircraft and spaceships as well as searchlight observations has consistently detected the aerosol layer at altitudes between 15 to 22 km with minimum dust amounts observed in the 25 to 30 km region.

The variety of observations that have already been discussed provide ample evidence that the lower stratosphere contains an appreciable amount of particulate material which appears to be a rather permanent feature of this region. The widespread nature of the aerosol layer is demonstrated by a recent photograph taken from a Soviet spaceship (Rosenberg and Nikolaeva-Tereshkova, 1965); this photograph of the earth's horizon at twilight is reproduced here as Fig. 2.

The eruption of the Mount Agung volcano on Bali ($8^{\circ}25'S$, $115^{\circ}30'E$) on 17 March 1963 has increased the aerosol content of the stratosphere and has therefore enhanced many of the phenomena that are associated with the presence of the dust layer. Optical effects, in particular, have been quite pronounced and have been reported by many observers. Volz (1965)

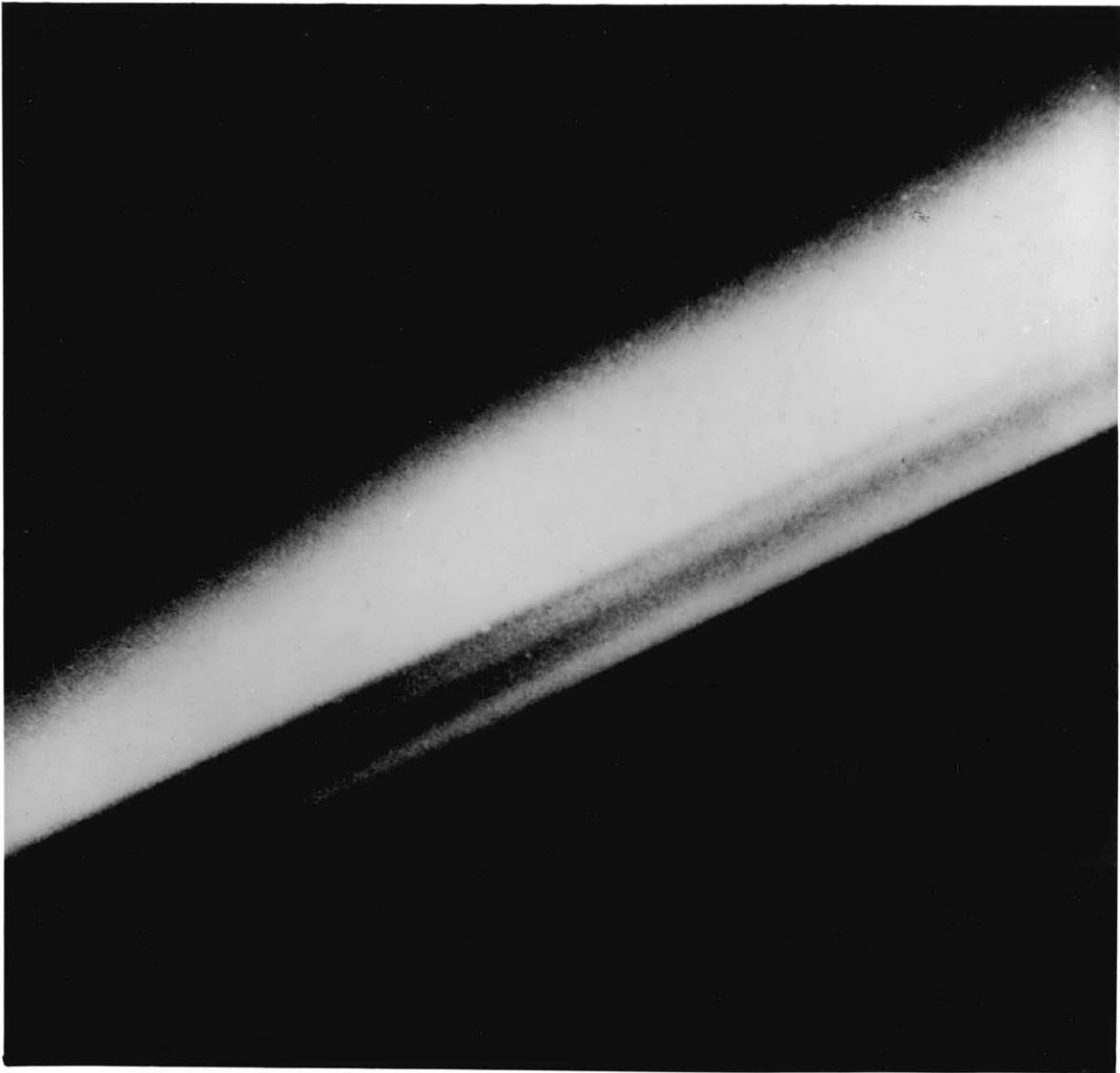


Fig. 2. Photograph showing some of the characteristics of the stratospheric aerosol layer as observed during twilight from the Soviet spaceship "Vostok 6" on 17 June 1963 (after Rosenberg and Nikolaeva-Tereshkova, 1965).

has recently summarized many of the visual observations associated with the increased dust content of the stratosphere as well as the results of various atmospheric turbidity measurements obtained since the volcanic eruption. In the Northern Hemisphere reports of unusual twilight effects (see, for example, Meinel and Meinel, 1963 and 1964; Volz, 1964) indicate that the dust content of the stratosphere increased substantially during fall 1963 and that the abnormal conditions have persisted at least throughout 1964.

Some quantitative measurements of the increase of stratospheric aerosol concentrations before and after the Agung eruption using the same method of observation are available. Volz (1964, 1965) has continued earlier measurements of the intensity of the twilight (Volz and Goody, 1962). These observations, obtained in Germany, show deviations from normal conditions beginning as early as May 1963; a pronounced increase in stratospheric turbidity in early winter 1963 was followed by abnormally high dust amounts since that time. Volz has estimated that if the enhanced turbidity was due to a layer that is only a few kilometers thick, the aerosol concentration may have exceeded that of the ordinary sulfate layer by a factor of 20 during winter 1963/64.

Recent studies of the aerosol layer using balloon-borne photoelectric particle counters (Rosen, 1964) also

indicate that particle concentrations between 15 to 20 km may be an order of magnitude larger than the results of the particle collections of Junge and his collaborators. A quantitative comparison between the results of the in situ particle counts and the particle concentrations obtained by analyzing impactor samples is, however, subject to some question; uncertainties associated with the collection efficiency of an impaction surface and the possible loss of volatile material makes it inherently difficult to match impactor data with results obtained using indirect optical techniques.

Fortunately, stratospheric particles have been collected with impactors both before and after the Agung event and, therefore, provide comparative information about the perturbed state of the aerosol layer. Particle number concentrations measured by Friend (Feely et al, 1963) from U-2 flights at latitudes near 30°N on 7 May 1963 and 30 July 1963 were approximately four times greater than values measured prior to the volcanic eruption. This was attributed to natural variations in the ordinary sulfate layer associated with the existence of a laminar structure. However, it now seems possible that these measurements may have recorded the incursion of volcanic material into the Northern Hemisphere with little delay from events in the Southern Hemisphere; this interpretation agrees with the results of photometric measurements of stratospheric turbidity that have

already been discussed.

Particle collections have been performed in the Southern Hemisphere before and after the Mount Agung eruption by Mossop (1963, 1964) who also collected particles on impaction surfaces mounted on U-2 aircraft. Aerosol concentrations up to 7 times those observed prior to the eruption were found in the impactor samples for almost a year after the eruption. Furthermore, the dimensions of many of the particles were much larger than observed in samples collected prior to the eruption. This was due not only to the presence of larger particles which could often be recognized as volcanic debris, but also to the existence of a layer of water-soluble material on these particles and, on occasion, a fluid layer surrounding the particle. Mossop suggested that the coating could be sulfate material or, in the case of fluid layers, sulfuric acid resulting from oxidation of the large quantities of gaseous sulfur compounds injected into the stratosphere by the eruption. It is therefore possible that the pronounced changes in the optical properties of the aerosol layer may be related to changes in the physical and chemical properties of the stratospheric aerosol, in addition to enhanced effects resulting from increased particle concentrations.

The aerosol layer in the stratosphere, whether in a natural or perturbed state, is of intrinsic interest as an atmospheric constituent for which only a small amount of basic quantitative data exists. The presence of the particulate

material is of definite concern in various fields of atmospheric research. The particles may be formed within the layer by chemical reactions; their presence could play a role in determining the chemical properties of the lower stratosphere. The variety of scattering phenomena associated with the layer presents ample evidence that its existence affects the optical properties of the stratosphere; the terrestrial radiation balance is affected by the presence of dust particles. Electrical properties of aerosols, such as their effect on the mobility of small ions, make them of interest in some fields of atmospheric electricity. The particles may have a potential role in rain formation since they could act as nuclei for water vapor condensation. The aerosol population of the stratosphere also plays a role in transporting radioactive fission products injected by nuclear weapons tests. Indeed, knowledge of the spatial and temporal variations of the layer could aid the study of horizontal and vertical transport mechanisms associated with the general circulation of the upper troposphere and lower stratosphere since various proposed models of atmospheric circulation would have to be consistent with the observed distribution of the particulate material as well as other trace substances in the stratosphere such as ozone, water vapor, and radioactive isotopes.

The present study is an exploratory attempt to provide routine observations of the aerosol layer by a very

new and promising technique for probing the earth's atmosphere, namely the use of a pulsed ruby laser as the source of radiation for an optical radar system. The apparatus developed for the study is described in the next chapter.

The use of light beams to derive information about the upper atmosphere is not a new concept; the ability to detect aerosol layers in the atmosphere by measuring light scattered from a searchlight beam has already been discussed. The use of searchlights was originally suggested by Synge (1930) as a means of measuring atmospheric densities; several investigators have since used searchlight beams to obtain atmospheric density profiles (see, for example, Elterman, 1954). Searchlight observations are usually performed by photometrically scanning a steady or modulated searchlight beam by photographic or electronic techniques from an observing site located a considerable distance from the source and employing triangulation for altitude determination. A pulsed searchlight, capable of being operated from a single site by using the time elapsed between the transmitted and received signal for altitude determination was used by Friedland, Katzenstein, and Zatzick (1956); however suitable light sources were not yet available to take full advantage of a pulsed system.

2. INSTRUMENTATION

The equipment used for the study of stratospheric aerosols is an optical radar, which uses a pulsed ruby laser as a source of radiation to extend the principles of radar to optical wavelengths. A Q-switched ruby laser acts as the transmitter and an astronomical telescope as the receiver for a monostatic radar system.

Fig. 3 is a schematic diagram of the apparatus. The laser head uses a cylindrical cavity of elliptical cross-section to provide efficient coupling of a straight xenon flashtube to a ruby rod with accurately polished ends; when the capacitor bank is discharged, light from the flashlamp is reflected from the walls of the cavity and absorbed by the ruby rod. A rotating prism (or mirror) is included in the optics of the laser system to prevent ordinary laser action until the device has rotated into exact alignment; this is the "Q-switch" for the pulsed laser system used in the apparatus. Electrical pulses from the rotating Q-switch are used to time a trigger pulse that discharges the capacitor bank at a predetermined time interval before the Q-switch has rotated into the proper position to fire the laser; this time interval is the time necessary to attain a maximum number of excited atoms of the active species in the ruby crystal.

The laser emits an intense beam of coherent monochromatic

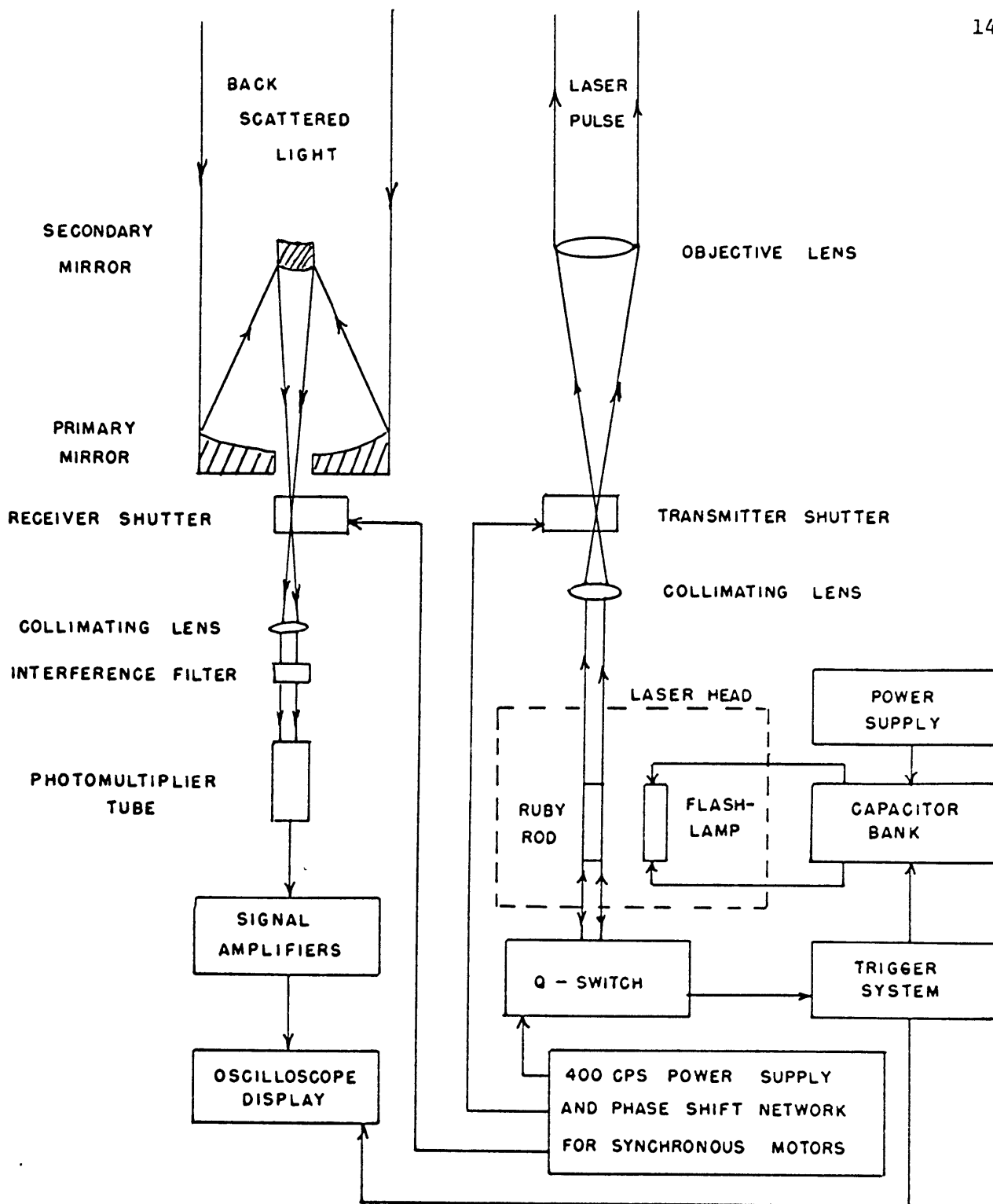


Fig. 3. Schematic diagram of the apparatus.

radiation with a wavelength of 0.694 micron and duration less than one microsecond. This light pulse is collimated by a refracting telescope and transmitted through the atmosphere. A small rotating shutter, synchronized with the Q-switching device, is incorporated into the transmitting unit to prevent the emission of fluorescent light after the laser pulse has been emitted.

Light from the transmitted laser pulse will be scattered by air molecules and particulate material suspended in the atmosphere; a certain fraction of the light will be scattered in the backward direction. Back-scattered light collected by the astronomical telescope is detected by a photometer which incorporates a narrow band interference filter, a photomultiplier tube, and another synchronized rotating shutter to prevent exposing the photomultiplier to the intense return obtained from scattering at short distances.

Each time that the laser is pulsed the current emitted by the photomultiplier cathode is amplified, displayed on an oscilloscope, and photographed. The oscilloscope is set up for single sweep operation and is triggered at the same time that the capacitor bank is discharged; the sweep is delayed until several microseconds before the mirror rotates into position to fire the laser. The signal is then photographed as the ordinary "A-scope" radar display in which the electron beam scans across the cathode ray tube at constant

speed and undergoes vertical deflections that are proportional to the received signal. These photographs provided the data records for the stratospheric aerosol study.

The observed photoelectron flux contains, in addition to the optical radar echoes, a noise component due to the sky background and to the photomultiplier dark current (at ambient temperatures this is due mostly to thermal emission from the photosurface and dynode structure). The interference filter in the photodetection system is incorporated to take advantage of the monochromatic nature of the laser pulse by eliminating background radiation in other spectral regions. However, the light from the daytime sky admitted through the filter was still very intense compared to the weak echoes received from the lower stratosphere and all observations were therefore performed at night. When the photomultiplier tube was cooled to reduce the dark current, the noise level could be reduced to negligible proportions for echoes from the lower stratosphere for nighttime observations.

Fig. 4 is a photograph of the optical radar unit as it appeared during summer 1965. The laser head, transmitter shutter, and a refracting telescope are mounted on a small optical bench which can be bolted directly to the metal box containing the receiving optics. The transmitting telescope, with a focal length of one meter and aperture of 10 cm, is used to collimate the laser beam. The receiving unit used a 40 cm aperture telescope of the Dahl-Kirkham type to collect

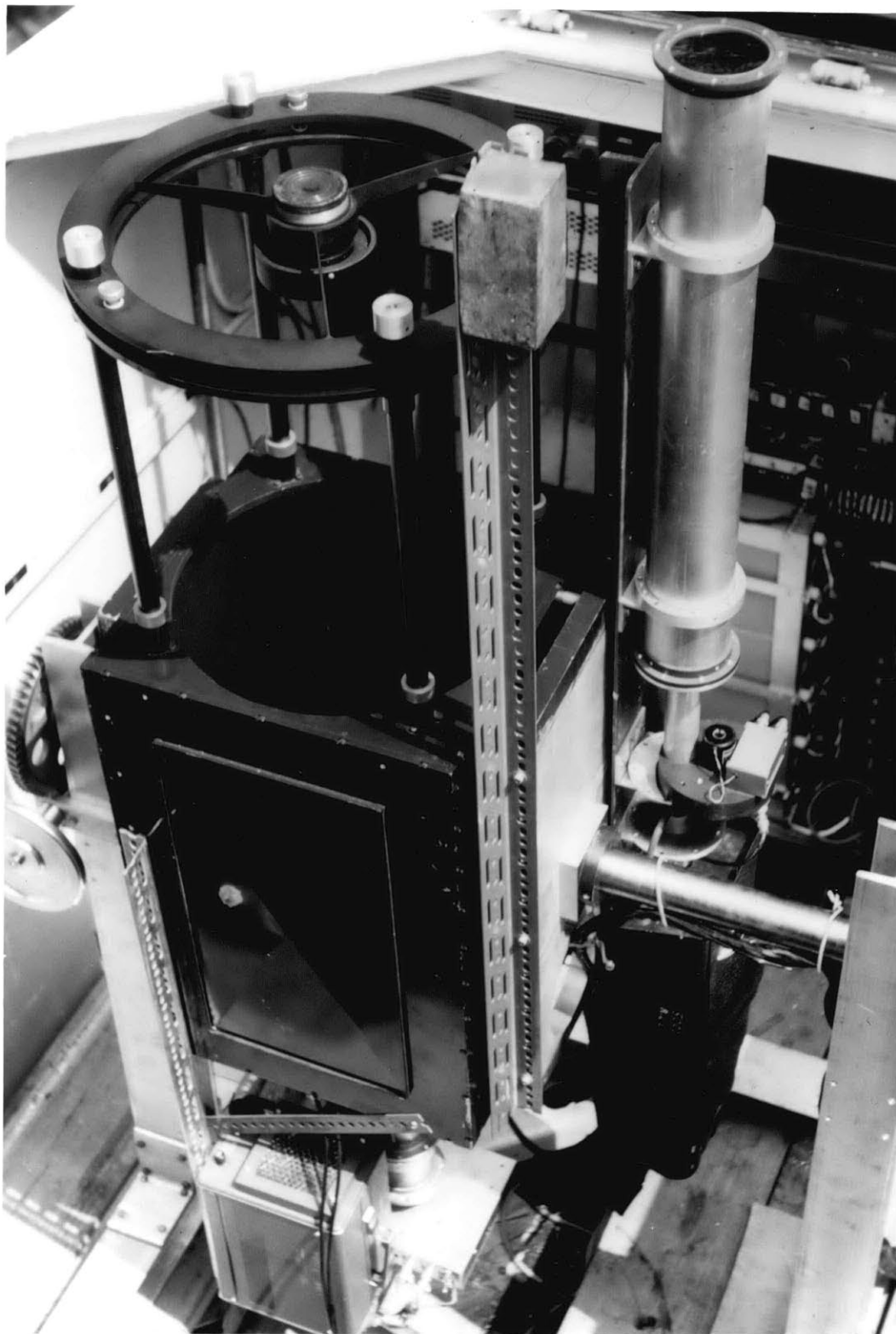


Fig. 4. Photograph of the apparatus.

the light back-scattered by atmospheric constituents. The photodetection system, attached to the back of the telescope, includes the receiving shutter, a narrow band interference filter, and an EMI 9558 A photomultiplier tube cooled with methanol and dry ice.

There have been two different lasers used during the stratospheric aerosol study. The first laser, built by the Radio Corporation of America, could emit pulses of approximately $1/2$ joule with a wavelength of 0.694 micron and duration shorter than one microsecond. Q-switching was achieved through the use of a rotating mirror. The three inch ruby rod used in this laser and the elliptical cavity in which the rod and a xenon flashlamp were located were cooled by dry nitrogen passed through a coil immersed in liquid nitrogen. After a considerable amount of experimentation to improve the performance of the laser unit, an Edgerton, Germeshausen, and Grier FX-42 flashlamp with a three inch arc length, modified for cooling with distilled water, enabled the laser to be fired at a maximum rate of about five pulses per minute.

A larger unit, built by Applied Lasers, Inc., was substituted in the fall of 1964. This laser is capable of delivering pulses of approximately two joules with a duration shorter than one microsecond at a pulse repetition rate of about thirty per minute. The ruby rod, flashlamp (EG & G FX-67 A), and elliptical cavity are cooled by closed loop circulation

of distilled water. The 90° orientation ruby rod is $6 \frac{5}{8}$ " long and $\frac{3}{8}$ " in diameter; a rotating prism is used for Q-switching the laser. The new unit enjoyed the benefits of rapidly improving laser technology and operated without interruption for repairs for the duration of the stratospheric aerosol study, in contrast to a considerable amount of developmental effort expended on the first unit.

Since the system has incorporated many improvements during the course of the study and since some observations taken in College, Alaska during the summer 1964 used a different telescope and photodetection unit from those described above, Table 1 has been constructed to summarize the characteristics of the optical radar units used throughout the study.

Table 1. General characteristics of various optical radar systems used during the study.

Observation period	January-May 1964	July-August 1964	October 1964-August 1965
Observation site	Lexington	College	Lexington
Transmitted wavelength	0.694 μ	0.694 μ	0.694 μ
Pulse length	<1 μ sec	<1 μ sec	<1 μ sec
Pulse energy	~ 1/2 joule	~ 1/2 joule	~ 2 joule
Pulse repetition rate	~ 0.1 sec ⁻¹	~ 0.1 sec ⁻¹	~ 0.5 sec ⁻¹
Transmitted beamwidth	<1 mrad	<1 mrad	<1 mrad
Transmitter efficiency (estimated)	~ 75%	~ 75%	~ 75%
Aperture of receiving telescope	40 cm	30 cm	40 cm
Receiver efficiency (estimated)	~ 30%	~ 30%	~ 30%
Quantum efficiency of photodetector	~ 5%	~ 5%	~ 5%
Bandwidth of receiver filter	20 Å	3 Å	6 Å

3. DETECTION OF AEROSOL LAYERS WITH OPTICAL RADAR

3.1 The optical radar equation.

Each time that the laser is fired a light pulse of duration τ containing n_τ photons is transmitted through the atmosphere. At any time t the photodetection system receives light back-scattered by the air molecules and aerosol particles illuminated by the laser beam that has traveled a distance $2R = ct$ for the front of the pulse and $2R - L = c(t - \tau)$ for the end of the pulse; R is the radar range and L is the length in space of the laser pulse. The volume illuminated by the laser pulse will therefore have a depth $\frac{L}{2}$ and a cross-sectional area ΩR^2 for $R \gg L$; here Ω is the solid angle subtended by the laser beam. The average intensity of the transmitted pulse illuminating this volume will be given by

$$\frac{n_\tau k_\tau k_A}{\Omega R^2 \tau} \quad (3.1)$$

if k_τ is the efficiency of the transmitting system and k_A is the atmospheric transmission. The radar cross-section σ is a measure of the efficiency of a particle to back-scatter radiation; it is defined as the area that intercepts the amount of power radiated by an isotropic scatterer which scatters energy in all directions with intensity equal to that back-scattered by the actual particle. Thus the intensity of light at the receiver that was

back-scattered from a single particle in the illuminated volume may be expressed as

$$\frac{n_T k_T k_A}{\Omega R^2 \tau} \cdot \frac{\sigma}{4\pi R^2} \cdot k_A \quad (3.2)$$

When scattering from an ensemble of particles is considered, a sum over all the contributions from each particle, taking phases into account, must be performed. If no systematic phase relation exists between the contributions of the various scatters, they are called independent and the expected scattered intensity is obtained by adding the intensities scattered by individual particles without regard to phase. If the volume illuminated by the light pulse contains M randomly distributed independent scatterers, the intensity of the light returned to the receiver becomes

$$\frac{n_T k_T k_A^2}{\Omega R^2 \tau} \cdot \frac{\beta}{4\pi R^2} \cdot \Omega R^2 \frac{L}{2} \quad (3.3)$$

where

$$\beta = \frac{1}{\Omega R^2 \frac{L}{2}} \sum_{m=1}^M \sigma_m \quad (3.4)$$

is the total radar cross-section per unit volume of atmospheric constituents at range R .

If A_R is the aperture of the receiving telescope and k_R the efficiency of the receiving system, the flux of photons at the photocathode is

$$\frac{n_T k_T k_A^2 L \beta}{8 \pi R^2 \tau} \cdot A_R k_R \quad (3.5)$$

Thus the expected flux of photoelectrons emitted at the photomultiplier cathode is

$$\frac{dn_R}{dt} = \frac{n_T k_T k_A^2 k_R A_R \eta c}{8 \pi} \cdot \frac{\beta}{R^2} \quad (3.6)$$

The energy transmitted per pulse is

$$W_T = n_T \frac{hc}{\lambda} \quad (3.7)$$

λ is the wavelength of the transmitted pulse and h is Planck's constant. This relation provides an alternate expression:

$$\frac{dn_R}{dt} = \frac{W_T k_T k_A^2 k_R A_R \eta \lambda}{8 \pi h} \cdot \frac{\beta}{R^2} \quad (3.8)$$

Equation 3.8 will be used as the optical radar equation to determine the rate at which photoelectrons are emitted at the photocathode.

3.2 Back-scattering from atmospheric constituents.

The necessity of providing quantitative estimates of the radar cross-section of various atmospheric constituents introduces the problem of determining the amount of energy absorbed and the amount and spatial distribution of the energy scattered by a particle in the field of electromagnetic wave. Air molecules scatter and absorb radiation, although the absorption is confined to specific wavelength regions. Aerosols with dimensions comparable to optical

wavelengths are efficient scatters and will contribute to the collective radar cross-section of the atmospheric constituents. Absorption of light by aerosols can often be neglected although the chemical composition of the particle must again be known.

Van de Hulst (1957) has reviewed the general theory for the scattering of light by small particles. His treatise is the basis for most of the scattering theory presented in the following discussion. The spatial distribution of the radiation scattered by a particle of arbitrary dimensions and composition requires the formal solution of Maxwell's equations. The scattered field may be specified in terms of two components of the amplitude of the scattered wave E_{\perp} and E_{\parallel} which are, respectively, perpendicular to and parallel to the scattering plane, that is the plane containing the source of radiation, the scattering particles, and the observer. The orientation of a particle of arbitrary form must be specified. The scattered field is then characterized by four complex amplitude functions S_1 , S_2 , S_3 , and S_4 , all functions of the scattering angle θ between the propagation vectors of the incident and scattered waves and the parameters describing the orientation of the particle. The functional relation is

$$\begin{pmatrix} E_{\parallel} \\ E_{\perp} \end{pmatrix} = \begin{pmatrix} S_2 & S_3 \\ S_4 & S_1 \end{pmatrix} \cdot \frac{e^{-ikR}}{ikR} \begin{pmatrix} E_{0\parallel} \\ E_{0\perp} \end{pmatrix} \quad (3.9)$$

here $k = \frac{2\pi}{\lambda}$ is the wave number, $i = \sqrt{-1}$, R is the distance from the particle, and $E_{o_{\perp}}$ and $E_{o_{\parallel}}$ are time dependent functions that describe the amplitudes of the electric vectors of the incident wave that are, respectively, perpendicular to and parallel to the scattering plane.

For homogeneous spherical particles $S_3 = S_4 = 0$ and scattering is described by just two of these amplitude functions, $S_1(\theta)$ and $S_2(\theta)$, which are functions only of the scattering angle θ . Thus

$$E_{\perp} = S_1(\theta) \frac{e^{-ikR}}{ikR} E_{o_{\perp}} \quad (3.10)$$

and

$$E_{\parallel} = S_2(\theta) \frac{e^{-ikR}}{ikR} E_{o_{\parallel}}. \quad (3.11)$$

By squaring the moduli, we obtain the intensity

$$I_{\perp} = \frac{|S_1(\theta)|^2 I_{o_{\perp}}}{k^2 R^2} \quad (3.12)$$

for the case of perpendicular polarization, and

$$I_{\parallel} = \frac{|S_2(\theta)|^2 I_{o_{\parallel}}}{k^2 R^2} \quad (3.13)$$

for parallel polarization.

For the special case in which the particles are very small compared to the wavelength of the incident radiation, they behave like dipoles and we obtain

$$I_{\perp} = \frac{k^4 p^2 I_{o_{\perp}}}{R^2} \quad (3.14)$$

and

$$I_{\parallel} = \frac{k^4 \rho^2 I_{0\parallel}}{R^2} \cos^2 \theta \quad (3.15)$$

where ρ is the polarizability of the particle. This special case was considered by Lord Rayleigh (1871) in his classical explanation of the blue color of the sky.

For back-scattered radiation ($\theta = 180^\circ$) no distinction can be made between the scattering planes and both equations reduce to

$$I = \frac{k^4 \rho^2 I_0}{R^2} \quad (3.16)$$

By the definition of the radar cross-section,

$$I = \frac{\sigma I_0}{4\pi R^2} \quad (3.17)$$

Thus the radar cross-section for Rayleigh scattering by a single molecule is

$$\sigma_R = 4\pi k^4 \rho^2 \quad (3.18)$$

The refractive index of a medium containing a large number of randomly distributed independent scatters can be determined from the scattering properties of the individual particles. If each unit volume of the medium contains N_A molecules of polarizability ρ , the index of refraction m is given by

$$m = 1 + 2\pi \rho N_A \quad (3.19)$$

This formula will be used to express the radar cross-section for Rayleigh scattering in terms of the refractive index:

$$\sigma_R = \frac{k^4}{\pi} \left(\frac{m-1}{N_A} \right)^2 = \frac{16\pi^3}{\lambda^4} \left(\frac{m-1}{N_A} \right)^2. \quad (3.20)$$

These expressions for the radar cross-section of a Rayleigh scatterer are valid for independent scattering by very small non-absorbing particles with isotropic polarizability. When any of the basic conditions are not met, it becomes more difficult to evaluate the intensity of the back-scattered radiation; atmospheric aerosols having dimensions comparable to optical wavelengths must be treated by rigorous scattering theory.

The fundamental contribution to general scattering theory has been the solution for scattering by homogeneous spherical particles of arbitrary size and composition (Mie, 1908). The result has the form of an infinite series of angular functions $\pi_n(\cos \theta)$ and $\tau_n(\cos \theta)$ with coefficients a_n and b_n determined by the boundary conditions on the spherical surface. The amplitude functions are given by

$$S_1(\theta) = \sum_{n=1}^{\infty} \frac{2n+1}{n(n+1)} \left\{ a_n \pi_n(\cos \theta) + b_n \tau_n(\cos \theta) \right\} \quad (3.21)$$

and

$$S_2(\theta) = \sum_{n=1}^{\infty} \frac{2n+1}{n(n+1)} \left\{ a_n \tau_n(\cos \theta) + b_n \pi_n(\cos \theta) \right\}. \quad (3.22)$$

In these formulae

$$\pi_n(\cos \theta) = \frac{dP_n(\cos \theta)}{d \cos \theta} \quad (3.23)$$

and

$$\tau_n(\cos \theta) = \cos \theta \cdot \pi_n(\cos \theta) - \sin \theta \frac{d\pi_n(\cos \theta)}{d \cos \theta}, \quad (3.24)$$

where $P_n(\cos \theta)$ is a Legendre polynomial of degree n . The coefficients a_n and b_n are combinations of spherical Bessel and Hankel functions of order $n + \frac{1}{2}$ and their derivatives. These coefficients are related to the size and composition of the spherical particle through the arguments α and $m\alpha$, where $\alpha = k_0 r = \frac{2\pi r}{\lambda}$ is a size parameter (r is the particle radius) and m is a complex index of refraction in which the imaginary portion is an absorption parameter. The series defining each of these functions are difficult to evaluate and extensive numerical calculations were not possible until recently when electronic computers could be used for the computations.

In order to illustrate the relation between the size of a Mie scatterer and its radar cross-section, it is necessary to obtain numerical solutions of the Mie formulae for back-scattered radiation. For this case $S_2 = S_3 = S$ and the intensity of the scattered light may be written as

$$I = \frac{|S|^2 I_0}{k^2 R^2} \quad (3.25)$$

From the definition of the radar cross-section (3.17), the radar cross-section of a Mie scatterer is

$$\sigma_M = \frac{4\pi |S|^2}{k^2} = \frac{\lambda^2}{\pi} |S|^2 \quad (3.26)$$

Another commonly used scattering parameter is the normalized radar cross-section, defined as the ratio between the radar cross-section and the projected area of the particle:

$$\frac{\sigma_M}{\pi r^2} = \frac{4 |S|^2}{k^2 r^2} = \frac{\lambda^2}{\pi^2 r^2} |S|^2 = \frac{4}{\alpha^2} |S|^2 \quad (3.27)$$

Fig. 5 shows the normalized radar cross-section of a Mie scatterer as a function of the size parameter $\alpha = kr$ for a refractive index $m = 1.5$. This value corresponds to the index of refraction of naturally occurring atmospheric aerosols (Volz, 1954) and, in particular, to the refractive index of ammonium sulfate and ammonium persulfate; these compounds make up over 90% of the mass of the stratospheric particles collected in direct sampling studies (Friend et al, 1961; Junge and Manson, 1961). The values plotted in the figure have been calculated for 0.05 increments of the scattering parameter to illustrate the rapid change in the radar cross-section associated with small increases of the scattering parameter. These results will be used to estimate the radar cross-section of the stratospheric aerosol to interpret the results of the laser back-scattering observations.

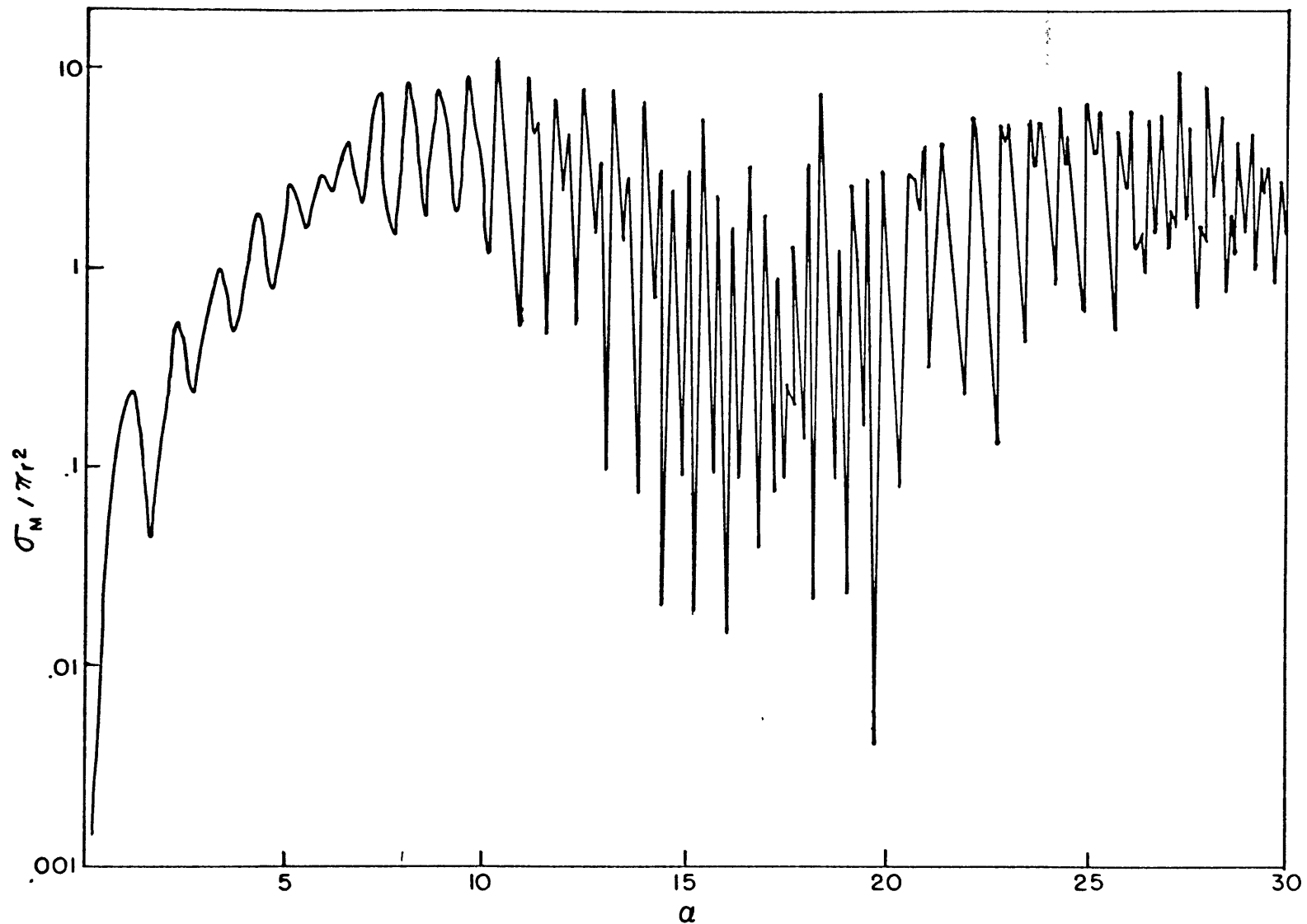


Fig. 5. Radar cross-section σ_M for spherical particles with refractive index 1.5 as a function of the Mie size parameter $\alpha = \frac{2\pi r}{\lambda}$ where r is the radius of the scattering particle and λ is the wavelength of the incident radiation. The calculated values are normalized to the geometric cross-section of the particle.

3.3 Quantitative estimates of atmospheric scattering parameters.

If the component of the optical radar signal due to molecular scattering can be evaluated, contributions due to the presence of particulate matter in the atmosphere might be detected. Quantitative estimates of the relative contributions of molecular and aerosol scattering will be obtained to determine the sensitivity of the system to changes in the aerosol content of the stratosphere.

The intensity of light back-scattered from air molecules may be treated by Rayleigh's scattering law for wavelengths at which absorption can be neglected. The wavelength of a ruby laser is a function of the temperature of the ruby crystal, increasing by approximately 0.04 Å per degree Kelvin. Long (1963) has measured the absorption spectrum of solar radiation at ruby wavelengths with a high-resolution spectrograph; the observed absorption spectrum shows relatively large ruby temperature differences between absorption lines. This allows the laser to be thermally tuned to wavelengths at which absorption can be neglected. Rayleigh's scattering law is therefore appropriate for determining the contribution of air molecules to the collective radar cross-section of atmospheric constituents. The radar cross-section per unit volume for molecular scattering is

$$\beta_R = N_A \sigma_R , \quad (3.28)$$

where N_A is the molecular number density. For air molecules illuminated by light with a wavelength of 0.6943 micron, equation 3.20 gives

$$\sigma_R = 2.5 \times 10^{-27} \text{ cm}^2. \quad (3.29)$$

The contribution of aerosols to the intensity of the radiation back-scattered from the atmosphere is more difficult to evaluate. It is possible to evaluate the radar cross-section of a single particle of known dimensions, composition, and spatial orientation by theoretical considerations if the surface of the particle can be approximated by a simple geometrical form or by experimental studies of scaled models with microwave radiation for geometrical surfaces that cannot be expressed analytically. Such estimates would be required for every particle illuminated by the light beam.

Photomicrographs and electron micrographs of stratospheric particles (Friend et al, 1961; Junge and Manson, 1961) indicate that the stratospheric aerosol is approximately spherical. Mie's formulae will therefore be used to estimate their radar cross-section.

Atmospheric aerosols often exhibit a regular decrease in concentration with increasing particle size that can be approximated by an inverse power law (Junge, 1952). The particle size distribution is usually expressed as a logarithmic radius-number concentration distribution:

$$\frac{dN}{d \log r} = \frac{c}{r^{\nu}} \tag{3.30}$$

where N is the number of particles of radius larger than r , c is a number determined by the total concentration, and ν is a constant. It is convenient to express this distribution function as a radius-number concentration distribution

$$\xi(r) = \frac{dN}{dr} = \frac{0.434c}{r^{\nu+1}} \tag{3.31}$$

Thus N_D , the number of dust particles with radii between r_1 and r_2 , is given by

$$N_D = \int_{r_1}^{r_2} \xi(r) dr = 0.434c \int_{r_1}^{r_2} \frac{dr}{r^{\nu+1}} = \frac{0.434c}{\nu} \left(\frac{1}{r_1^{\nu}} - \frac{1}{r_2^{\nu}} \right) \tag{3.32}$$

Also, the total radar cross-section of the dust particles in the indicated size interval is

$$\beta_D = \int_{r_1}^{r_2} \sigma(r) \cdot \xi(r) dr, \tag{3.33}$$

where $\sigma(r)$ is the Mie radar cross-section at the radius r . Since Mie calculations are performed as a function of the scattering parameter $\alpha = \frac{2\pi r}{\lambda}$ it is desirable to transform variables and express the integral in terms of the scattering parameter α at the fixed wavelength λ of the ruby light. This gives

$$\beta_D = 0.434c \int_{r_1}^{r_2} \frac{\sigma(r) dr}{r^{\nu+1}} = 0.434c \left(\frac{2\pi}{\lambda} \right)^{\nu} \int_{\alpha_1}^{\alpha_2} \frac{\sigma(\alpha) d\alpha}{\alpha^{\nu+1}} \tag{3.34}$$

which may also be expressed in terms of the total number of particles in the indicated size interval by using equation 3.32.

Mie radar cross-sections for a refractive index 1.5 were calculated as a function of the scattering parameter α from $\alpha=0$ to $\alpha=30$ in steps of 0.05. These results were punched on data processing cards and were used to compute the total radar cross-section of aerosol particles as a function of the radius limits of the particle size distribution and the slope of the distribution function, by numerically evaluating the integral in equation 3.34.

Junge et al (1961) found that the size distribution of stratospheric particles followed an inverse square law for particle sizes between 0.1 and 1μ ; a simultaneous study by Friend et al (1961) indicated a steeper slope when the dimensions of flattened particles on the impaction surfaces were changed to the dimensions of equivalent spheres. This correction changed the slope of the size distribution determined by the particle collections to $\nu=3.5$ (Junge, 1963). Newkirk and Eddy (1964) assumed a power law distribution function for particle sizes to interpret light scattering measurements by a balloon-borne coronagraph. The observed angular distribution of the scattered light was compared to calculated distributions for Mie scatterers; the results were also consistent with a value $\nu=3.5$ for stratospheric aerosols.

Although the first particle collection measurements indicated that the power law approximation could be applied to particle sizes from 0.1 to about 1μ , subsequent investigations by Friend (Feely et al, 1963) indicate that a break in the size distribution occurs at slightly larger particle sizes to give a distribution function that is approximately symmetrical about 0.275μ radius. These results suggest that the size distribution function for the sulfate particles found in the stratosphere may be approximated by a power law with a slope characterized by $n=3.5$ for particle sizes larger than 0.275μ but is not very well known for smaller particles. At some radius between about 0.1 and 0.275μ the number concentration is known to decrease rapidly with decreasing particle size. The exact location of this break in the power law distribution function is not accurately known because the region where the cut-off occurs is within a size interval where the direct sampling measurements require large corrections for impaction efficiency and optical techniques are rather insensitive to changes in the size distribution.

The upper limit of the distribution function extends to at least 1μ . Above this size the low particle concentrations are subject to a large amount of statistical fluctuation. The total radar cross-section calculations extended the size distribution to the largest scattering parameters for which Mie formulae were evaluated. This

corresponds to $\alpha=30$ or $n=33\mu$ at the ruby wavelength. The results, however, are rather insensitive to the upper radius limit. For $\nu=3.5$ the total cross-section would be decreased by $\sim 20\%$ if the scattering parameter appropriate to 1μ were used as the upper limit.

Since the lower radius limit and the slope of the size distribution are also not precisely known the calculations have been performed for a variety of size distributions characterized by different slopes and different cut-off radii at the lower limit of the distribution function. In order to summarize the results of these calculations two figures have been constructed. Fig. 6 presents a number concentration parameter associated with the size distribution characterized by a slope $\nu=3.5$ and lower radius limit $r_c = 0.275\mu$, taken to be a good estimate of the actual distribution function for larger particle sizes. The diagram shows N_D the total number of particles having radii larger than 0.275μ necessary for the aerosol return to exactly equal the molecular return at the indicated altitudes, as determined from the number densities for air molecules tabulated in the U.S. Standard Atmosphere, 1962 and Rayleigh radar cross-section given in equation 3.31.

Fig. 7 illustrates the effect of changing the size distribution function. N_D must be multiplied by the indicated numbers if different particle distributions characterized by the slope ν and cut-off radius r_c are used

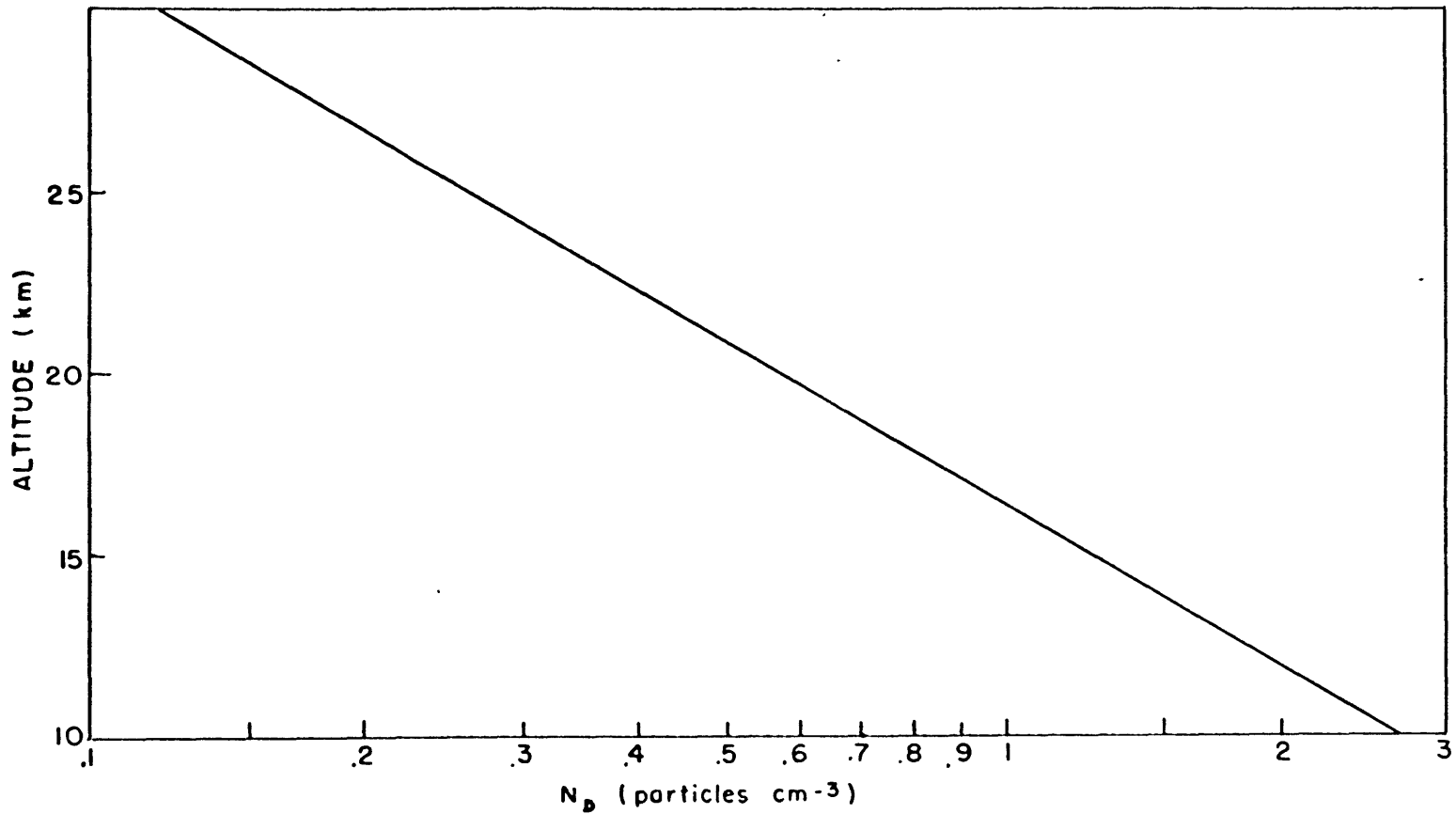


Fig. 6. Number of dust particles required to back-scatter the same amount of light as the molecular return from the lower stratosphere at the ruby wavelength. The dust particles are assumed to be Mie scatterers with refractive index 1.5 with sizes prescribed by a distribution function $dN = C r^{-3.5} d \log r$; the lower cut-off for the size distribution function is assumed to be 0.275μ . The molecular number density has been obtained from the U. S. Standard Atmosphere, 1962.

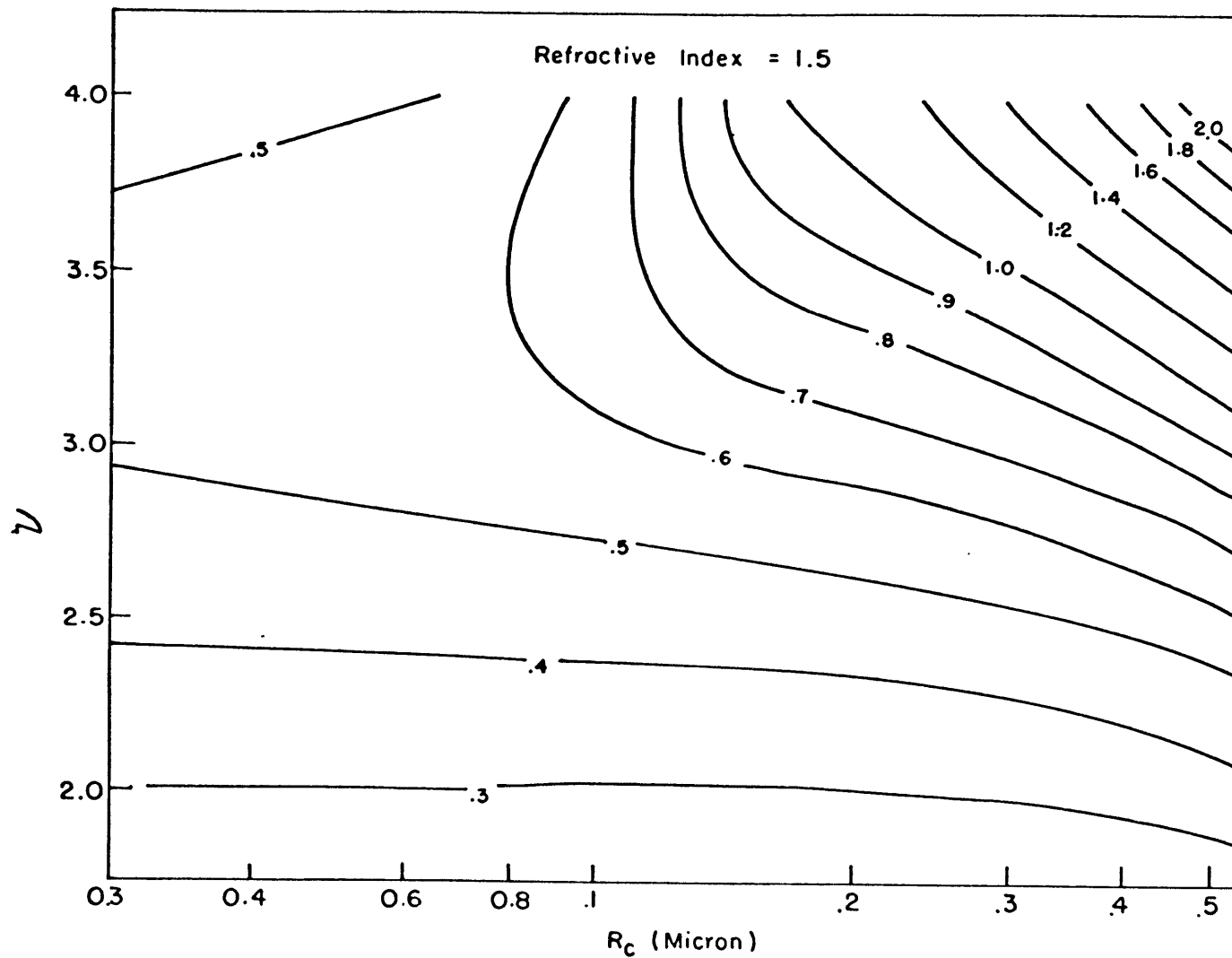


Fig. 7. Correction constants for Fig. 6 for different size distribution functions characterized by the slope ν and cut-off radius R_c .

in the scattering calculation. Since most studies place r_c between 0.1 to 0.3 μ and ν between 3 and 4, it appears that different size distributions will not change the estimated value of N_D by more than 30%. The almost constant factor for $\nu \lesssim 2.5$ reflects the fact that back-scattering intensity functions decrease very rapidly with decreasing particle size and the smaller particles do not make a significant contribution to the back-scattered radiation unless they are present in very large amounts. The important parameter of the size distribution function for numerical scattering calculations is therefore the radius at which a break in a power law occurs, and the exact form of the subsequent decrease with smaller particle sizes will not affect the results appreciably.

The previous calculations were performed for a refractive index 1.5; the same parameters have also been calculated for a refractive index 1.33, appropriate to water droplets. This computation shows that, for the range of size distribution parameters shown in Fig. 5, all values must be increased by a factor of ~ 3 . This indicates that the use of Mie calculations for a 1.33 refractive index to interpret optical radar returns from the stratosphere may overestimate the particle concentration by this amount if the particles are indeed composed of the sulfates that have been detected in the impactor samples.

Recent in situ particle concentration measurements by

Rosen (1964) with a photoelectric particle counter provide profiles of the number concentration of stratospheric particles having radii larger than certain predetermined values. The size cut-off for the particles sampled with the device corresponds rather closely with the 0.275μ lower cut-off used to calculate N_D . The published profiles show maximum concentrations of approximately 1 to 2 particles cm^{-3} near 16 km altitude. According to the calculations summarized in Fig. 6, 1.1 Mie particles cm^{-3} at 16 km altitude will back-scatter the same amount of radiation as the molecular return from that height. Thus the echoes received from those altitudes should be approximately twice that expected from a dust-free atmosphere at the altitude of maximum dust concentrations.

4. DATA REDUCTION AND ANALYSIS

Most of the 1964 data was recorded with a Hewlett-Packard Model 196 A oscilloscope camera capable of recording several consecutive optical radar echoes on a Polaroid print. An accurate tracing of one of these photographs is shown in Fig. 8; this shows five optical radar traces, recorded at five second intervals at approximately 1930 EST on 4 November 1964. The photocathode current was registered as an A-scope display; the vertical deflections are proportional to the received signal and the horizontal distance from the initial deflection to any point on the curve is directly related to the distance from the instrument to the volume illuminated by the laser beam. A scale has been drawn at the bottom of the tracing to indicate altitudes; while the range increases from left to right according to the conventional A-scope display, the photocathode current was registered as a negative deflection of the trace. The time base of the oscilloscope was set to give a maximum range of about 40 km for the display. The gain was adjusted to obtain the largest possible deflection of the oscilloscope beam for altitudes above ~ 10 km.

The vertical deflections of the observed traces are digitized to provide quantitative information for comparison with the expected echoes from a dust-free atmosphere as prescribed by the optical radar equation. The data recorded on Polaroid prints were digitized by use of a grid etched onto a

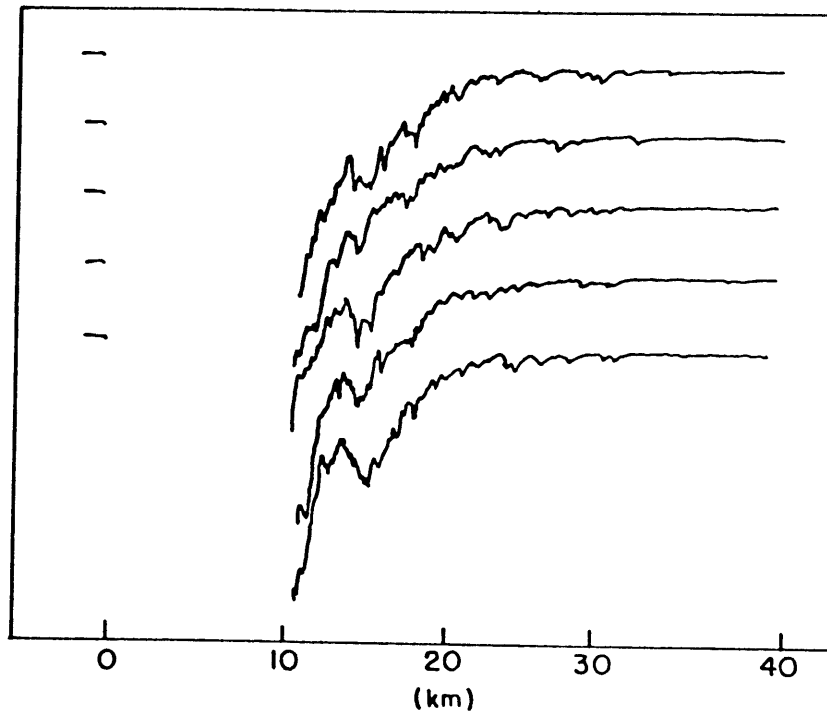


Fig. 8. Sample data record showing five consecutive optical radar returns. An altitude scale is included at the bottom of the figures; enhanced echoes near 16 km are evident in the tracing.

transparent overlay for which the grid spacing was carefully drawn with reference to photographed calibration signals displayed on the same oscilloscope used to record the optical radar traces.

From January 1965 to the end of the study, data were recorded on 100 ft rolls of 35 mm film with a Fairchild 556-BH1 radarscope camera modified for use on an oscilloscope. When the laser was pulsed, the return signals detected by the photomultiplier were displayed on an Tektronix 555 dual beam oscilloscope and photographed. At the end of the display sweep a relay was activated to advance the film to the next frame. A 24 hour clock, a 4-digit electric counter, and a data card were photographed on each frame for identification purposes. Two traces were recorded simultaneously; both traces measured the current emitted at the photodetector cathode. The upper trace displayed the optical radar echoes at altitudes less than 40 km. The lower trace extended the observation to a range of about 200 km by using a time base 5 times longer than used for the 40 km display sweep. At altitudes above 30 km the flux density of the echoes had decreased to such an extent that a continuous current was no longer recorded and when the gain was increased by a factor of ~ 100 , the display consisted of "spikes" representing the emission of single photoelectrons by the photomultiplier. The 200 km data was analyzed by counting the number of "spikes" observed in specified altitude intervals

for a large number of traces. The presence of scattering layers at latitudes from 60 to 140 km could be determined by a statistical analysis of the accumulated photoelectron counts (Fiocco and Smullin, 1963).

The 40 km trace was digitized, in principle, in exactly the same manner as the data recorded on Polaroid prints. The data reduction has been accomplished with the aid of an "Oscar F" semi-automatic oscilloscope record analyzer manufactured by the Benson-Lehner Corporation. The image of each oscilloscope trace was projected onto a viewing screen; when cross-hairs were manually moved on the screen to follow the photographed oscilloscope trace, the machine digitized the observed coordinates of the trace through an analog-to-digital converter and provided a printed record of the digitized coordinates. These coordinates were then punched on data processing cards for subsequent analysis. The coordinates were digitized with reference to a linear coordinate system; calibration traces have also been digitized to provide corrections for any non-linearity of the oscilloscope display or camera system, just as the Polaroid data was digitized with respect to a coordinate system determined with photographed calibration traces.

The digitized vertical deflections of the optical radar traces were used to derive quantitative information on the dust content of the stratosphere by comparing the observed echoes with the expected return from a clear molecular

atmosphere calculated from the optical radar equation (3.8). This equation was obtained with an implicit assumption that the range resolution of the signal could not exceed the depth of the volume illuminated by the laser beam since the derivation used the average intensity of the transmitted pulse. The pulse lengths of both lasers used during the study were less than 1μ sec; the range resolution of the system could therefore be about 150 meters. While the detail afforded by this resolution is highly desirable, the shape of the observed traces (see Fig. 8) exhibited a great deal of variability from trace to trace.

This variation had the appearance of random fluctuations superimposed on a mean return. Numerical calculations have verified this observation. More than 200 consecutive traces, taken at 5 second intervals on 18 December 1964, were digitized and used to study these fluctuations. The mean and standard deviation of the digitized coordinates at each altitude were calculated. If the variations in the photoelectron flux recorded on the oscilloscope traces are indeed random variations, the calculated values of the standard deviation should vary as $\sqrt{\frac{dn_p}{dt}}$ where $\frac{dn_p}{dt}$ is the observed photoelectron flux at the photocathode. The computed values of the mean and standard deviation of the optical radar return at each altitude are plotted in Fig. 9 on logarithmic graph paper. If the standard deviation does vary as $\sqrt{\frac{dn_p}{dt}}$ the plotted points should lie on a line with a slope equal to 1/2.

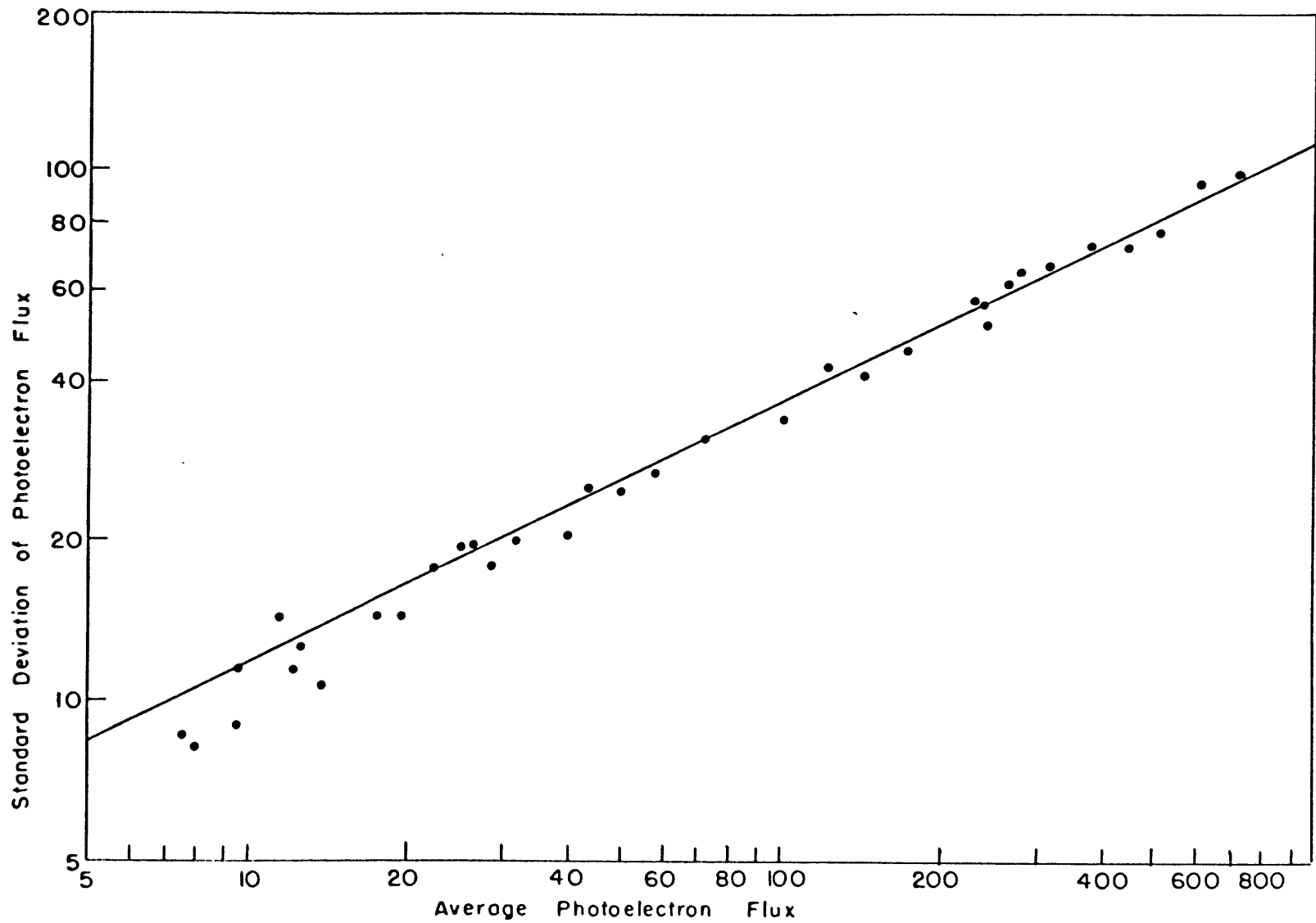


Fig. 9. Root-mean-square fluctuations of the photoelectron flux as a function of the average photoelectron flux observed for various 1/2 km altitude intervals. Relative units.

A line with this slope has been drawn through the points and the agreement is quite satisfactory. Other calculations also corroborate a conclusion that the fluctuations are random. For example, autocorrelation coefficients at one lag were calculated at each altitude and found to be very small with a mean value of almost zero and having absolute values ≤ 0.1 .

The fluctuations are primarily due to shot noise affecting the photomultiplier current, and also, possibly, due to phase effects in the propagation of the wave; it is considered unlikely that the fluctuations represent variations in scattering particle concentrations. Uncertainties associated with statistical fluctuations of the signal can be eliminated only by integrating a sufficient number of optical radar returns. The effect of this in reducing the random fluctuations of the signal is summarized in Fig. 10 which shows isopleths of rms fluctuations of the echoes received by the apparatus used in the study as a function of the number of traces added together and of the altitude of the echo. The fluctuations are expressed as percentage deviations from the mean photoelectron flux observed at each altitude. The curves represent smoothed values of the results of computations performed on the same series of digitized traces that were used to construct Fig. 9. The expected rms fluctuations do, of course, increase with altitude and with smaller numbers of traces used to compute the mean. This

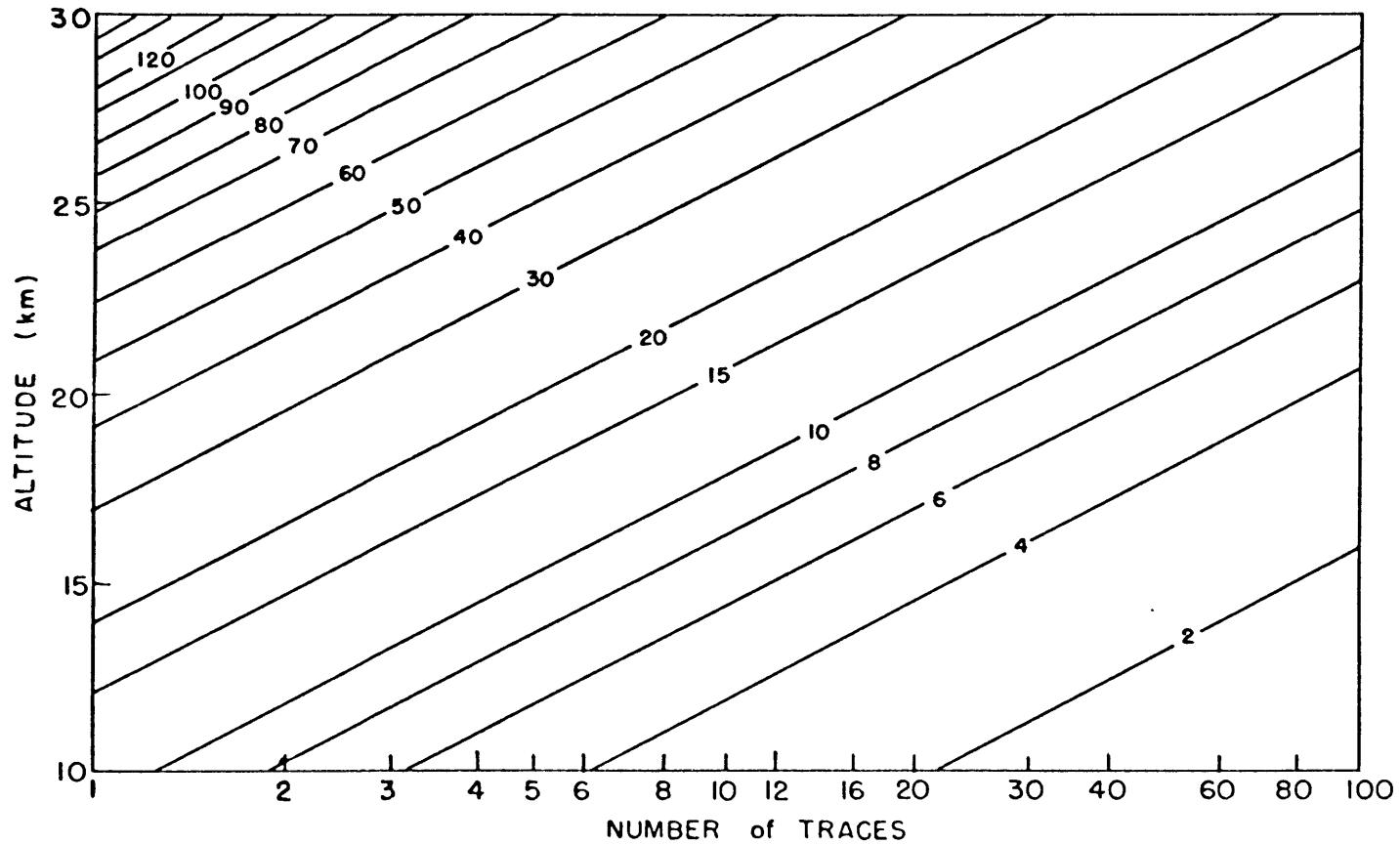


Fig. 10. Estimated rms fluctuations of the average optical radar return for 1/2 km altitude intervals in the lower stratosphere as a function of the number of individual traces used to determine the average return. The fluctuations are expressed as a percent of the average signal for each altitude interval.

figure indicates the expected error associated with the experimental returns for 1/2 km altitude intervals. If, indeed, the fluctuations are random and if, in addition, they are not correlated with fluctuations at contiguous altitudes, values appropriate to 1 km averages should be reduced by a factor $\frac{1}{\sqrt{2}}$. The values are calculated for a single night of observation and at best can be used only as a guide in evaluating the error in the experimental results for the entire series since day-to-day variations in the sensitivity of the apparatus will change the photoelectron flux at the photocathode and thereby change the expected rms fluctuations for each altitude (see Fig. 9).

In view of the random nature of the signal, it is necessary to integrate a number of successive traces and obtain an average optical radar return for the given time interval. The number of traces required to reduce the statistical fluctuations of the received signal to an acceptable level, the relatively large range interval used for the study, and the difficulty of determining the exact position of very small range intervals, especially on the Polaroid prints, made it necessary to decrease the range resolution. The data records were digitized by using average vertical coordinates for 1 km altitude increments for the Polaroid data and 1/2 km increments for the data recorded on microfilm. The observed coordinates for consecutive traces were summed to provide an integrated optical radar return for each

period of observation. This average signal was then compared to the expected signal from a molecular atmosphere to construct vertical profiles of the dust content of the stratosphere. Thus, to derive the dust profiles, it is necessary to evaluate the intensity of the echoes for a dust-free atmosphere by using equation 3.8 for the case of Rayleigh scattering by air molecules.

With the laser systems used in the study, the energy transmitted W_T was not constant from pulse to pulse; however, it could in principle be determined by an appropriate monitoring system and used to evaluate the equation. Similarly, k_T and k_R , the efficiencies of the transmitting and receiving systems, respectively, could also be measured and utilized in the calculation. The only parameters that vary with altitude in the equation are the atmospheric transmission k_A , the Rayleigh radar cross-section per unit volume $\beta_R = N_A \sigma_R$ where N_A is the molecular number density and σ_R is the radar cross-section for Rayleigh scattering, and the range R . Thus, the average photoelectron flux for a given series of traces could be derived from a relation

$$\frac{d\pi_R}{dt} = \text{constant} \cdot \frac{N_A k_A^2}{R^2} \quad (4.1)$$

For the stratospheric dust study the optical radar was zenith-oriented so that the range was the distance above the instrument; slant path transmission was not involved in the calculations. For a vertical path in the atmosphere a light

beam suffers almost all of its attenuation in the troposphere; in the attenuation model proposed by Elterman (1964) atmospheric optical parameters have been calculated that include attenuation by molecular and aerosol scattering and by ozone absorption. The parameters computed for 0.7 micron radiation indicate that the k_A^2 term does not vary by more than 3% over the entire altitude interval from 10 to 30 km. Attenuation of the laser beam was therefore neglected in the analysis of the data, and the atmospheric attenuation term was regarded as a constant. Thus the optical radar return was approximated by the relation

$$\frac{dn_R}{dt} = \text{constant} \cdot \frac{N_A}{R^2} . \quad (4.2)$$

If the number concentration of air molecules is known, the molecular return could be evaluated by determining the constant in this equation. This requires some relatively simple measurements of the transmission efficiencies of the transmitting and receiving systems, as well as a complete knowledge of the energy transmitted in each pulse and the atmospheric transmission in the troposphere at the time that the measurement was performed. Most of the data was obtained with considerable difficulty because of the fact that the optical radar unit was in a developmental stage, and full-time effort was devoted to other improvements on the instrument which would increase its capabilities and eliminate undesirable features which became evident when

attempts were made to collect data on a routine basis. Therefore the data analysis was conducted without the benefit of complementary data on atmospheric transmission or the output of the laser for each pulse.

A computer program was written to analyze the digitized optical radar traces. The computational scheme is analogous to a graphical procedure that has been described in a note reporting preliminary observations of the stratospheric aerosol layer (Fiocco and Grams, 1964). The calculation, in effect, determines the radar constant of equation 4.2 by using observed optical radar returns to calibrate the apparatus. The calculation is initiated by computing the average vertical coordinates of a number of consecutive traces to eliminate statistical fluctuations of the signal. Ratios are then computed between the average optical radar return and the values calculated from the optical radar equation for an arbitrary radar constant and tabulated number densities of air molecules in the U.S. Standard Atmosphere, 1962. Then these ratios are normalized by dividing each ratio by the average ratio calculated for all altitudes greater than or equal to 25 km. The resulting numbers are taken to be the scattering ratio, called $\frac{\sigma}{\sigma_R}$ and interpreted as the ratio of observed to molecular radar cross-sections. By the normalizing procedure the average value of the scattering ratio for altitudes above 25 km is unity; the technique has therefore assumed that the contribution from

aerosols at altitudes above 25 km is negligible compared to the molecular returns. This assumption was based on the shape of a large number of profiles constructed during the preliminary analysis of the data; these profiles, obtained by the graphical technique, normally showed minimum ratios with appreciable scatter about a constant ratio for the entire region above 25 km and much larger scattering ratios at lower altitudes. The assumption is supported by the results of Rosenberg, Sandomirsky, and Poldmaa (1966). In principle, the use of the smallest calculated ratio for the normalizing procedure would be a better assumption; however the normalizing procedure would then be severely affected by the statistical fluctuations of the signal at the calibration altitude which, according to Fig. 10, are unacceptably large.

On occasion the procedure could produce scattering ratios less than unity at some altitude below 25 km. The signal below 25 km was considered to be sufficiently reliable for calibration purposes so that the scattering ratios for the lower regions should therefore be equal to or greater than one (the observed signal should be at least equal to that expected from a clear atmosphere). Therefore the computation scheme tested the scattering ratios calculated for the region below 25 km; if one or more of these ratios was less than one, they were recalculated with the normalizing procedure applied to the minimum ratio observed

in the lower regions (i. e., all the computed ratios are then divided by this minimum ratio to obtain the scattering ratio).

Fig. 11 has been constructed to show the effect of systematic fluctuations of the digitized signal. Curve a is an idealized optical radar echo and curve b is the expected molecular return associated with the echo; both curves are plotted on a logarithmic scale to fix their shape. The ratio between curve a and curve b is the scattering ratio $\frac{\sigma}{\sigma_R}$, plotted as curve c in the inset figure. Curves a⁺ and a⁻ have been constructed to qualitatively illustrate the effect of adding or subtracting, respectively, a systematic error equal to 50% of the expected return at 30 km; since the theoretical return at 30 km is about two orders of magnitude less than the 10 km return, this amounts to $\sim 0.5\%$ of the full-scale deflection of the recorded oscilloscope trace. Curves c⁺ and c⁻ in the inset figure show the $\frac{\sigma}{\sigma_R}$ profiles calculated from curves a⁺ and a⁻, respectively, according to the computational scheme that has been outlined. The systematic increase in the calculated return has slightly reduced the $\frac{\sigma}{\sigma_R}$ ratios in the 10-20 km latitude interval and has also created a false indication of enhanced dust concentrations at higher altitudes. The effect of a systematic decrease in the calculated return has created a larger scattering ratio in the lower stratosphere and has also provided a result indicating scattering ratios appreciably

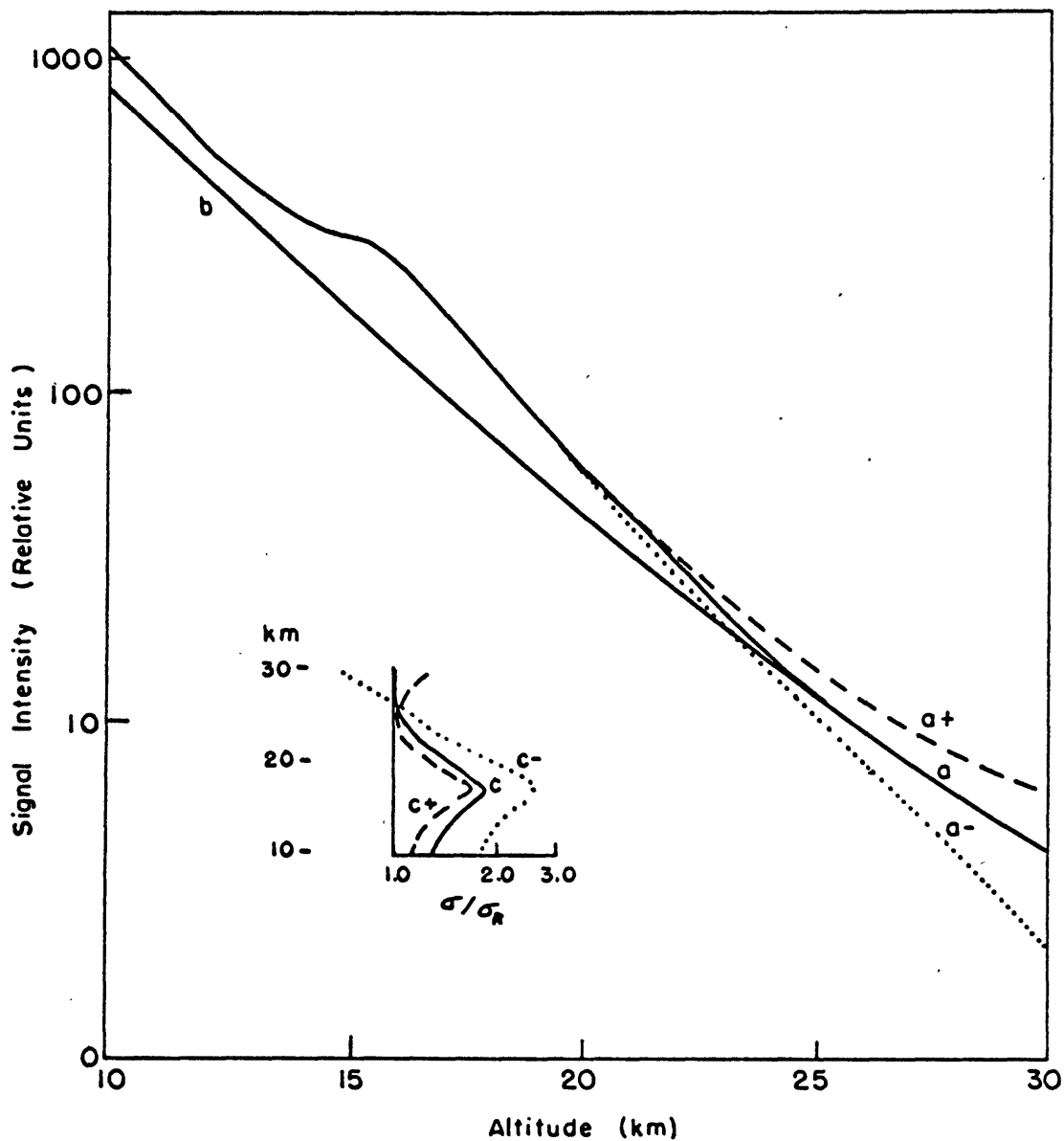


Fig. 11. Graphical description of the effect of a systematic fluctuation of the digitized optical radar signal. Curve a: idealized optical radar echo; curve b: theoretical return from a molecular atmosphere; curve c: scattering ratios σ/σ_R derived from curves a and b. Curves a⁺ and a⁻ illustrate the effect of adding or subtracting, respectively, a constant signal level from curve a; curves c⁺ and c⁻ are the consequent scattering ratio profiles.

less than one in the high altitude intervals, contrary to the definition of the scattering ratio. Although the observed signal fluctuations are considered to be random and such systematic effects should disappear when a sufficient number of traces are averaged together, systematic errors could arise by a parallax error in digitizing traces, the sky background on a moonlit night, or other equally realistic factors. Observed profiles, although showing nearly constant mixing ratios above 25 km on the average, often display the characteristic forms shown as curves c^+ and c^- . The calibration technique that has been previously described tends to reduce the numerical fluctuations of the calculated scattering ratios for lower altitudes that can be associated with systematic errors in the digitized signal.

In some of the early 1964 data, a transient response to overload of a photomultiplier preamplifier made it necessary to keep the synchronized rotating shutter on the receiver closed until the echoes were acceptably small. For this case the shutter frequently was still opening when the signal from the lower stratosphere was received and the observed data, therefore, required a shutter correction. This was accomplished by comparing the calculated scattering ratios at altitudes below 15 km with the average profile obtained for the entire study, excluding those profiles requiring the shutter correction. A linear regression formula was applied to this result to determine the shutter

opening rate to recover the portion of the profile affected by the shutter. It is not possible to estimate the uncertainty associated with the correction, but it is pointed out the use of the average profile to determine the shutter correction should cause the resulting scattering ratios to tend toward average values.

Another source of error lies in the use of a model molecular atmosphere for computing the expected optical radar echo. A cursory examination of temperature profiles for Bedford, Massachusetts (plotted, for example, on the ozonograms of Hering and Borden, 1965) indicates that density fluctuations at altitudes between 10 and 30 km seldom exceed 5% of the molecular density specified in the U.S. Standard Atmosphere, 1962. Variations in atmospheric density were therefore neglected to maintain the logistic simplicity of the observations and are recognized as a source of uncertainty. Also, it is not possible to estimate the error associated with the calibration procedure which assumes that the aerosol contribution to the optical radar signal at the calibration altitudes can be neglected. The assumption does introduce the possibility that the observed scattering ratios are higher; the technique may underestimate the dust content of the stratosphere.

5. OBSERVATIONS OF STRATOSPHERIC AEROSOLS

Optical radar observations of stratospheric aerosols were made during the time period from January 1964 to August 1965 on as many nights as acceptable viewing conditions and the existence of a properly functioning instrument would allow. Most of these observations were conducted at Lexington, Massachusetts (geographical coordinates $42^{\circ}25'N$, $71^{\circ}15'W$); data was also obtained at College, Alaska ($64^{\circ}53'N$, $148^{\circ}3'W$), simultaneously with studies of noctilucent clouds during the summer 1964 (Fiocco and Grams, 1966). This investigation has provided quantitative information on the vertical distribution of the particulate material in the altitude region from 10 to 30 km during the observation period.

The aerosol data is obtained from computed vertical profiles of a scattering ratio $\frac{\sigma}{\sigma_R}$ which is interpreted as the ratio between the observed radar cross-section σ of the atmospheric constituents to the radar cross-section σ_R of a model dust-free atmosphere. One of these profiles has been published previously (Fiocco and Grams, 1964) and is included as Fig. 12. This profile was obtained during a 16-minute period on 14 February 1964 at Lexington. Curve a is the observed optical radar return obtained by averaging the 20 consecutive traces recorded in the given time interval. The expected return from a dust-free atmosphere is plotted

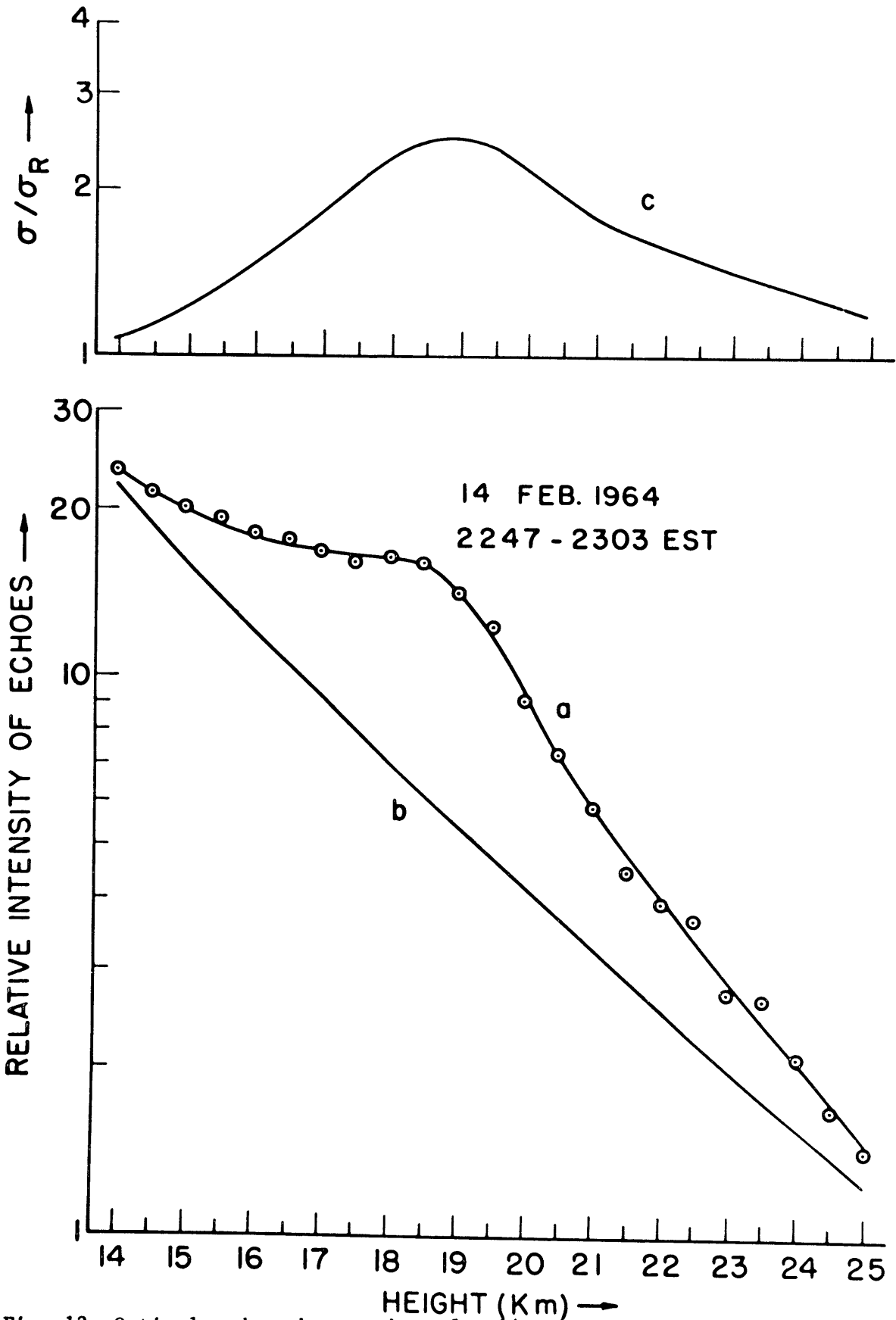


Fig. 12. Optical radar observations for 14 February 1964. Curve a: observed intensity of echoes from a vertically pointing optical radar. Curve b: expected intensity of echoes from a purely molecular atmosphere. Curve c: ratio of curve a to curve b, interpreted as the ratio of observed to molecular cross-sections.

as curve b. The scattering ratio σ/σ_r is curve c, the ratio between these two curves.

The scattering ratio did have a maximum near 20 km in agreement with the results of Junge et al and the broad-scale features of the profile were in agreement with profiles derived by other optical techniques (e.g., Volz and Goody, 1962; Bigg, 1964, Elterman and Campbell, 1964). The Mie scattering calculations presented in Section 3.3 had not yet been performed at the time that this preliminary result was published so it was not possible to comment on the particle concentrations inferred by the measurement. The scattering computations have since shown that at the altitude of the maximum scattering ratio the estimated particle concentration of Mie scatters with a refractive index of 1.5 is about 1 cm^{-3} for particles with radii greater than 0.275 micron. This was about an order of magnitude larger than the results of the particle collections of Junge and his collaborators although it agrees with the photoelectric particle counts obtained during the same year by Rosen (1964). The large increase in particle concentration can be attributed to the perturbed conditions existing after the eruption of the Mount Agung volcano.

The stratospheric dust layer exhibited appreciable fluctuations throughout the period of observation. Day-by-day variations, however, were not so pronounced and hourly variations seemed to exhibit little fluctuation other than those associated with the calibration procedure

used to evaluate the scatter ratio. Fig. 13 shows ten hourly profiles taken during a single night of observation on 11-12 March 1965. Each profile was obtained by digitizing 25 consecutive traces taken at two second intervals at the indicated observation times. The curves are lines connecting plotted values of the scattering ratio for 1/2 km altitude intervals.

The scattering ratios have been plotted on a logarithmic scale as a function of altitude. The shape of the profile is not affected by changing the radar constant since multiplication is graphically accomplished by adding a length that is proportional to the multiplier. All scattering ratios are therefore multiplied by the same constant when the curve is shifted in the horizontal direction, parallel to lines of constant altitude. This means that the shape of the curve is fixed by the semilogarithmic representation, although the exact location of the curve on the logarithmic scale is subject to the calibration uncertainty.

The parameter

$$b = \frac{\sigma}{\sigma_R} - 1 \quad (5.1)$$

may be thought of as an "aerosol mixing ratio" if the size distribution of the aerosols is independent of altitude since it defines a number that is proportional to the aerosol component of the optical radar return measured

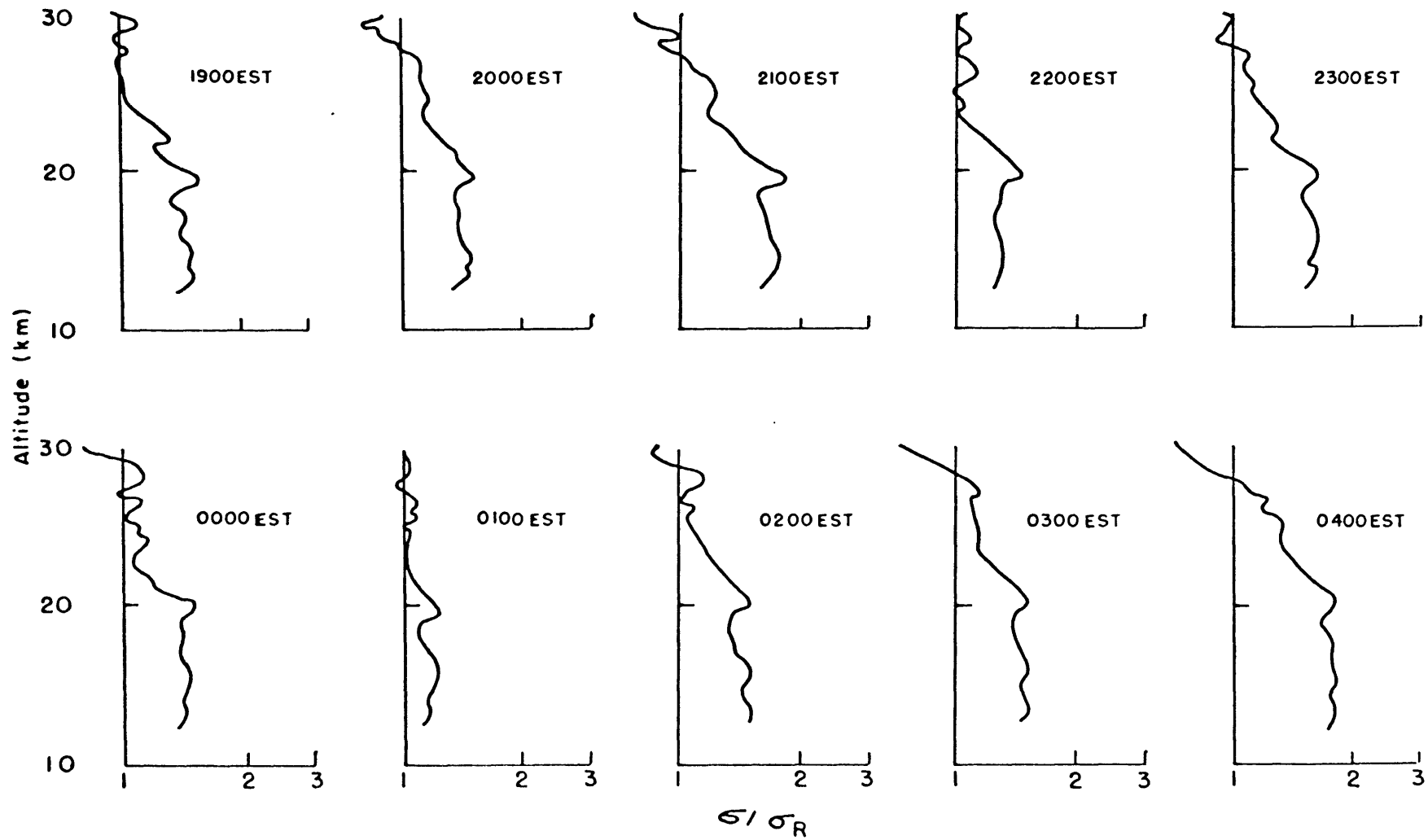


Fig. 13. Ten consecutive hourly profiles obtained on 11-12 March 1965 showing scattering ratios σ/σ_R for 1/2 km altitude intervals at the indicated observation times.

relative to molecular concentrations. This parameter is equal to one when the aerosol component of the optical radar echo is equal to the molecular return ($\sigma/\sigma_R = 2$). Thus concentration profiles may be obtained by multiplying the observed aerosol mixing ratio b by the number density of air molecules at each altitude and an appropriate factor. In effect, this has been done for $b=1$ in Fig. 6; number concentrations may therefore be obtained by multiplying the values of N_D given by the diagram with observed values of the aerosol mixing ratio b at each altitude. These concentrations represent approximately one-half of the total concentration of dust particles if the size distribution found by Friend (Feely et al, 1963) adequately described the size distribution function throughout the period of observation.

The most noticeable feature of the observed scattering ratios is a prominent local maximum near 19 km altitude with a relatively constant mixing ratio at lower altitudes which tends to peak at about 16 km. The general features of the vertical distribution of dust did not exhibit any systematic changes during the entire night of observation. Numerical fluctuations are evident from one profile to the next, but these are associated with statistical fluctuations of the echoes received from the calibration altitudes. Indeed, the observed rms fluctuation of the scattering ratio at 16 km was $\sim 12\%$ as expected from the results summarized

in Fig. 10.

These hourly profiles and many other sequential profiles separated by time intervals as short as one minute consistently show little qualitative change from one profile to the next for those altitudes where statistical fluctuations of the optical radar echoes are small. The rms fluctuation of the photoelectron flux for 1/2 km range intervals when 25 consecutive radar return is, according to Fig. 10, less than 10% of the observed signal below ~ 20 km and, indeed, the profiles shown in Fig. 13 are quite similar, even with one hour time differences, below this altitude. However, considerable variability is observed at higher altitudes; these variations are attributed only to statistical fluctuations of the signal and are not used to derive a complicated wave structure for thin aerosol layers at these altitudes as inferred by Collis and Ligda (1966) from optical radar measurements with an apparatus having comparable sensitivity.

A graphical summary of all the data that have been analyzed for the stratospheric aerosol study is presented in Figs. 14, 15, and 16. Again, the scattering ratio has been plotted as a function of altitude on a semi-logarithmic display to preserve the shape of the curve. The curves show lines connecting plotted values of the scattering ratio averaged over 1 km altitude intervals for the indicated time periods. Each profile is identified by the date and time that the observation was performed

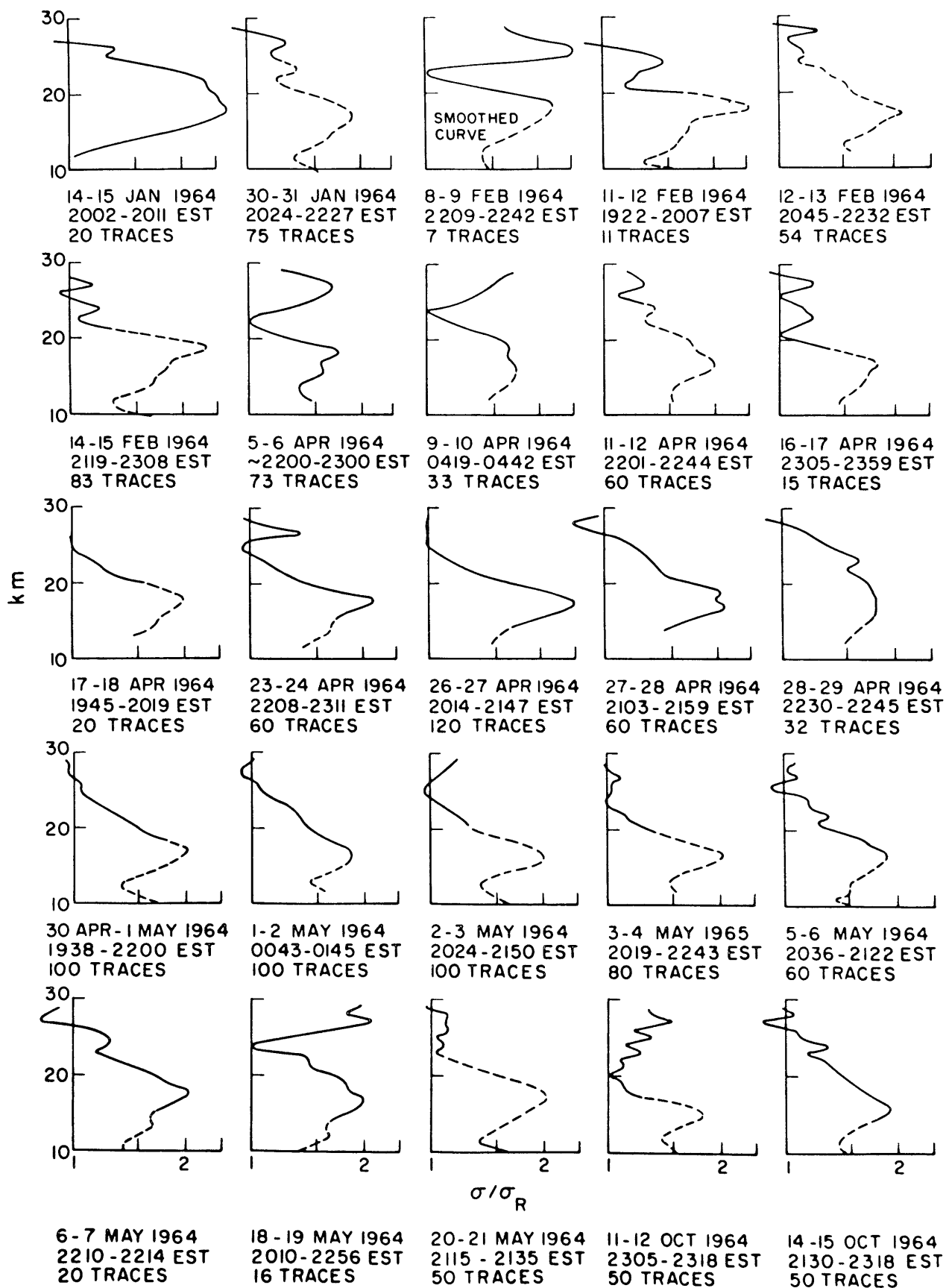


Fig. 14. Graphical summary of optical radar data showing nightly average scattering ratios σ/σ_R for 1 km intervals in the lower stratosphere. Part 1.

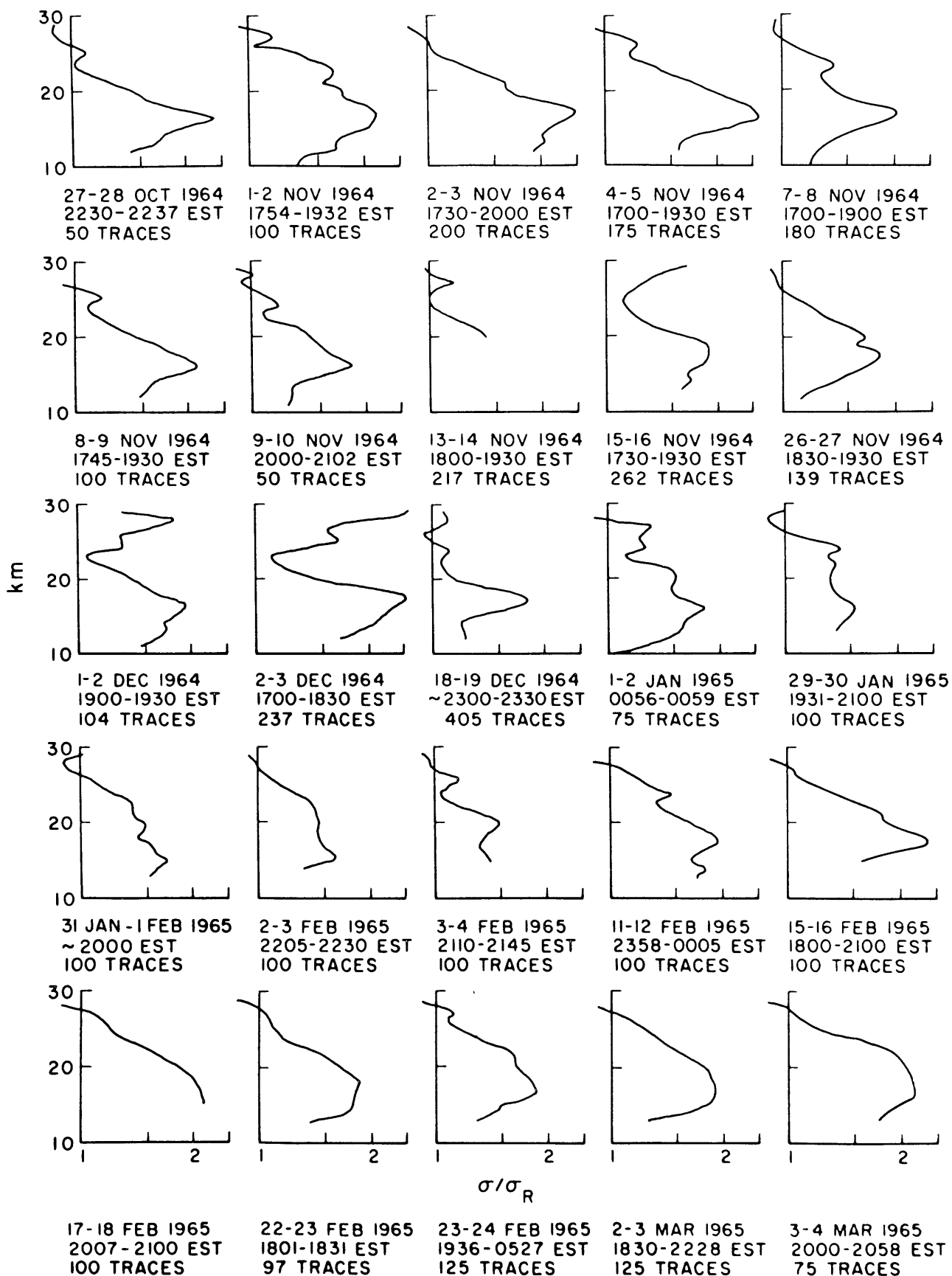


Fig. 15. Graphical summary of optical radar data. Part 2.

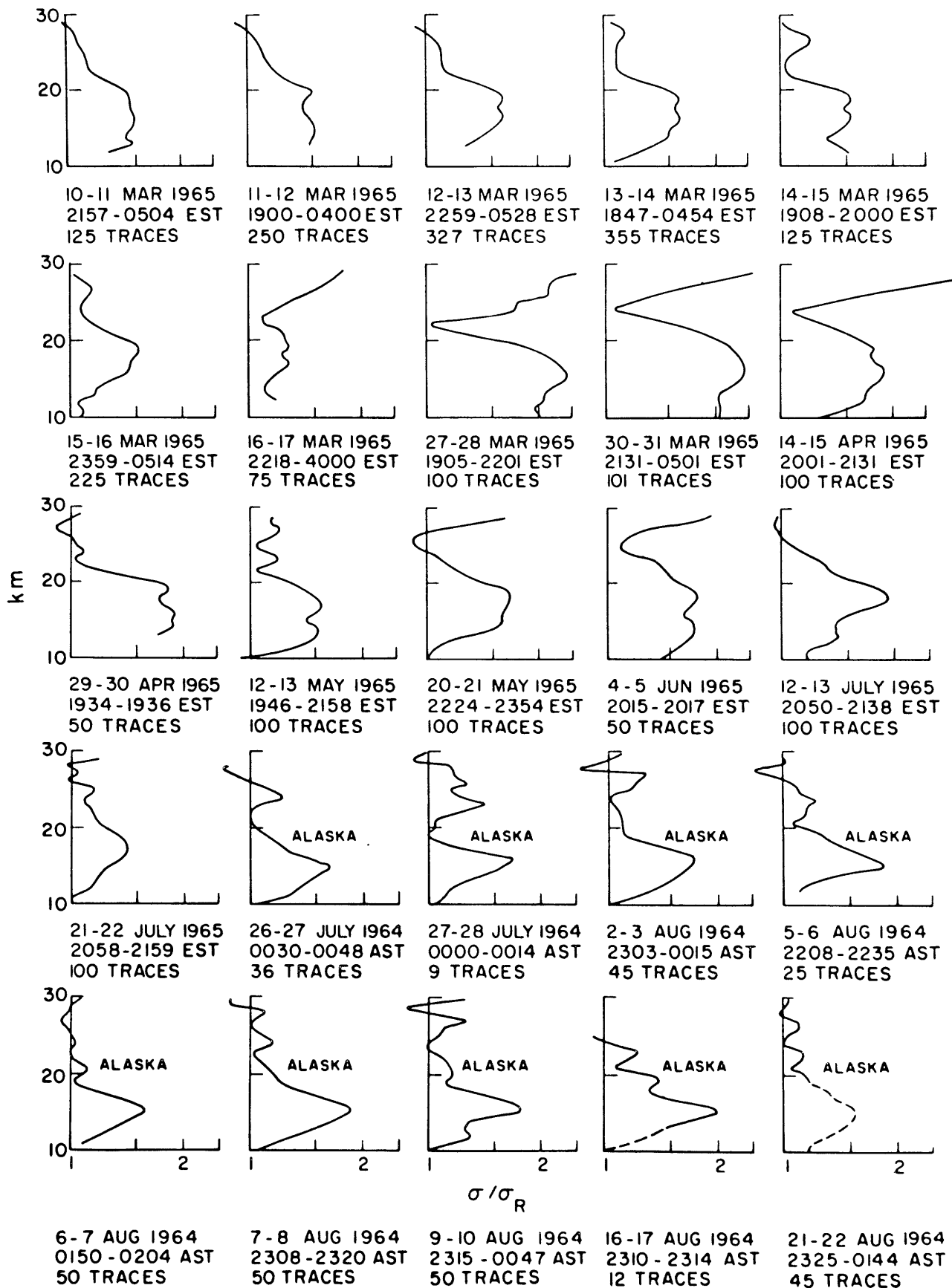


Fig. 16. Graphical summary of optical radar data. Part 3.

and the number of traces that were digitized to derive the profile. Numerical values of the nightly average scattering ratios are tabulated in the appendix.

Error bars have not been drawn for the profiles presented in the graphical summary; estimates of the expected root-mean-square fluctuation of the optical radar echoes, expressed as a percent deviation from the mean optical radar return at each altitude, have been shown in Fig. 10 as a function of the number of traces used to derive a dust profile. Some of the earlier data were obtained from a small number of traces when the instrument was in a developmental stage and subject to failures which could halt the observations if the malfunction could not be repaired at the observation site. Even though these traces are subject to some statistical fluctuation, the resulting profiles are treated as the best estimate of the stratospheric dust content for the night of observation and are given equal weight in all the calculations that have been performed using the quantitative data derived during the stratospheric aerosol study.

The lowest portion of about 20 of the profiles obtained in the first part of the study is drawn as a dashed line in the data summary. The dashed lines represent scattering ratios recovered from early data for which the shutter in the photodetection system was still opening while echoes were being received from the shorter ranges; these profiles

incorporate the shutter correction previously described.

The aerosol layer is prominently displayed as a maximum in the aerosol mixing ratio that was always observed in the lower stratosphere between 10 and 20 km altitude. The observed return from the aerosol layer was approximately 1.9 times the expected return from the model molecular atmosphere; the daily rms fluctuation of the scattering ratio was found to be approximately 0.3, showing variations of $\sim 30\%$ for the aerosol mixing ratio.

The profiles derived for the summertime polar stratosphere in 1964 are also included in the data summary. Slightly smaller dust amounts were observed at the College, Alaska observation site; an average scattering ratio of about 1.7 with rms fluctuations ~ 0.15 were observed at the altitude of the maximum scattering ratio. The aerosol layer was located at slightly lower altitudes than at Lexington; this is in accordance with other observations (Manson and Junge, 1961; Rossler, 1963; Clemesha, Kent, and Wright, 1966) which indicate that the height of the aerosol layer approximately follows latitudinal changes in the tropopause height.

Rosen (1964) compared the particle concentrations at the concentration maximum of the aerosol layer with particle concentrations at 85 km altitude obtained from rocket soundings (Hemenway and Soberman, 1962) and infers a constant dust mixing ratio to at least 85 km. He concludes that the source must lie at least above 85 km and that the

particles are probably of extraterrestrial origin. However in view of the composition of the particles (Friend et al, 1961; Junge et al, 1961) and the omnipresent minimum scattering ratio above 20 km observed in this study, it appears that the particles may be formed within the layer as suggested by Junge et al or, at least, can be associated with the spatial distribution of the debris injected into the stratosphere by the eruption of the Mount Agung volcano.

The stratospheric aerosol data obtained in this study were compared on a day-to-day basis with tropopause heights. Radiosonde observations are not obtained routinely in the Boston area; tropopause data were obtained from microfilm records of Northern Hemisphere Data Tabulations for Nantucket Island in Massachusetts (about 41°N , 70°W). The center of mass of the aerosols between 12 and 24 km was calculated from the optical radar measurements and compared with the tropopause height observed at Nantucket on all days for which nearly simultaneous observations existed during the time period from January 1964 to February 1965. Fig. 17 summarizes these results; a scatter diagram has been constructed with the center of mass of the aerosol layer as the ordinate and the corresponding tropopause height at the radiosonde station as the abscissa. Points plotted as open circles on this diagram and all subsequent diagrams refer to dust observations that incorporate a shutter correction. No pronounced trend is evident although the regression line

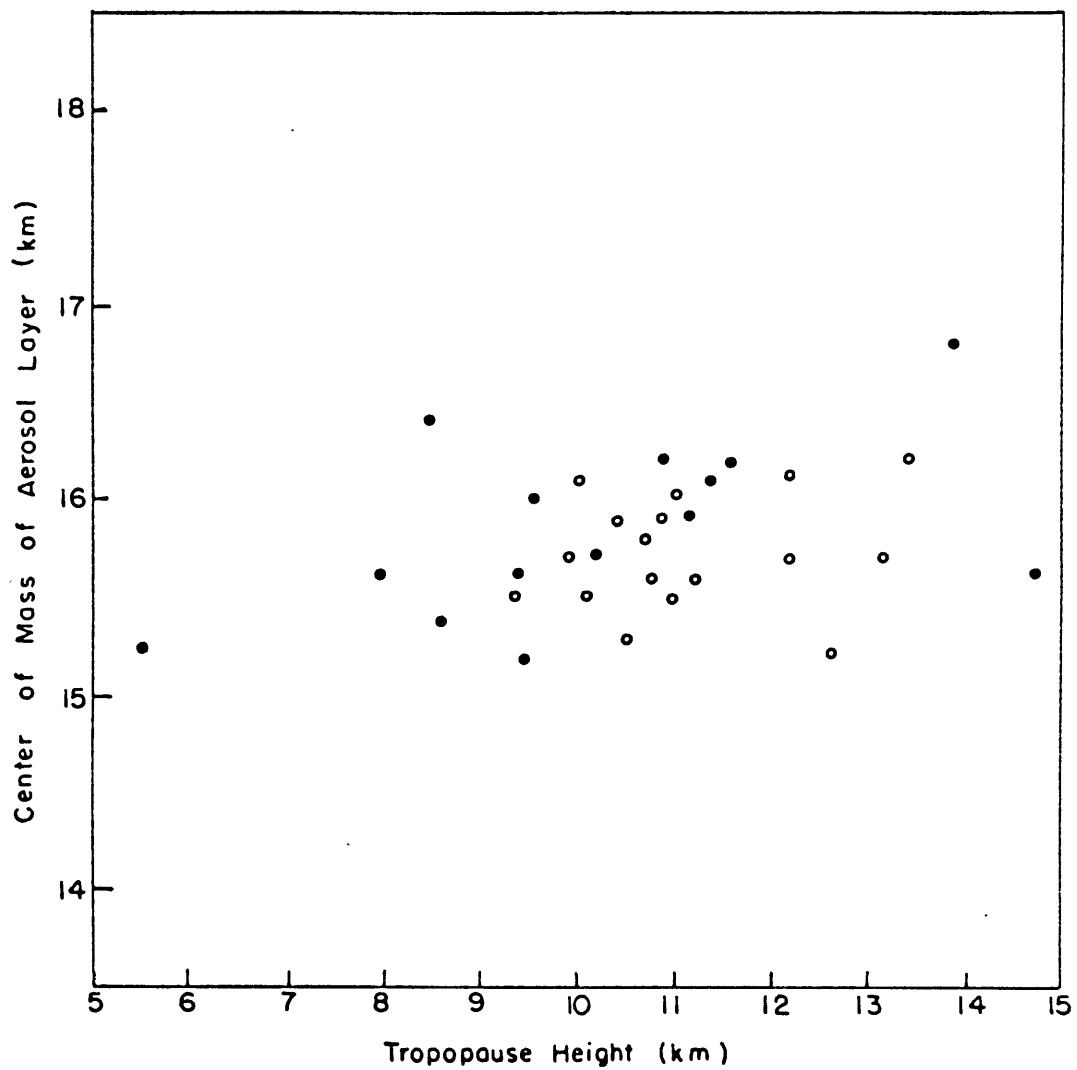


Fig. 17. Relation between the height of the center of mass of the aerosol layer and the height of the tropopause.

drawn through the points on the scatter diagram has a slope of approximately +0.1, indicating that changes in the tropopause height can have a small effect on the distribution of mass in the aerosol layer. Fig. 1, from Manson and Junge (1961), also does not exhibit pronounced changes in the vertical distribution of aerosols following daily changes in the height of the tropopause.

According to Fig. 17 the center of mass of the aerosol layer was usually located near 16 km. Fig. 18 has been constructed to indicate day-to-day fluctuations of dust amounts at 16 km as a function of time. The time scale shown at the bottom of the figure includes a date index used for various computations as well as the date of the observation. The data collection was interrupted from mid-February 1964 until the first week of April 1964 when repairs to the laser were required. Another break in the collection of data at Lexington occurred in summer 1964 when optical radar observations of noctilucent clouds were performed; data for the summertime high-altitude stratosphere were, however, obtained during this time period.

The observed scattering ratios exhibited an appreciable amount of scatter without pronounced seasonal trends (see Fig. 22, page 82, showing daily variations of atmospheric ozone measured at Bedford, Massachusetts during the same time period). Several features of the daily fluctuations deserve comment. A high dust content was indicated for the

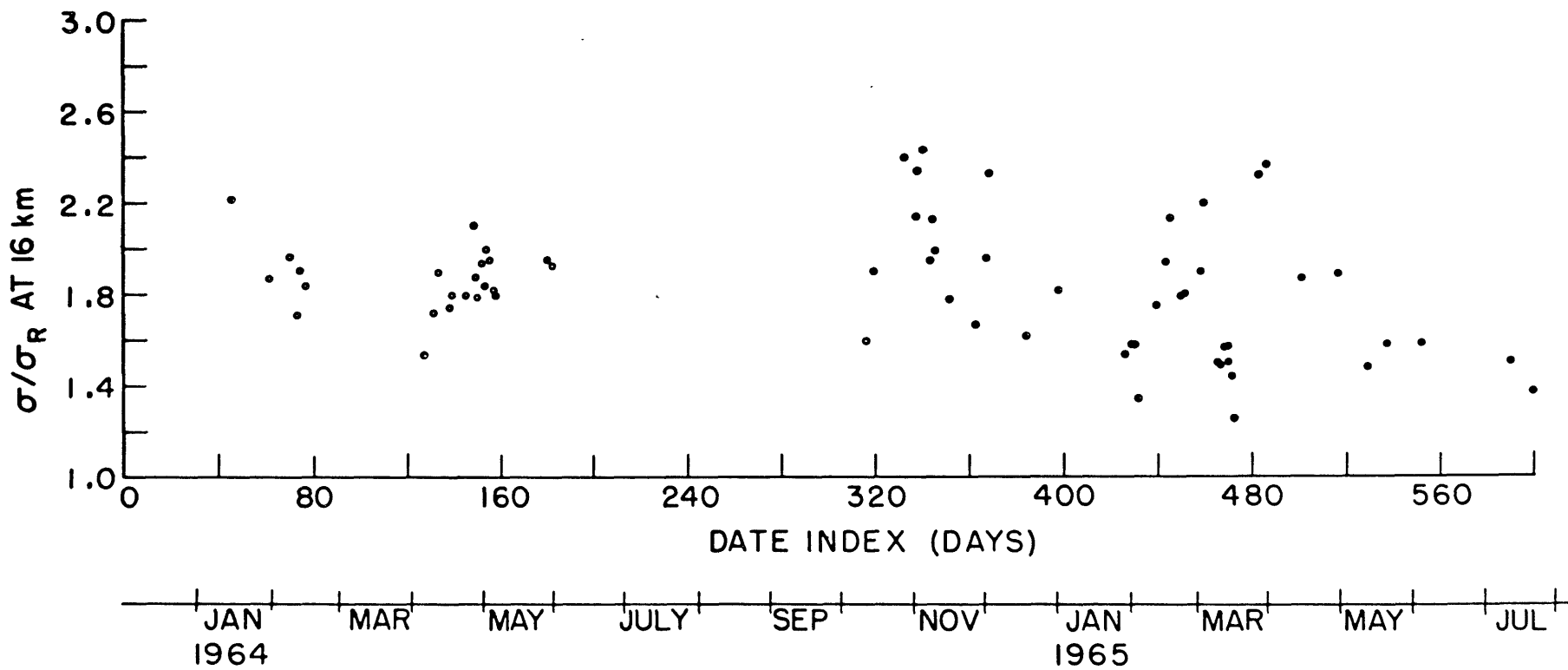


Fig. 18. Daily variation of the observed scattering ratio σ/σ_R at 16 km altitude during the optical radar study.

first observation with the apparatus on 14-15 January 1964; this high aerosol concentration, followed by decreased amounts during spring 1964, follows the same trend as the twilight observations of Volz (1965) during the same time period. Fall 1964 was also a period of high aerosol concentration with decreasing dust amounts indicated during early winter 1964/65. Except for a short period of low dust amounts during mid-March 1965, the aerosol concentration increased again during spring 1965. A subsequent decrease during summer 1965 suggests that the stratospheric aerosol layer may be returning to normal conditions. Low dust amounts during summer 1965 have also been found by Volz (1965) and are corroborated by other investigations such as studies of the small-ion density in the stratosphere (Paltridge, 1966). The considerable length of time required for the turbidity of the stratosphere to return to normal conditions is comparable to the classic and well-documented Krakatoa eruption in 1883 (see, for example, Wexler, 1951).

In view of the enhanced dust amounts resulting from the Mount Agung eruption in the Southern Hemisphere, a latitudinal gradient in dust concentration may exist, with smaller amounts of dust in the high latitudes and larger amounts in tropical regions. Indeed, some evidence in this respect has been observed by the results of optical radar measurements. The data collected in mid-latitudes

at Lexington, Massachusetts exhibited a scattering ratio ~ 1.9 while the observations performed at high latitudes at College, Alaska showed slightly less dust amounts with a maximum ratio ~ 1.7 . A single profile obtained in Kingston, Jamaica (about $18^{\circ}\text{N}, 77^{\circ}\text{W}$) with a similar apparatus (Clemesha, Kent, and Wright, 1966) shows a maximum scattering ratio of ~ 2.1 between 20 and 25 km. With an rms fluctuation of about 0.3 for the scattering ratio observed at the Lexington site this difference is not large, although it shows the expected trend with latitude.

With a latitudinal gradient in dust amounts the effects of horizontal advection by stratospheric air motions should be evidenced by higher dust amounts associated with air originating in low latitudes than for air from high latitude regions. An attempt was made to verify such a relation for the dust measurements by comparing dust concentrations with wind data at 100 mb from the Northern Hemisphere Data Tabulations for the radiosonde station at Nantucket Island. Fig. 19 shows a scatter diagram displaying the observed relation between dust amounts at 16 km and the northward component of the wind at 100 mb; Fig. 20 shows dust amounts at 16 km and the wind direction at 100 mb. The dust and wind data do not show the expected effect; the plotted points exhibit an appreciable amount of scatter, and contrary to the predicted relation, even suggest that northerly winds may be associated with higher dust amounts than southerly

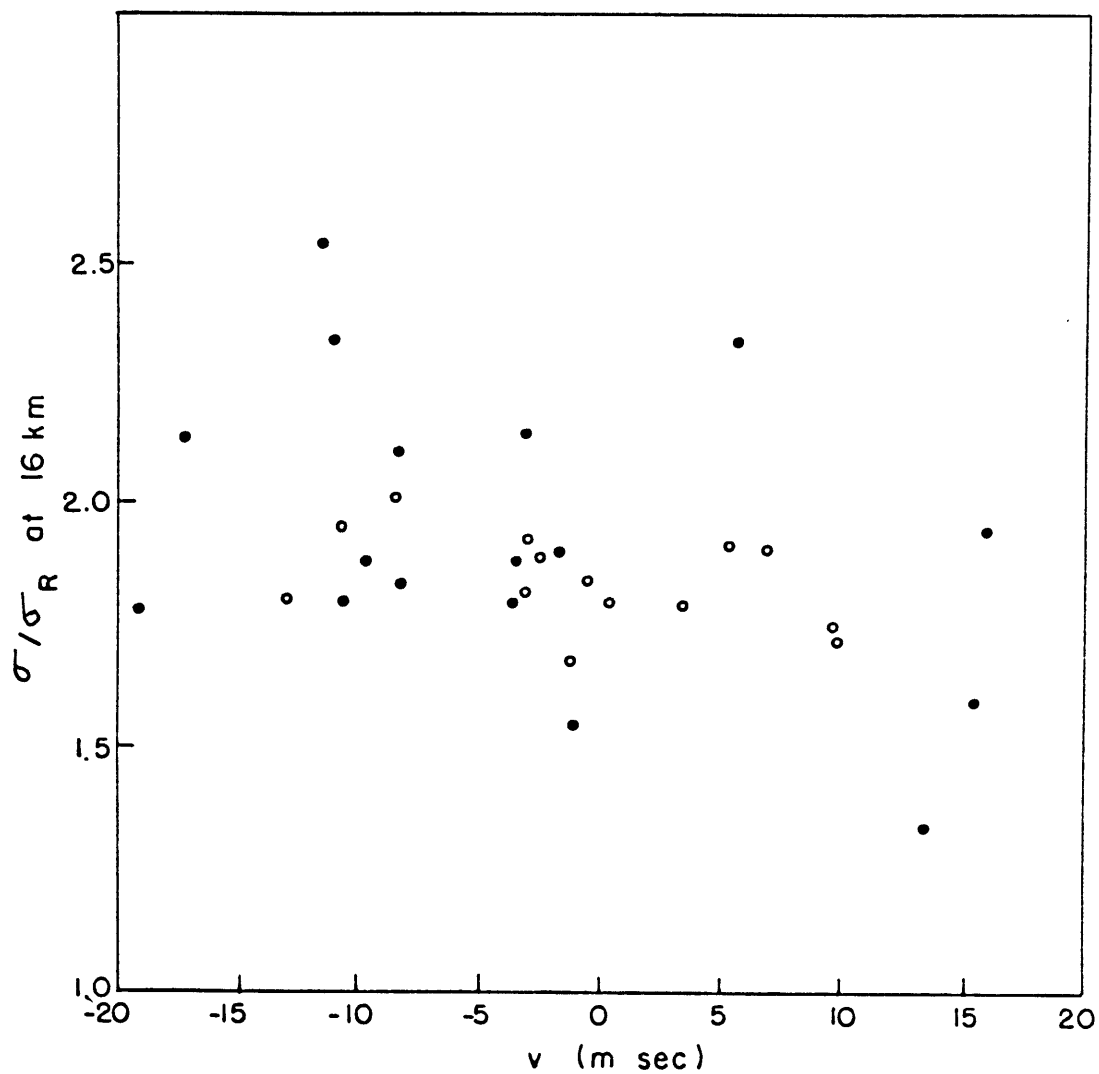


Fig. 19. Relation between the observed scattering ratio σ/σ_R at 16 km altitude and the northward component of wind velocity at 100 mb.

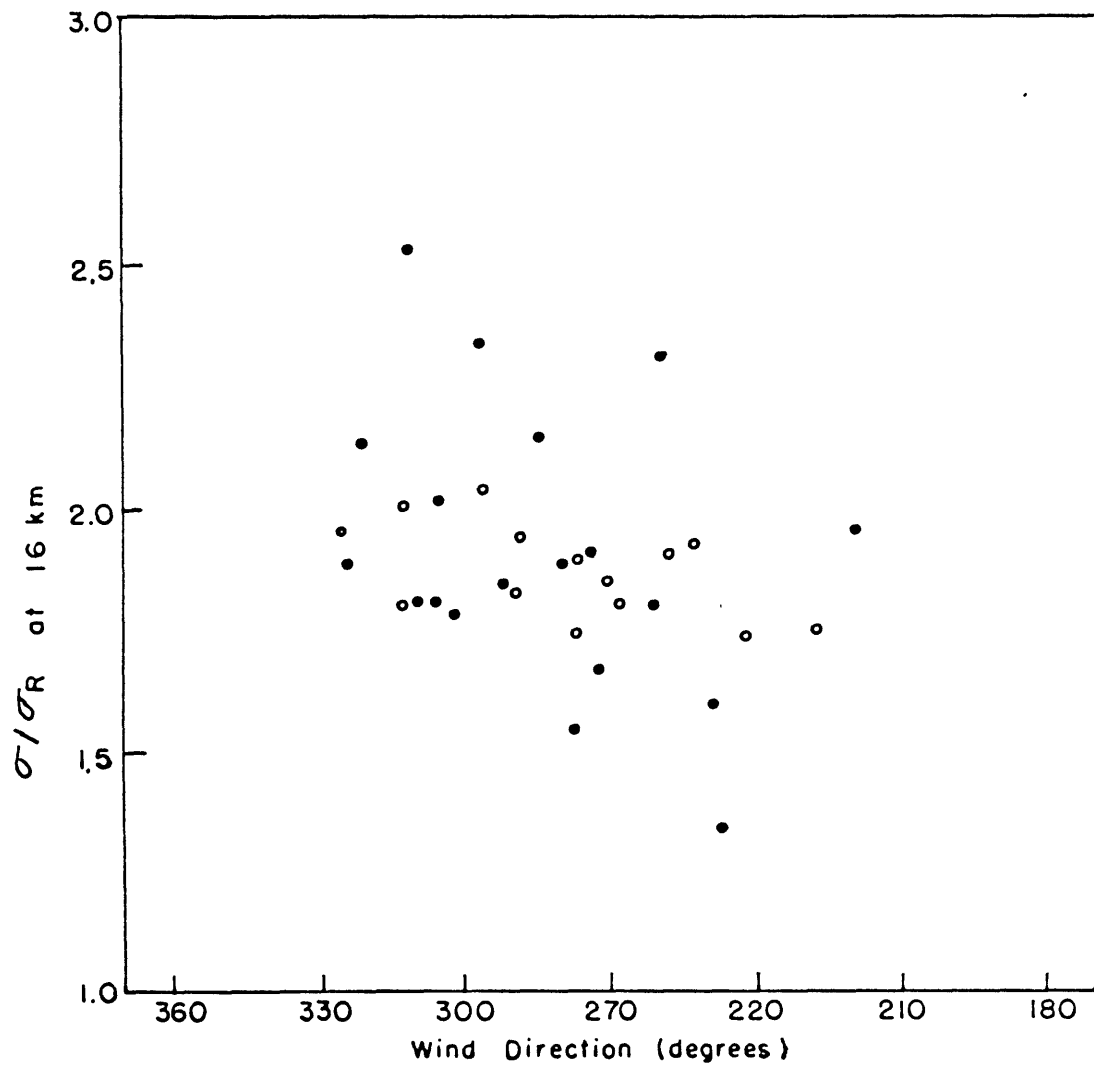


Fig. 20. Relation between the observed scattering ratio σ/σ_R at 16 km altitude and the wind direction at 100 mb.

winds. This would not rule out the possibility of advective effects, however, since the observed wind direction does not necessarily indicate the origin of the air and different results might be obtained by constructing trajectories.

Various statistical calculations have been performed with the dust data. Using the 1 km average scattering ratios that were plotted in the graphical summary of the data, autocorrelation coefficients were calculated at each altitude for lags up to 30 days from the irregularly spaced dust observations which fit each lag category; with 66 different profiles available for the statistical calculations, ~ 15 data pairs could be assembled for each lag category. Autocorrelation functions for dust measurements at 15, 16, and 17 km are shown in Fig. 21. All curves are plotted together to illustrate the statistical fluctuation of the correlation coefficients that is expected for small samples. The correlogram shows large values of the autocorrelation coefficients for lags up to six days before falling to smaller values. Unfortunately, the autocorrelation function has been calculated from a non-homogeneous sample in which the number of data pairs decreases as the time lag increases so that the statistical reliability of the correlations decreases for the larger lags. The form of the autocorrelation function that has been calculated may suggest the presence of a periodicity of approximately one month. Such a

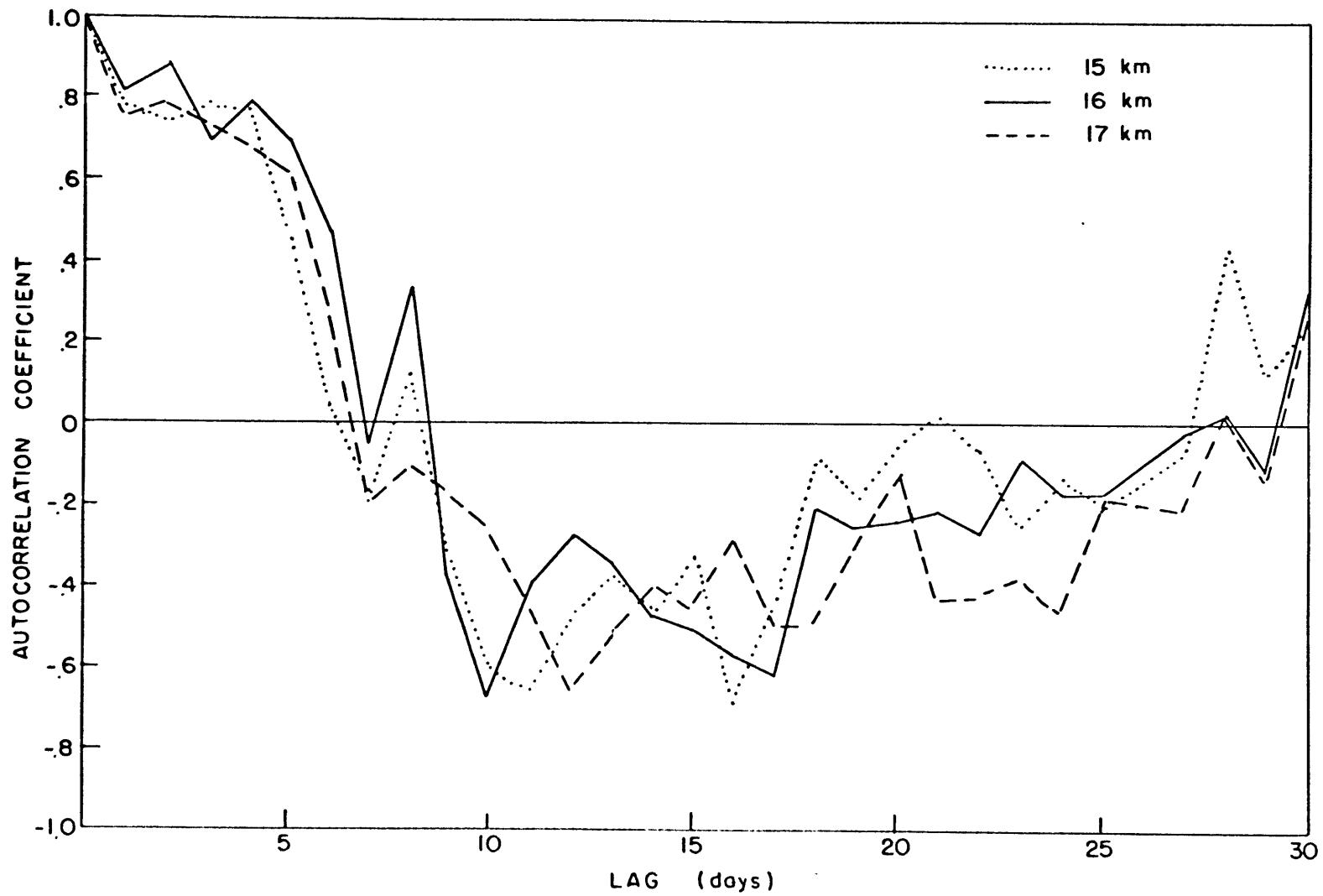


Fig. 21. Autocorrelation coefficients for dust observations near the center of mass of the aerosol layer.

periodicity is interesting, especially since Bigg and Miles (1964) have observed a lunar influence on ice nuclei concentrations measured at a network of surface stations in Australia. However, the statistical uncertainty associated with the autocorrelation coefficients computed for large lags does not allow a definite conclusion to be drawn and additional research is required.

The stratospheric dust layer has also been compared with atmospheric ozone. Most of the variations of atmospheric ozone are associated with changes in the ozone content of the lower stratosphere, where maximum concentrations are observed. The most common parameter for describing the ozone content of the atmosphere is the total amount of ozone in a vertical column above the earth's surface. This quantity is usually expressed as the height of an equivalent column of ozone reduced to standard temperature and pressure; observed values are only about 0.15 to 0.5 cm at STP. This small amount of ozone first attracted attention in the early part of this century when it was discovered that the cut-off in the solar spectrum for wavelengths less than about 0.3μ was due to the presence of ozone in the atmosphere. This trace gas has since been found to have great geophysical importance, and ozone is now perhaps the most extensively studied minor constituent of the atmosphere. It is formed photochemically at altitudes above 25 to 30 km and is transported to lower regions by mixing processes. Ozone is generally

considered to be a photochemically quasi-conservative property in the lower stratosphere and has frequently been used as a tracer to indicate atmospheric motion. Various aspects of ozone research including the photochemistry of the ozone layer, methods of measuring atmospheric ozone, and the meteorological processes that affect ozone have been reviewed by various authors (see, for example, Craig, 1965; Vassey, 1965).

The basic method for determining the total amount of ozone in a vertical column compares the flux of solar radiation at different wavelengths in a spectral region where solar energy is absorbed by ozone but still reaches the surface of the earth with sufficient intensity to be detected by a spectrophotometer. Details of the standard ozone spectrophotometer and the technique used to obtain the total ozone measurement are given by Dobson (1957). The temporal and spatial distribution of total ozone has been studied for several decades. Although daily fluctuations of total ozone often exceed seasonal changes, the climatological data obtained by averaging large numbers of observations show a maximum ozone amount in spring and a minimum in fall, with the largest seasonal fluctuations observed at high latitudes; Fig. 22 shows daily total ozone amounts measured at Bedford, Massachusetts (near Lexington) which are obtained routinely as part of a global network of ozone observations.

Many methods of observing the vertical distribution of

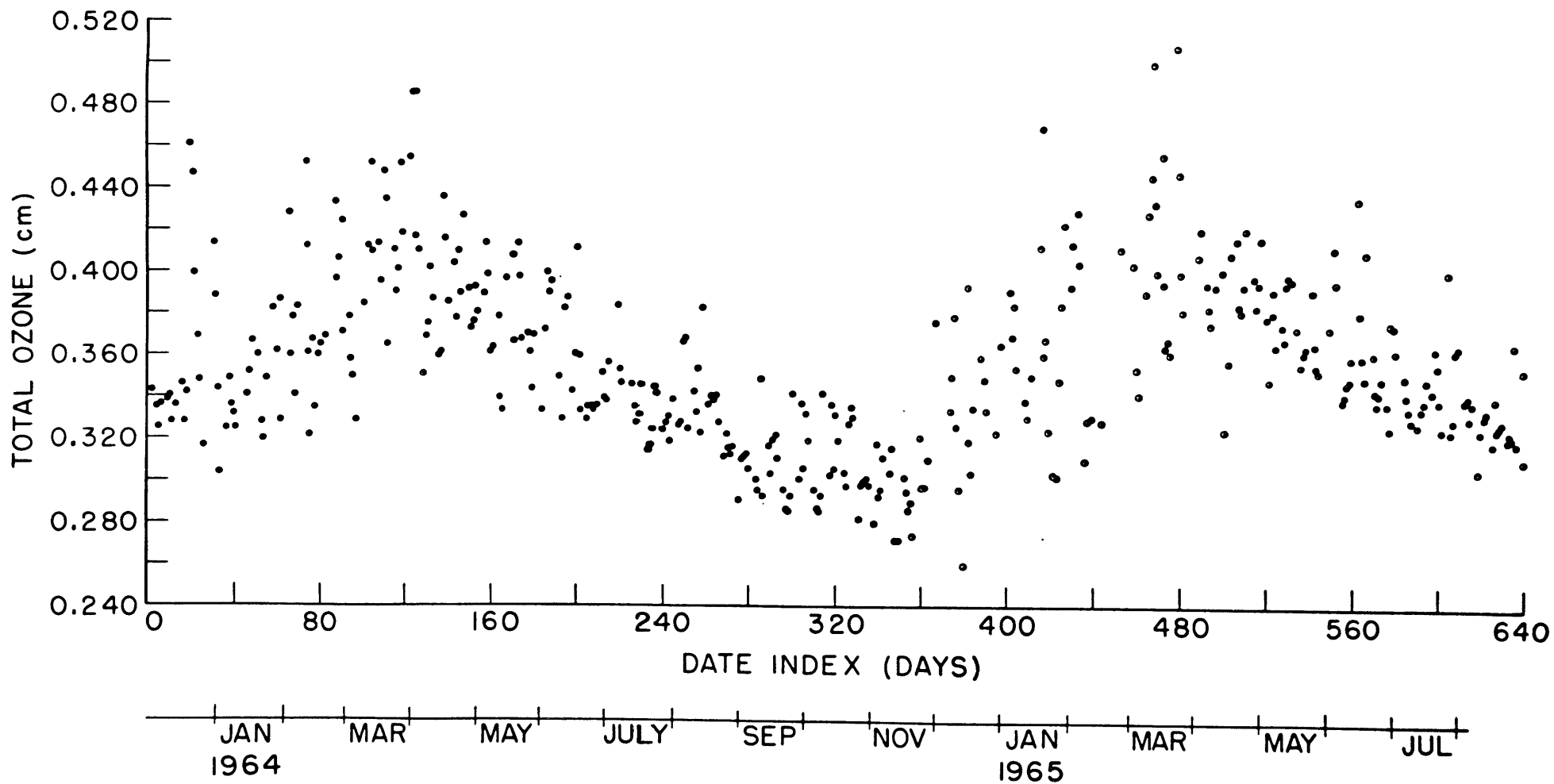


Fig. 22. Daily variation of the total amount of ozone in a vertical atmospheric column reduced to standard temperature and pressure.

ozone are available (Craig, 1965). Systematic observations of the vertical ozone distributions have been performed at a network of North American Stations since January 1963 in a program organized by the Air Force Cambridge Research Laboratories (Hering, 1964; Hering and Borden, 1964, 1965a). A chemiluminescent device designed by Regener (1964) was used in the ozonesonde network. The balloon-borne instrument provides detailed profiles of the vertical distribution of ozone; absolute calibration of the apparatus relies on a surface measurement of the total ozone with the Dobson spectrophotometer. An analysis of the errors involved in the ozonesonde measurements has been presented by Hering and Dütsch (1965).

Ozone and dust amounts were correlated using dust profiles derived from the optical radar observations and ozone data supplied by W. Hering and T. Borden. This included vertical ozone profiles obtained at Bedford, Massachusetts as part of the regular ozonesonde program, as well as more numerous complementary data on the total ozone amounts measured daily at Bedford. Dust and ozone profiles were expressed in terms of their average concentration in 1 km altitude intervals in the lower stratosphere, and correlation coefficients were then calculated for each altitude interval. The results are given in Fig. 23 which shows the correlation between dust and ozone for altitudes from 12 to 24 km for several different time lags between their respective

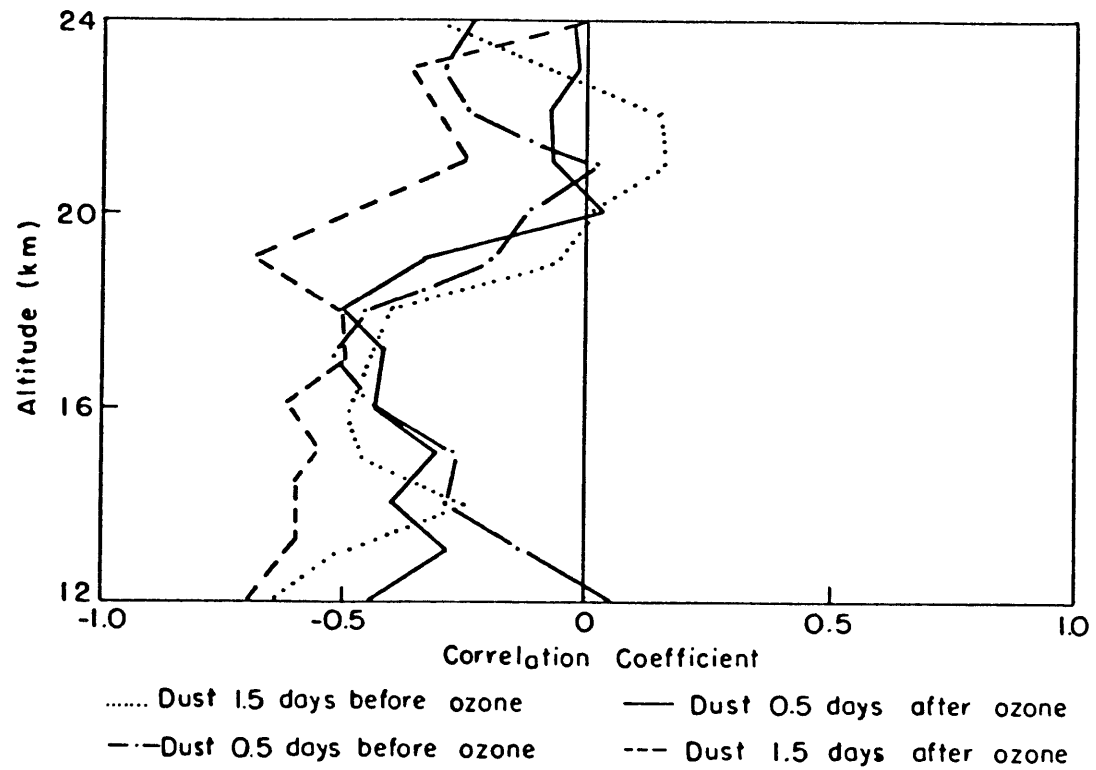


Fig. 23. Correlation coefficients for measurements of the ozone and dust content of the lower stratosphere as a function of altitude for several different time lags between the observations.

measurements. The ozone profiles used for the calculation were obtained according to a predetermined schedule which provides weekly observations of the vertical distribution of ozone and some additional observations made in situations having special meteorological interest. The observation dates for dust and ozone did not always coincide since the attempt to correlate the two parameters was not initiated until fall 1964, when the stratospheric aerosol study was well underway. Furthermore, the optical radar observations are dependent on tropospheric cloud conditions, and observations with the apparatus could not always be performed at times near the scheduled ozone soundings. Nevertheless, approximately 15 to 20 pairs of ozone and dust profiles could be assembled for various time lags using the 66 dust observations obtained during the study and the available ozone profiles. Simultaneous data did not exist; optical radar observations were performed at night, typically near 2100 EST, while the ozone observations were usually scheduled at 0700 EST. Thus, the observations were normally obtained about 1/2 day apart. The correlation coefficients displayed in Fig. 23 are cross-correlations between ozone and dust with dust measured approximately 1/2 and 1 1/2 days before and after the ozone observation. The correlation coefficients for altitudes near the center of mass of the aerosol layer are all negative, having values of approximately -0.5 for the lag categories shown in the diagram. When small samples are compared

it is possible to obtain a high correlation coefficient by chance; the correlations were extended to 30 days lag in order to establish a frequency distribution of correlation coefficients for presumably uncorrelated data. The observed coefficients of approximately -0.5 at altitudes near the center of mass of the aerosol layer are thereby found to be ~ 1.9 standard deviations from the mean value of the correlation coefficient at large lags; the probability of exceeding 1.9 standard deviations is about 6% for a normal distribution. Thus a significant anticorrelation between dust and ozone is obtained in the region where maximum dust amounts were observed during the optical radar study.

Most changes in total ozone are highly correlated with changes in the ozone content of the lower stratosphere. Mateer and Godson (1960) found, for example, a correlation coefficient of $+0.97$ for total ozone and the ozone in the 12 to 24 km altitude interval for a Canadian station. Hering and Borden (1965b) have correlated ozone concentrations obtained from the ozonesonde network with total ozone; the highest correlation coefficients were usually obtained at altitudes between 8 and 20 km.

The aerosol data have also been correlated with the measurements of total ozone obtained at Bedford, Massachusetts to provide additional statistical evidence of a relation between the aerosol layer and stratospheric ozone, on the assumption that the changes in the total ozone amounts were

indeed indicative of corresponding changes in stratospheric ozone. Since total ozone observations are performed on a daily rather than a weekly basis, a larger number of data pairs would be expected and the statistical significance of the results would be increased. The results are summarized in Fig. 24, which shows isopleths of constant correlation coefficients displayed as a function of the altitude of the dust measurement and the lag, in days, between the dust and total ozone observations. Again, simultaneous observations were not obtained. The total ozone measurements were taken near 1200 EST and, as it has been previously pointed out, the dust observations were performed at night. The calculations show a very high anticorrelation between total ozone and the dust at 16 km (the center of mass of the dust layer) which falls off rapidly with increasing lag. The computed correlation is -0.70 which exceeds the mean correlation coefficient at large lags by almost 4 standard deviations. This result verifies the relationship between stratospheric dust and ozone during the study.

Fig. 25 is a scatter diagram showing observed values of $\frac{\sigma}{\sigma_z}$ at 16 km and total ozone for data pairs with dust measured the night after ozone ($\sim 1/3$ day lag); if ozone data were missing for that lag category, the ozone observation obtained the day after the dust measurement (dust $\sim 2/3$ day before ozone) has been used in the diagram. Total ozone has been plotted as the ordinate and the dust parameter as

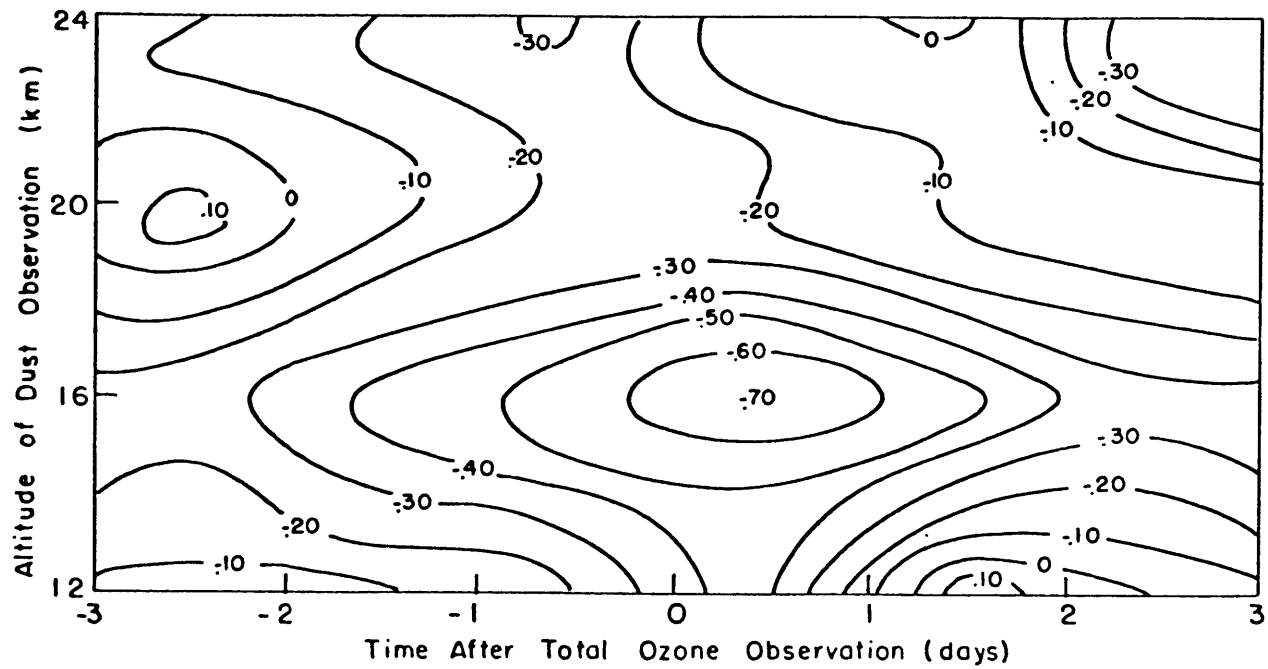


Fig. 24. Correlation coefficients for total ozone measurements and the dust content of the lower stratosphere as a function of the time lag between the observations and the altitude of the dust measurements.

the abscissa in the display; data pairs in which the dust parameter has a shutter correction are again plotted as open circles. The negative correlation is quite evident in the figure, with the largest dust amounts associated with low ozone values and maximum ozone amounts observed only when dust concentrations are low.

It has been pointed out in reference to Fig. 18 that high dust amounts were observed in fall 1964 and some low values were obtained in spring 1964 and 1965. Since the total ozone measurement always exhibits characteristically high values in spring and low values in fall, it was considered necessary to recalculate the correlation coefficients using ozone data with the well known seasonal variation of ozone removed to eliminate the possibility that the correlation was fortuitously obtained by the incursion of large amounts of dust from the Southern Hemisphere during seasons having minimum ozone content and subsequent decreasing trends of dust concentration during seasons with increased ozone amounts. Thirty-day running means were, therefore, subtracted from the observed total ozone amounts to eliminate seasonal variations of ozone. The correlation coefficients calculated for this case are shown in Fig. 26 in the same format as Fig. 24. As would be expected with regard to the seasonal effects that have been described, the magnitudes of the correlation coefficients have been reduced. However, the dust amounts at altitudes near the

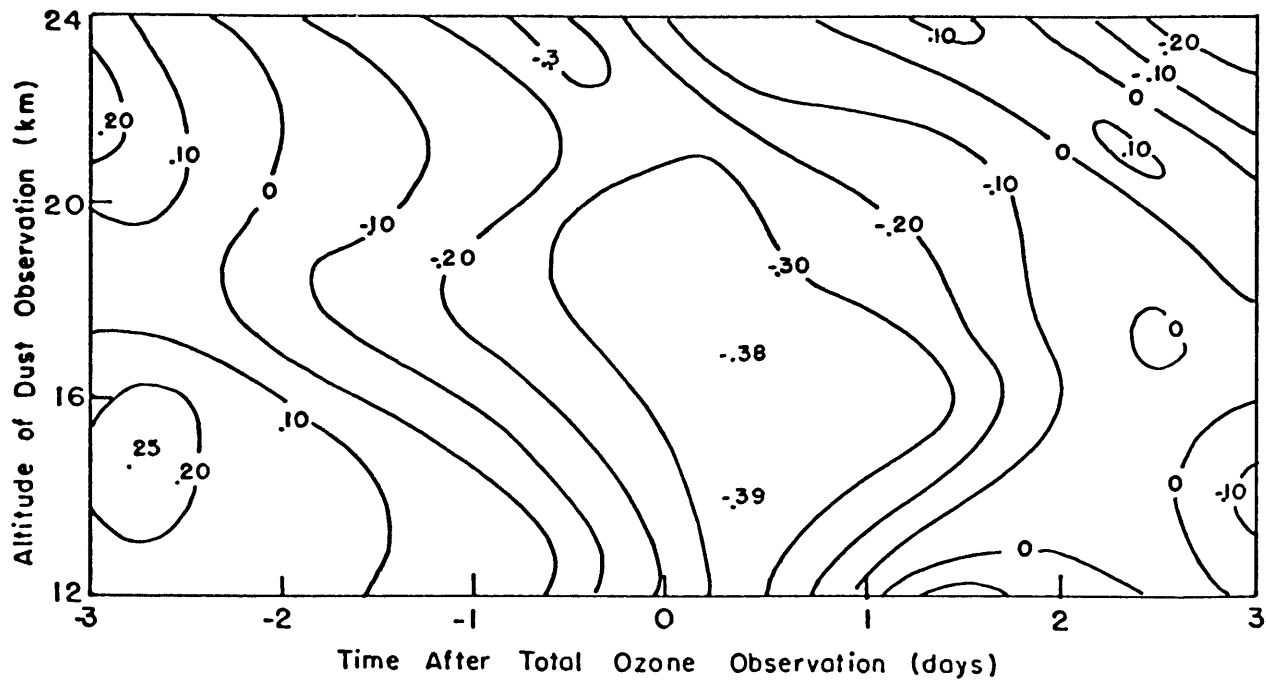


Fig. 26. Correlation coefficients for deviations from the monthly mean of ozone measurements and the dust content of the lower stratosphere as a function of the time lag between the observations and the altitude of the dust measurements.

the center of mass of the aerosol layer and total ozone remain negatively correlated for lags up to two days. Observed correlation coefficients have values of approximately -0.35 , exceeding the mean of correlation coefficients computed for longer lags by over two standard deviations and thereby remaining statistically significant at the 5% level of confidence. A scatter diagram for dust amounts at 16 km and deviations from the monthly mean of total ozone has been constructed and is shown as Fig. 27. Again, a negative trend in the observations is indicated with high dust amounts tending to be associated with negative deviations and large positive deviations occurring only when dust concentrations are low.

The calculations that have been described apply to the time period from January 1964 to April 1965 for which vertical profiles of atmospheric ozone were available. Total ozone amounts were available up to August 1965; data pairs using all available total ozone observations were used in constructing the scatter diagrams in Figs. 25 and 27. The correlations between dust and total ozone measurements were recalculated including dust data for the extended time period which essentially concurred with the observed trend toward natural conditions in the stratospheric dust layer and was characterized by low dust amounts. For the case of the dust-total ozone correlation, the maximum coefficient was decreased from -0.70 to -0.57 ; the calculated coefficients

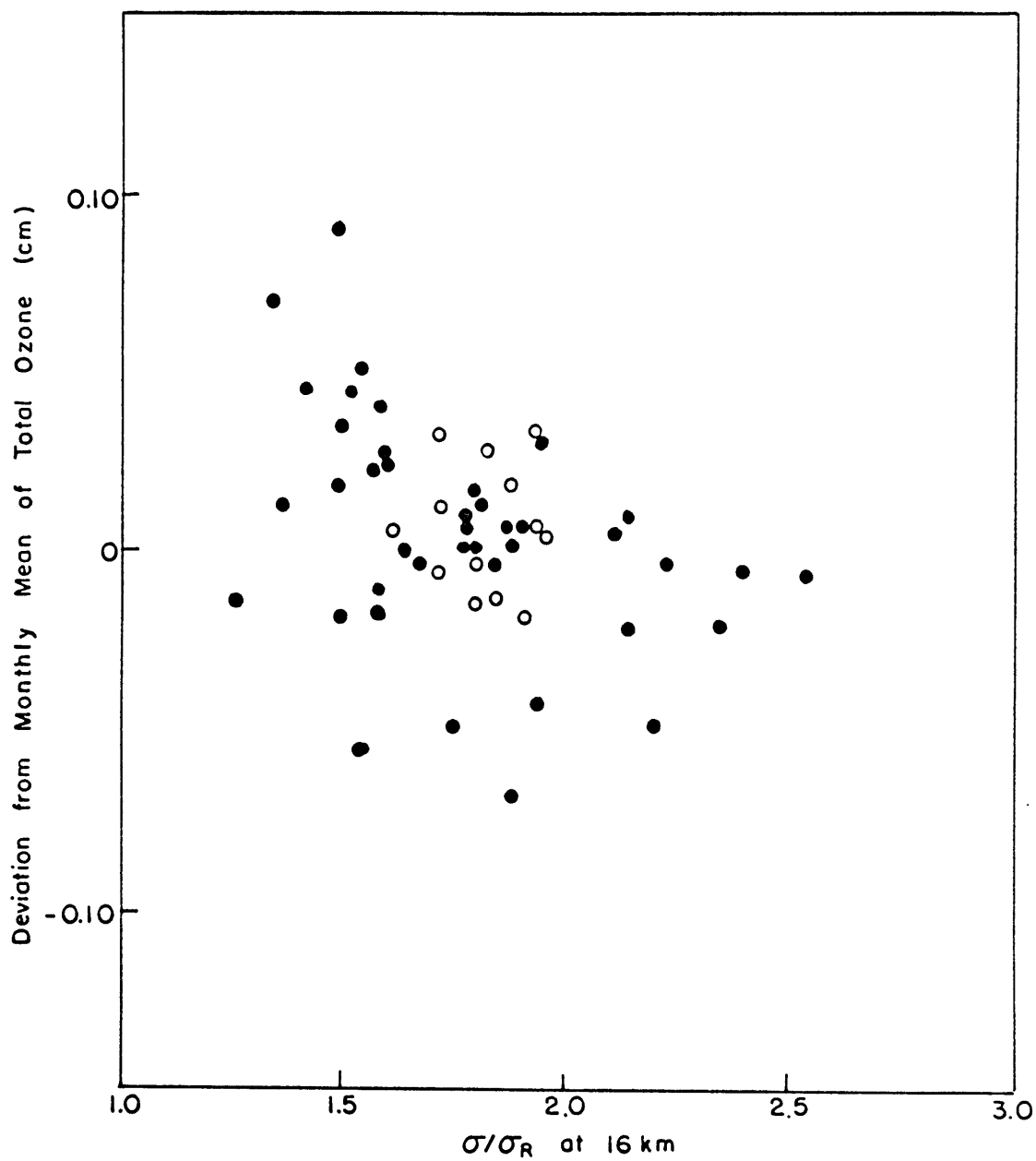


Fig. 27. Relation between the observed scattering ratio σ/σ_R at 16 km altitude and deviations from the monthly mean of the total amount of ozone in the atmosphere.

for data with the monthly mean of ozone removed were also reduced by about 20% of their values when the summer 1965 data was included. The calculations indicate that the relationship was not as pronounced in the presence of smaller dust amounts; this is also visually observed in Figs. 25 and 27 by the trend for increased scatter in the data points associated with lower dust concentrations.

In order to compare the temporal behavior of ozone with that of the stratospheric aerosol layer, autocorrelation functions for ozone concentrations at each altitude have been calculated in an analogous manner to the procedure used for the dust profiles. Some of the results are shown in Fig. 28; the considerable amount of persistence displayed by the dust data is lacking; the autocorrelation function decreases to insignificant values within one or two days. Similar calculations performed with total ozone are shown in Fig. 29. The autocorrelation function again falls rapidly but then remains significantly correlated for at least a month; this is taken to reflect the seasonal trend in the total ozone. The calculations for Fig. 28 were made using only the ozone profiles obtained within a few days of the dust profiles and the apparent lack of a seasonal variation may be due to preferential selection of data or the statistical fluctuations associated with small data samples; the total ozone correlogram used continuous observations for the entire period of observation

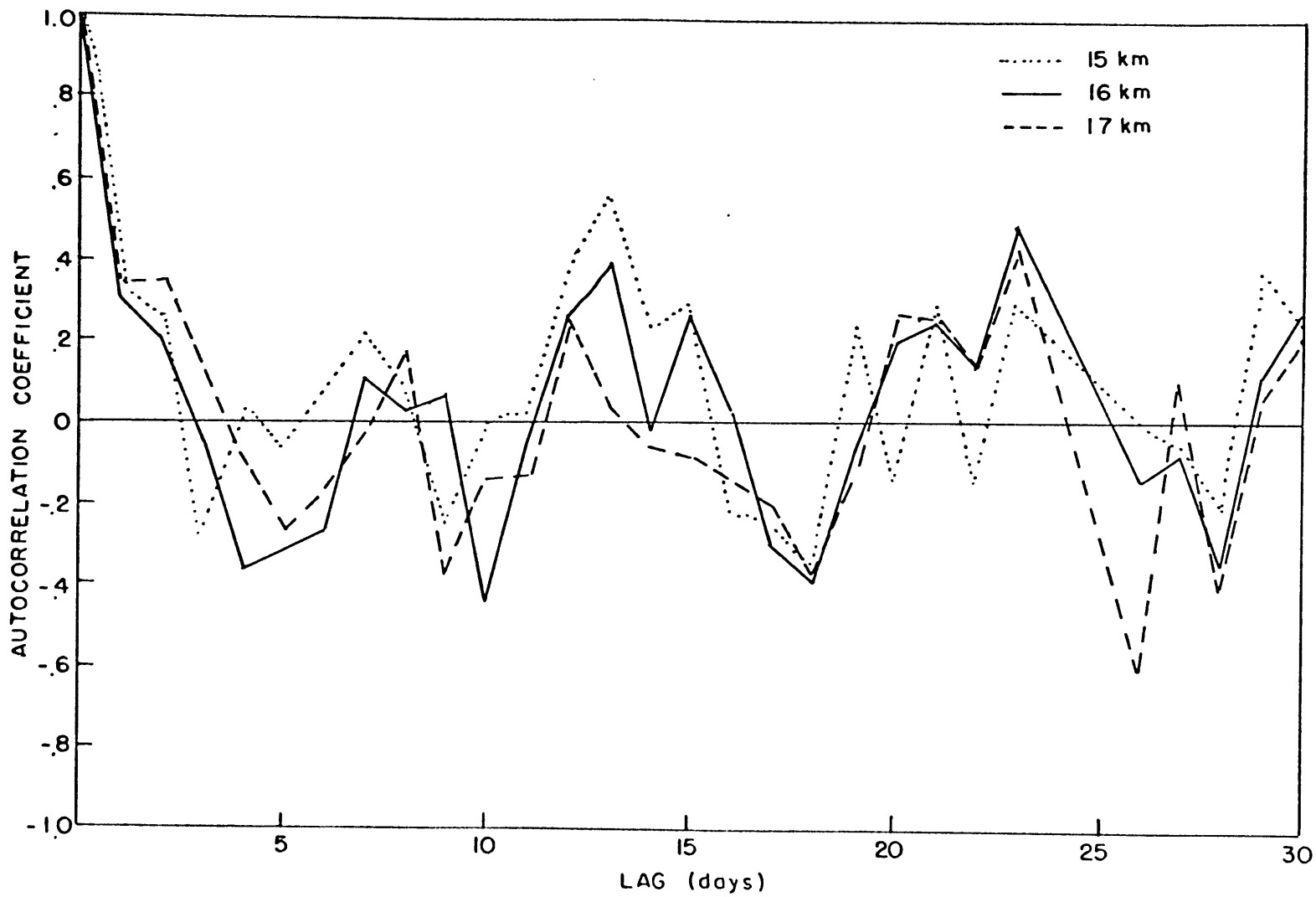


Fig. 28. Autocorrelation coefficients for stratospheric ozone observations near the center of mass of the aerosol layer.

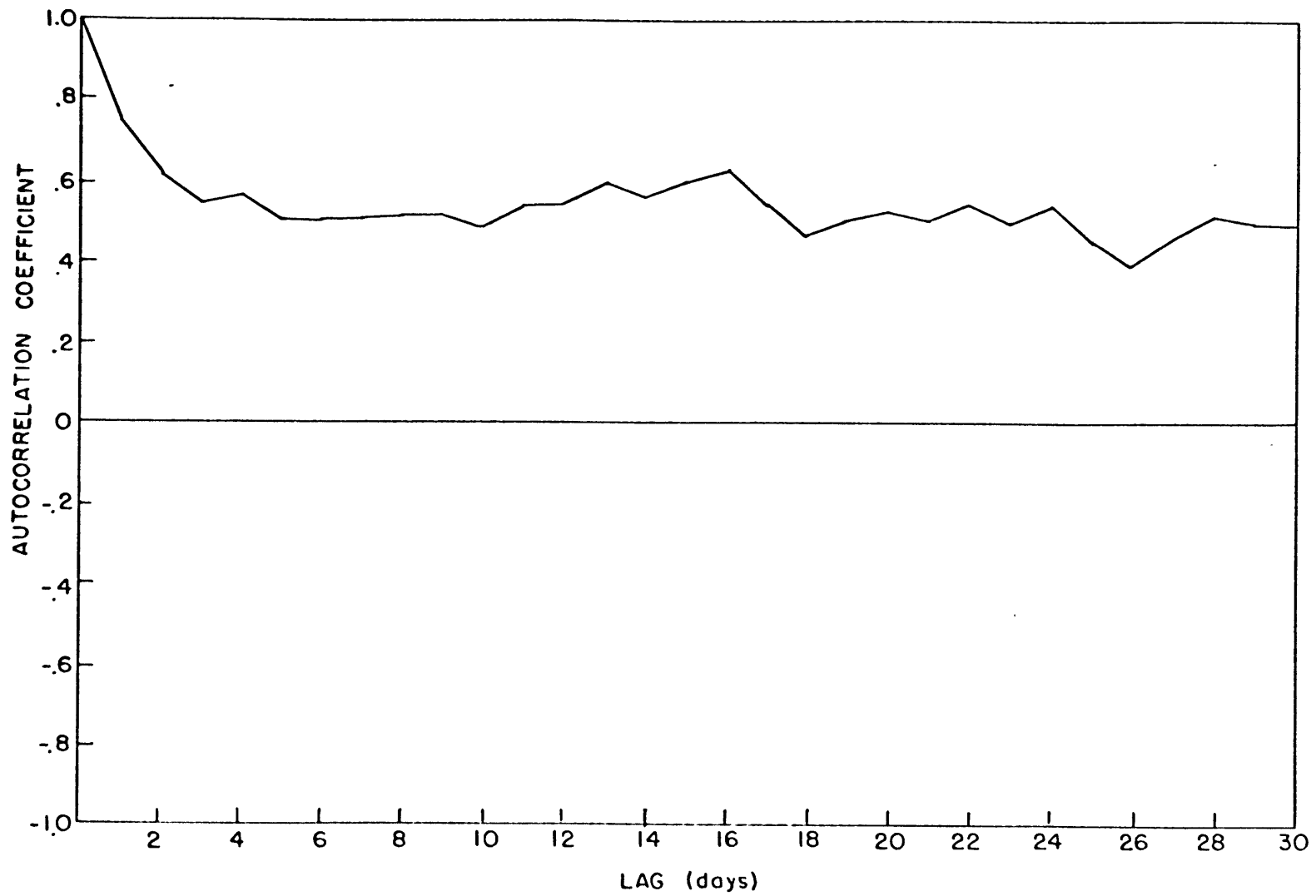


Fig. 29. Autocorrelation coefficients for the total amount of ozone in a vertical atmospheric column:

and therefore represents a larger and considerably more homogeneous sample from which to calculate the autocorrelation function.

It is appropriate to speculate on the cause for the observed negative correlation between stratospheric dust and the ozone layer. Many other meteorological parameters associated with the conditions in the lower stratosphere have been compared with the total ozone and significant correlations have been found (see, for example, Normand, 1951). The interrelationships between the daily fluctuations of total ozone amounts and the various parameters that are known to be correlated with these values can, in part, be explained by the systematic operation of certain meteorological factors such as vertical motions in the stratosphere and horizontal advection associated with synoptic scale weather patterns (Reed, 1950).

This study finds a significant relationship between ozone and aerosols in the lower stratosphere that acts in such a way that daily fluctuations of each parameter are negatively correlated. The aerosol study was conducted during a perturbed state of the atmosphere when particle concentrations were perhaps an order of magnitude larger than the natural population of stratospheric aerosols and the physical and chemical properties of the particulate material were likely to be different from the natural state. The enhanced optical phenomena associated with the perturbed

state of the atmosphere after the volcanic eruption on Bali island must first be considered. Since the total ozone measurement is based on an optical technique, the presence of a layer of scattering dust particles in the stratosphere introduces the possibility that attenuation of solar radiation by these particles may introduce a systematic error. Such an error would also be reflected in the vertical profiles obtained with the chemiluminescent sensor used by the Air Force Cambridge Research Laboratories since the absolute calibration of the ozonesonde is obtained by a simultaneous measurement of the total amount of ozone with a Dobson spectrophotometer.

The standard ozone spectrophotometer and details of its use have been described by Dobson (1957). The instrument measures the relative intensity of solar ultraviolet radiation at two wavelengths which, though separated by only about 0.02μ , have very different ozone absorption coefficients. Two statements of the Bouguer-Lambert law incorporating the effects of ozone absorption and scattering by molecules and dust particles are written and combined into an equation for the total amount of ozone in a vertical column necessary to produce the observed relative extinction of the two wavelengths. This equation contains a term which is proportional to the difference $\delta(\lambda_1) - \delta(\lambda_2)$ between dust scattering coefficients $\delta(\lambda_1)$ and $\delta(\lambda_2)$ for the wavelength pair λ_1 and λ_2 . On the assumption that scattering

by dust particles is independent of wavelength, this quantity vanishes and the total ozone amount is computed from the measured relative flux of solar radiation using calculated values of Rayleigh molecular scattering parameters and ozone absorption parameters determined from laboratory measurements. Since the assumption that the particle scattering is independent of wavelength is not valid for particles having dimensions comparable to the wavelength of the light, two pairs of wavelengths are measured in the standard procedure. Then although $\delta(\lambda_1) - \delta(\lambda_2)$ may not be zero, it is assumed to have the same value for the two wavelength pairs and the effects of particle scattering are assumed to cancel in the second approximation. The procedure would appear to minimize the effects of particle scattering although quantitative estimates of the error involved in the technique cannot be obtained without reasonably complete knowledge of the optical properties of the dust particles between the instrument and sun. It seems unlikely, however, that the enhanced particle concentrations in the stratosphere could produce appreciable errors in the total ozone measurement, especially since most of the particle scattering occurs in the lower troposphere. However, the possibility cannot be completely discounted in view of the perturbed nature of the dust layer. The observed peak in the size distribution of stratospheric aerosols at $\sim 0.3\mu$ (Feely et al, 1963) introduces another possibility that could provide an appreciable

wavelength dependence. The standard wavelength pairs used for the Dobson measurement are 0.3055 and 0.3254 μ and 0.3176 and 0.3398 μ ; since these wavelengths may be very close to a cut-off in a particle size distribution having abnormally large number concentrations, the wavelength dependence could arise from the enhanced scattering cross-sections exhibited by particles whose dimensions are nearly equal to the wavelength of the incident radiation.

Another possible influence on the total ozone measurement that could be related to the perturbed state of the lower stratosphere lies in the fact that sulfur dioxide is another atmospheric constituent that absorbs ultraviolet radiation in the same wavelength region as ozone (Dobson, 1963); sulfur dioxide has been associated with the formation of sulfate particles in the aerosol layer. Although Dobson could not detect the presence of a sufficient amount of sulfur dioxide to affect ozone measurements, the possibility that abnormal amounts of sulfur dioxide in the stratosphere followed the eruption of Mount Agung could introduce a systematic error if the sulfur dioxide content of the stratosphere was sufficiently large and if it was related to the dust concentration. Again no quantitative estimates of this effect can be made without a basic knowledge of the distribution of sulfur dioxide in the atmosphere.

Thus, the possibility exists that the ozone measurement may be affected by improper treatment of particulate

scattering or by failure to account for absorption by sulfur dioxide when calculating ozone amounts. Craig (1965, pg. 180) notes that values of total ozone differ by ~ 10 percent between nearly simultaneous measurements using different wavelength pairs or even different pairs of wavelength pairs, indicating that not all parameters involved are completely understood. In view of a lack of definite evidence that the ozone measurement itself may be the cause for the relationship between the two parameters, other explanations for the anticorrelations will be considered.

Some evidence has been obtained from the optical radar observations that the enhanced dust amounts from the Mount Agung eruption in the Southern Hemisphere have been distributed with a latitudinal gradient in dust concentration having smaller amounts of dust in high latitudes and larger amounts in tropical regions. Since maximum ozone amounts occur in high latitudes, horizontal advection processes could explain the observed anticorrelation; a polar air mass should contain high ozone amounts and low dust concentrations, while the opposite would be expected for air originating from low latitudes. Indeed, day-to-day ozone variations are associated with the systematic effects of horizontal advection and vertical motions associated with synoptic-scale weather patterns (Reed, 1950); even seasonal variations can be explained in terms of the meridional

transport of ozone by large-scale quasi-horizontal mixing processes (Newell, 1963, 1964). However, a crude attempt to relate fluctuations of observed dust amounts to the north-south component of the wind did not conform to the concept that the mean latitudinal distribution of the stratospheric aerosol could be strictly applied to explain daily fluctuations in terms of horizontal transport mechanisms. However, no definitive conclusions are possible without more extensive data, perhaps from a network of simultaneous observations.

Another relationship between the dust layer and ozone has recently been suggested. Kroening (1965) has pointed out that the stratospheric aerosol, located in a region where ozone concentrations are much higher than near the surface of the earth, may be an important sink for the chemical decomposition of ozone. Pittcock (1965) has reported a persistent "hole" in the vertical ozone distribution at about 20 km altitude in early 1964 for ozone profiles obtained at Boulder, Colorado that could be attributed to the presence of an ozone sink; he suggested that atmospheric ozone was being destroyed at that altitude by a concentrated layer of volcanic dust injected into the stratosphere by The Mount Agung eruption.

Rosen (1966) states that ozone decomposition by a thin dust layer near 20 km is unlikely because the dust distributions obtained with the photoelectric particle

counter do not show thin dust layers in that region. However, this statement is contradicted by the dust profile obtained in early 1964 that shows a layered structure near 20 km (Rosen, 1964); evidence presented by the few dust profiles obtained with the particle counter does not appear to be definitive.

The process of ozone decomposition in the atmosphere is poorly understood, but it is generally assumed that the primary sink for the chemical destruction of ozone is the surface of the earth. Some evidence that ozone may be chemically destroyed in tropospheric clouds and by particulate material and trace gases near the ground does exist; these observations have been discussed by Junge (1963b) with reference to tropospheric ozone. If the anomaly in the vertical ozone distribution observed by Pittcock was actually caused by chemical destruction of ozone by particulate material associated with the volcanic eruption, the abnormally high aerosol concentrations that have existed at least until late spring 1965 may have been generally responsible for the destruction of significant amounts of ozone during that time period. The observed negative correlation may, therefore, have resulted from chemical decomposition of ozone in the presence of the perturbed dust population of the stratospheric aerosol layer which, in addition to enhanced number concentrations, may also have had a different chemical composition than the ordinary

sulfate particles found in the natural state of the layer (Mossop, 1964). In fact, none of the results of this study can be taken as evidence against chemical destruction of ozone by the perturbed aerosol layer. The correlation between dust and total ozone had a maximum value near the center of mass of the aerosol layer. Correlations between dust and ozone concentrations at latitudes near the center of mass of the layer were significantly negative. Also, the correlations remained significantly high when seasonal effects were removed from the ozone data, indicating that the daily fluctuations were related.

If an explanation based on an interaction between ozone and dust was to have a physical foundation, the average time between collisions of an ozone molecule and a dust particle should be short compared to the time scale over which the correlations are observed. A simple estimate of the time required for interaction between the ozone molecules and dust particles has been made. Consider N_D aerosol particles per unit volume and an ozone molecule with velocity v . The average cross-section per unit volume presented by the particles will be $\pi r^2 N_D$ where r is the particle radius. The number of collisions per unit time will therefore be $\pi r^2 N_D v$. The average particle radius is taken to be 0.3μ ; the velocity of the ozone molecule is taken to be 340 m/sec, the root-mean-square thermal velocity of ozone at stratospheric temperatures. The collision rate Γ^{-1} is

therefore given by $\pi r^2 N_D v \approx 10^{-4} N_D \text{ sec}^{-1}$ if N_D is expressed in cgs units. The average time between collisions is therefore $T \sim \frac{10^4}{N_D}$ seconds. With particle concentrations of approximately 1 cm^{-3} the average time for each ozone molecule to collide with an aerosol particle is about three hours and the possibility of a chemical reaction between the aerosol and ozone cannot be ruled out. The dust particles would, however, have to act as a catalyst in such a reaction since the mass of the ozone in the stratosphere exceeds that of the stratospheric aerosol by at least two orders of magnitude.

6. CONCLUSIONS

An optical radar system has been developed to obtain information on the vertical distribution of stratospheric aerosols during a two year study of the dust layer near 20 km. The data obtained with the apparatus consistently showed a maximum in the relative concentration of aerosols between 15 and 20 km altitude. The study was conducted during a period when the aerosol layer was perturbed from its normal state by the eruption of the Mount Agung volcano on Bali Island in early 1963 and the results may represent anomalous conditions in the lower stratosphere. The observed maximum of the aerosol mixing ratio in the lower stratosphere is, therefore, likely to be associated with the spatial distribution of the volcanic debris and the observations could not be used to infer the origin of the natural population of sulfate particles.

The vertical distribution of the aerosol particles was obtained by comparing the optical radar return with the expected return from a molecular atmosphere, using the observed echoes from 25-30 km altitude to calibrate the instrument. At the observation site in Lexington, Massachusetts the observed return from the layer was approximately 1.9 times the expected return from the model atmosphere. The daily rms fluctuation of the scattering ratio was approximately 0.3 and hourly fluctuations were much smaller. In

the summer 1964 some observations were also performed at College, Alaska. For this series of observations the maximum scattering ratio was ~ 1.7 with daily fluctuations of about 0.15.

The observed scattering ratios have been related to the number of particles per unit volume illuminated by the laser beam by evaluating Mie scattering functions for back-scattered radiation. Calculated particle concentrations were found to be in agreement with independent studies by other investigators, especially with the particle counts of Rosen (1964).

The observations have been compared with other meteorological parameters in the lower stratosphere. The center of mass of the layer was usually very close to 16 km; day-to-day changes in the tropopause height were accompanied by a tendency for small vertical displacements of the layer. The optical radar observations performed in Alaska agree with the concept that the height of the layer approximately follows latitudinal changes in the tropopause height.

Although the data obtained in this study at the two observation sites in Alaska and Massachusetts, as well as another profile obtained by other workers in Jamaica, suggest a latitudinal gradient in dust concentrations, the effect was not evident when an attempt to relate fluctuations in the dust content of the stratosphere to the north-south component of the wind was made. Little relation between

the two parameters was found; in fact the data seem to indicate that higher dust amounts are associated with northerly flow.

Stratospheric aerosol measurements were found to be correlated with measurements of atmospheric ozone. A significant negative correlation was found between dust concentrations and ozone concentrations as derived from the results of this study and from ozone profiles obtained from the Air Force Cambridge Research Laboratories, respectively; the anticorrelation was also obtained using total ozone observations. This result supports the suggestion by Pittcock (1965) that stratospheric ozone may be chemically decomposed in the presence of the debris injected into the atmosphere by the eruption of the Mount Agung volcano. The observed correlation, however, may also be related to large-scale horizontal mixing processes that transport dust and ozone from different source regions. The possibility also exists that the observed correlation may reflect systematic errors in the ozone measurement resulting from the perturbed conditions in the stratosphere.

The optical radar apparatus used for this study is, in its present state of development, capable of obtaining vertical profiles of the back-scattered laser pulse at a rate in excess of 30 per minute. Unfortunately, the signal intensity from the lower stratosphere is too weak to derive useful information from each pulse, and many echoes must be

averaged to obtain reliable profiles of the 20 km aerosol layer. However, the signal intensity from tropospheric levels is much higher; the individual profiles have greater quantitative value and could be used for studying short-period fluctuations of scattering discontinuities in the troposphere.

The ability of the technique to study the 20 km layer, albeit accompanied by a considerable data reduction effort, has been demonstrated. Although the basic apparatus can obtain data at a rapid rate, routine observations are accompanied by a large collection of data records; further efforts directed at increasing the signal strength or electronically averaging the individual echoes are necessary for routine observations. Also, complementary data on atmospheric transmission and the total energy radiated in each laser pulse would increase the quantitative reliability of the observations and appropriate instrumentation to obtain such data should be developed.

The technique of using the back-scattered radiation to detect layers of scattering particles is perhaps the most simple application of laser scattering as an atmospheric probe. Other light scattering applications are being considered by our group, as well as other workers, to derive data on the temperature distribution, atmospheric velocities, and vertical profiles of individual molecular species.

APPENDIX

Numerical values of the nightly average scattering ratios for 1 km intervals between 12 and 24 km altitude are presented in tabular form. For each table the first column gives the observation period for which data have been analyzed; the time periods listed in this column refer to Eastern Standard Time or, in the case of the data obtained in College, to Alaska Standard Time. The second column identifies the date, month, and year of the observation. Column three lists the number of individual traces used to obtain the average profile; the statistical reliability of each profile may be estimated by referring to Fig. 10, page 48.

Subsequent columns give the observed scattering ratios σ/σ_R at the indicated altitudes. Scattering ratios which incorporate a shutter correction are denoted by an asterisk after the number.

Table A1: Numerical summary of optical radar data. Part 1.

TIME	DATE	TRACES	12km	13km	14km	15km	16km	17km	18km	19km	20km	21km	22km	23km	24km
2002-2011	14-01-64	20	1.07	1.27	1.49	1.89	2.22	2.46	2.68	2.56	2.51	2.35	2.30	1.94	1.67
2024-2227	30-01-64	75	1.38*	1.52*	1.66*	1.71*	1.87*	1.93*	1.86*	1.71*	1.40*	1.27*	1.21*	1.39*	1.28*
2209-2242	8-02-64	7	1.40*	1.44*	1.60*	1.79*	1.97*	2.06*	2.11*	2.10	1.79	1.31	1.07	1.00	1.48
1922-2007	11-02-64	11	1.43*	1.57*	1.62*	1.71*	1.71*	1.90*	2.48*	2.24*	1.66*	1.16	1.19	1.28	1.46
2045-2232	12-02-64	54	1.54*	1.48*	1.56*	1.76*	1.91*	2.11*	1.96*	1.70*	1.53*	1.52*	1.35*	1.32*	1.11*
2119-2308	14-02-64	83	1.32*	1.51*	1.70*	1.70*	1.84*	1.87*	2.18*	2.31*	1.79*	1.34*	1.10	1.09	1.20
2200-2308	5-04-64	73	1.48	1.37	1.37	1.51	1.54	1.54	1.70	1.66	1.34	1.15	1.01	1.00	1.27
0419-0442	9-04-64	33	1.46*	1.51*	1.65*	1.69*	1.72*	1.70	1.64	1.67	1.57	1.41	1.18	1.10	1.00
2201-2244	11-04-64	60	1.51*	1.53*	1.53*	1.76*	1.90*	1.97*	1.78*	1.72*	1.67*	1.52*	1.31*	1.28*	1.35*
2305-2359	16-04-64	15	1.45*	1.53*	1.64*	1.70*	1.74*	1.83*	1.66*	1.39*	1.11	1.00	1.11	1.23	1.16
1945-2019	17-04-64	20		1.48*	1.68*	1.69*	1.80*	1.94*	1.99*	1.80*	1.58*	1.29	1.21	1.14	1.04
2208-2311	23-04-64	60	1.42*	1.56*	1.67*	1.67*	1.80	2.07	2.13	1.72	1.45	1.27	1.18	1.10	1.00
2014-2147	26-04-64	120	1.48*	1.50*	1.62*	1.84	2.10	2.46	2.44	2.10	1.67	1.40	1.29	1.18	1.07
2103-2159	27-04-64	60			1.45	1.60	1.88	2.09	1.96	2.02	1.75	1.47	1.38	1.35	1.28
2230-2245	28-04-64	32	1.46*	1.55*	1.59*	1.72*	1.79*	1.77	1.78	1.70	1.68	1.57	1.50	1.61	1.53
1938-2200	30-04-64	100	1.35*	1.40*	1.61*	1.80*	1.93*	2.02*	1.82*	1.57	1.48	1.35	1.27	1.16	1.09
0043-0145	1-05-64	100	1.54*	1.44*	1.60*	1.75*	1.84	1.83	1.67	1.59	1.40	1.36	1.31	1.26	1.13
2024-2150	2-05-64	100	1.38*	1.36*	1.54*	1.87*	2.00*	1.94*	1.70*	1.49*	1.29*	1.24	1.16	1.07	1.00
2019-2243	3-05-64	80	1.54*	1.47*	1.55*	1.77*	1.95*	2.02*	1.76*	1.55*	1.31*	1.15	1.12	1.04	1.00
2036-2122	5-05-64	60	1.50*	1.50*	1.60*	1.74*	1.82*	1.86*	1.70	1.57	1.30	1.24	1.30	1.19	1.15
2210-2214	6-05-64	20	1.51*	1.62*	1.61*	1.66*	1.80	2.02	2.06	1.76	1.65	1.44	1.28	1.16	1.19
2010-2256	18-05-64	16	1.60*	1.57*	1.61*	1.77	1.95	1.97	1.83	1.76	1.63	1.43	1.41	1.07	1.00
2115-2135	20-05-64	50	1.39*	1.49*	1.61*	1.76*	1.93*	2.02*	1.95*	1.76*	1.48*	1.30*	1.17*	1.03*	1.07
2305-2318	11-10-64	50	1.37*	1.48*	1.70*	1.70*	1.60*	1.23*	1.12	1.08	1.00	1.08	1.08	1.20	1.12
2130-2318	14-10-64	50	1.42*	1.52*	1.65*	1.81	1.90	1.78	1.69	1.53	1.46	1.32	1.27	1.15	1.31
2230-2237	27-10-64	50	1.43	1.70	1.78	1.99	2.40	2.15	1.76	1.57	1.48	1.25	1.13	1.04	1.03

Table A2: Numerical summary of optical radar data. Part 2.

TIME	DATE	TRACES	12km	13km	14km	15km	16km	17km	18km	19km	20km	21km	22km	23km	24km
1754-1932	1-11-64	100	1.70	1.70	1.82	2.09	2.14	2.20	2.06	1.79	1.77	1.60	1.68	1.66	1.46
1730-2000	2-11-64	200	1.92	2.07	2.01	2.17	2.35	2.50	2.26	1.77	1.64	1.62	1.43	1.27	1.17
1700-1930	4-11-64	175	1.59	1.58	1.75	2.17	2.53	2.53	2.47	2.15	1.93	1.72	1.48	1.39	1.23
1700-1900	7-11-64	180	1.27	1.35	1.50	1.68	1.95	2.02	1.73	1.46	1.38	1.32	1.29	1.38	1.28
1745-1930	8-11-64	100	1.47	1.57	1.60	1.90	2.13	1.98	1.76	1.68	1.46	1.33	1.21	1.11	1.07
2000-2102	9-11-64	50	1.30	1.29	1.36	1.65	1.88	1.78	1.59	1.51	1.45	1.37	1.15	1.10	1.20
1800-1930	13-11-64	217									1.42	1.34	1.20	1.10	1.03
1730-1930	15-11-64	262		1.60	1.68	1.66	1.78	1.88	1.89	1.89	1.61	1.36	1.25	1.18	1.14
1830-1930	26-11-64	139	1.13	1.22	1.39	1.48	1.67	1.81	1.80	1.61	1.67	1.57	1.40	1.28	1.22
1900-1930	1-12-64	104	1.65	1.72	1.70	1.83	1.94	1.91	1.61	1.53	1.40	1.29	1.12	1.06	1.32
1700-1830	2-12-64	237	1.72	1.91	2.13	2.20	2.33	2.51	2.44	1.87	1.47	1.26	1.15	1.13	1.38
2300-2330	18-12-64	405	1.23	1.23	1.20	1.32	1.62	1.80	1.72	1.51	1.14	1.09	1.06	1.09	1.11
0056-0058	1-01-65	75	1.46	1.57	1.60	1.70	1.83	1.64	1.49	1.50	1.53	1.50	1.26	1.13	1.27
1931-2100	29-01-65	100		1.38	1.43	1.52	1.54	1.46	1.35	1.36	1.33	1.33	1.39	1.31	1.40
2000	31-01-65	100		1.53	1.61	1.67	1.59	1.55	1.44	1.48	1.48	1.39	1.39	1.39	1.22
2205-2230	2-02-65	100			1.32	1.61	1.59	1.47	1.48	1.45	1.47	1.45	1.42	1.39	1.23
2110-2145	3-02-65	100				1.40	1.34	1.32	1.37	1.46	1.49	1.34	1.18	1.06	1.06
2358-0005	11-02-65	100		1.72	1.79	1.65	1.75	1.92	1.94	1.84	1.72	1.51	1.35	1.35	1.45
1800-2100	15-02-65	100				1.57	1.93	2.34	2.32	2.03	1.83	1.82	1.65	1.45	1.33
2007-2100	17-02-65	100				2.14	2.13	2.11	2.04	1.98	1.85	1.67	1.57	1.39	1.26
1801-1831	22-02-65	97		1.38	1.71	1.79	1.79	1.84	1.87	1.81	1.65	1.54	1.42	1.27	1.15
1936-0527	23-02-65	125		1.29	1.46	1.50	1.80	1.85	1.83	1.73	1.63	1.64	1.62	1.45	1.28
1830-2228	2-03-65	125		1.27	1.58	1.78	1.88	1.90	1.89	1.85	1.76	1.66	1.52	1.39	1.30
2000-2058	3-03-65	75		1.74	1.85	1.92	2.19	2.19	2.12	2.13	2.06	2.00	1.93	1.69	1.48
2157-0504	10-03-65	125	1.28	1.48	1.44	1.47	1.50	1.50	1.47	1.47	1.41	1.33	1.19	1.14	1.13
1900-0400	11-03-65	250		1.48	1.49	1.50	1.49	1.44	1.41	1.45	1.50	1.36	1.25	1.16	1.13

Table A3. Numerical summary of optical radar data. Part 3.

TIME	DATE	TRACES	12km	13km	14km	15km	16km	17km	18km	19km	20km	21km	22km	23km	24km
2259-0528	12-03-65	327		1.26	1.38	1.45	1.57	1.59	1.56	1.63	1.60	1.43	1.21	1.10	1.12
1847-0454	13-03-65	355	1.22	1.35	1.48	1.50	1.58	1.59	1.55	1.58	1.52	1.38	1.18	1.08	1.08
1908-2000	14-03-65	125	1.53	1.42	1.31	1.41	1.50	1.52	1.47	1.53	1.48	1.29	1.08	1.04	1.03
2359-0514	15-03-65	225	1.03	1.16	1.19	1.30	1.44	1.44	1.47	1.51	1.44	1.27	1.16	1.10	1.05
2218-4000	16-03-65	75	1.21	1.12	1.12	1.19	1.26	1.27	1.24	1.28	1.26	1.23	1.12	1.09	1.22
1905-2201	27-03-65	100	2.06	2.06	2.19	2.35	2.33	2.22	2.06	1.83	1.59	1.19	1.04	1.44	1.71
2131-0501	30-03-65	101	2.02	2.02	2.15	2.29	2.37	2.33	2.29	2.21	2.04	1.81	1.64	1.34	1.07
2001-2131	14-04-65	100	1.67	1.69	1.74	1.84	1.87	1.80	1.74	1.76	1.68	1.46	1.40	1.16	1.09
1934-1936	29-04-65	50		1.73	1.86	1.87	1.89	1.77	1.73	1.82	1.68	1.34	1.10	1.04	1.08
1946-2158	12-05-65	100	1.42	1.51	1.50	1.42	1.48	1.56	1.51	1.42	1.29	1.16	1.05	1.19	1.16
2224-2354	20-05-65	100	1.07	1.24	1.49	1.59	1.58	1.63	1.64	1.66	1.51	1.28	1.19	1.08	1.05
2015-2017	4-06-65	50	1.55	1.68	1.68	1.67	1.59	1.65	1.74	1.73	1.56	1.47	1.42	1.34	1.15
2050-2138	12-07-65	100	1.30	1.40	1.37	1.39	1.49	1.69	1.91	1.87	1.67	1.47	1.36	1.28	1.20
2058-2159	21-07-65	100	1.14	1.17	1.21	1.33	1.37	1.41	1.39	1.30	1.23	1.19	1.14	1.07	1.12
ALASKA															
0030-0048	26-07-64	36	1.34	1.41	1.56	1.63	1.46	1.26	1.19	1.12	1.05	1.03	1.00	1.04	1.23
0000-0014	27-07-64	9	1.15	1.25	1.46	1.61	1.67	1.33	1.10	1.00	1.05	1.06	1.19	1.42	1.23
2303-0015	2-08-64	45	1.32	1.44	1.53	1.64	1.67	1.46	1.28	1.08	1.09	1.07	1.06	1.03	1.00
2208-2235	5-08-64	25	1.10	1.22	1.35	1.79	1.80	1.59	1.40	1.30	1.24	1.07	1.15	1.16	1.22
0150-0204	6-08-64	50	1.20	1.30	1.46	1.57	1.51	1.33	1.13	1.03	1.07	1.11	1.01	1.00	1.04
2308-2320	7-08-64	50	1.32	1.54	1.72	1.86	1.77	1.51	1.35	1.21	1.15	1.10	1.04	1.04	1.15
2315-0047	9-08-64	50	1.34	1.30	1.34	1.72	1.71	1.52	1.24	1.11	1.16	1.14	1.11	1.01	1.00
2310-2314	16-08-64	12	1.30	1.42	1.69	2.00	1.84	1.40	1.31	1.39	1.33	1.08	1.16	1.23	1.04
2325-0144	21-08-64	45	1.26	1.37	1.49	1.51	1.51	1.38	1.32	1.18	1.15	1.04	1.10	1.13	1.00

REFERENCES

- Bigg, E.K., 1956: The detection of atmospheric dust and temperature inversions by twilight scattering. J. Meteor., 13, 262-268.
- Bigg, E.K., 1964: Atmospheric stratification revealed by twilight scattering. Tellus, 16, 76-83.
- Bigg, E.K. and G.T. Miles, 1964: The results of large-scale measurements of natural ice nuclei. J. Atmos. Sci., 21, 396-403.
- Bull, G.A., and D.G. James, 1956: Dust in the stratosphere over Western Britian on April 3 and 4, 1956. Meteor. Mag., 85, 293-297.
- Chagnon, C.W., and C.E. Junge, 1961: The vertical distribution of sub-micron particles in the stratosphere. J. Meteor., 18, 746-752.
- Clemesha, B.R., G.S. Kent, and R.W.H. Wright, 1966: Laser probing the lower atmosphere. Nature, 209, 184-185.
- Collis, R.T.H., and M.G.H. Ligda, 1966: Note on lidar observations of particulate matter in the stratosphere. J. Atmos. Sci., 23, 255-257.
- Craig, R.A., 1965: "The Upper Atmosphere: Meteorology and Physics", New York, Academic Press, 176-233.
- Dobson, G.M.B., 1957: Observers' handbook for the ozone spectrophotometer. Ann. I.G.Y., 5, 46-89.
- Dobson, G.M.B., 1963: Note on the measurement of ozone in the atmosphere. Quart. J. R. Meteor. Soc., 89, 409-411.
- Elterman, L., 1954: Seasonal trends of temperature, density, pressure to 67.6 km obtained with the searchlight probing technique. J. Geophys. Res., 59, 351-358.
- Elterman, L., 1964: Atmospheric attenuation model, 1964, in the ultraviolet, visible, and infrared regions for altitudes to 50 km. Air Force Cambridge Research Laboratories Report, AFCRL-64-740.
- Elterman, L., and A.B. Campbell, 1964: Atmospheric aerosol observations with searchlight probing. J. Atmos. Sci., 21, 457-458..

- Feely, H.W., B. Davidson, J.P. Friend, R.J. Lagomarsino, M.W.M. Leo, 1963: Ninth quarterly report on Project Star Dust. U.S. Dept. of Defense report DASA-1309, 22-66.
- Flocco, G., and G. Grams, 1964: Observations of the aerosol layer at 20 km by optical radar. J. Atmos. Sci., 21, 323-324.
- Flocco, G., and G. Grams, 1966: Observations of the upper atmosphere by optical radar in Alaska and Sweden during the summer 1964. Tellus, 18, 34-38.
- Flocco, G. and L.D. Smullin, 1963: Detection of scattering layers in the upper atmosphere (60-140 km) by optical radar. Nature, 199, 1275-1276.
- Friedland, S.S., J. Katzenstein, and M. Zatzick, 1956: Pulsed searchlighting the atmosphere. J. Geophys. Res., 61, 415-434.
- Friend, J.P., H.W. Feely, P.W. Krey, J. Spar, A. Walton, 1961: The High Altitude Sampling Program, Vol. 5, U. S. Dept. of Defense report DASA-1300, 1-153.
- Gruner, P., 1942: Dämmerungserscheinungen. In "Handbuch der Geophysik", Bd. 8, Berlin, Borntrager, 432-526.
- Gruner, P., and H. Kleinert, 1927: Die Dämmerungserscheinungen. "Probleme der Kosmischen Physik", Bd. 10, Hamburg, Henri Grand.
- Henenway, C.O., and R.K. Soberman, 1962. Studies of micro-meteorites obtained from recoverable sounding rockets. Astron. J., 67, 256-266.
- Hering, W.S., 1964: Ozonesonde observations over North America. Air Force Cambridge Research Laboratories Report, AFCRL-64-30 (I).
- Hering, W.S., and T.R. Borden, 1964: Ozonesonde observations over North America. Air Force Cambridge Research Laboratories Report, AFCRL-64-30 (II).
- Hering, W.S., and T.R. Borden, 1965a: Ozonesonde observations over North America. Air Force Cambridge Research Laboratories Report, AFCRL-64-30 (III).
- Hering, W.S., and T.R. Borden, 1965 b: Mean distributions of ozone density over North America, 1963-1964. Air Force Cambridge Research Laboratories Report, AFCRL-65-913.

- Hering, W.S., and H.U. Dütsch, 1965: Comparison of chemiluminescent and electrochemical ozonesonde observations. J. Geophys. Res., 70, 5483-5490.
- Jacobs, L., 1954: Dust clouds in the stratosphere. Meteor. Mag., 83, 115-119.
- Junge, C., 1952: Gesetzmässigkeiten in der Grossenverteilung atmosphärischer Aerosole über dem Kontinent. Ber. Deut. Wetterdienstes US-Zone, 35, 261-177.
- Junge, C.E., 1963 a: Sulfur in the atmosphere. J. Geophys. Res., 68, 3975-3976.
- Junge, C.E., 1963 b: "Air chemistry and Radioactivity", New York, Academic Press, 37-59.
- Junge, C.E., C.W. Chagnon, and J.E. Manson, 1961: Stratospheric Aerosols. J. Meteor., 18, 81-108.
- Junge, C.E., and J.E. Manson, 1961: Stratospheric aerosol studies. J. Geophys. Res., 66, 2163-2182.
- Kroening, J.L., 1965: Stratosphere and troposphere: transport of material between them. Science, 147, 862-864.
- Long, R.K., 1963: Atmospheric attenuation of ruby lasers. Proc. IEEE, 51, 859-860.
- Mateer, C.L., and W. L. Godson, 1960: The vertical distribution of atmospheric ozone over Canadian stations from Umkehr observations. Quart. J. R. Meteor. Soc., 86, 512-518.
- Megrelishvili, T.V., 1958: The possibility of investigating aerosol layers by the twilight method. Bull. Acad. Sci. U.S.S.R. Geophys. Series, 315-317.
- Meinel, M.P., and Meinel, A.B., 1963: Late twilight glow of the ash stratum from the eruption of Agung volcano. Science, 142, 582-583.
- Meinel, A.B., and Meinel, M.P., 1964: Height of the glow stratum from the eruption of Agung on Bali. Nature, 201, 657-658.
- Mie, G., 1908: Beitrag zur Optik trüber Medien. Ann. Physik, 25, 377-445.
- Mossop, S.C., 1963: Stratospheric particles at 20 km. Nature, 199, 325-326.

- Mossop, S.C., 1964: Volcanic dust collected at an altitude of 20 km. Nature, 203, 824-827.
- Newell, R.E., 1963. Transfer through the tropopause and within the stratosphere. Quart. J. R. Meteor. Soc., 89, 167-204.
- Newell, R.E., 1964: Further ozone transport calculations and the spring maximum in ozone amount. Pure and Appl. Geophys., 59, 191-206.
- Newkirk, G. Jr., and J. A. Eddy, 1964: Light scattering by particles in the upper atmosphere. J. Atmos. Sci., 21, 35-60.
- Normand, Sir Charles, 1951: Some recent work on ozone. Quart. J. R. Meteor. Soc., 77, 474-478.
- Paltridge, G.W., 1966: Stratospheric small-ion density measurements from a high-altitude jet aircraft, J. Geophys. Res., 71, 1945-1952.
- Pittock, A.B., 1965: Possible destruction of ozone by volcanic material at 50 mbar. Nature, 207, 182.
- Rayleigh, Lord, 1871: On the light from the sky, its polarization and colour. Phil. Mag., 41, 107-120, 274-279.
- Reed, R.J., 1950: The role of vertical motions in ozone-weather relationships. J. Meteor., 7, 263-267.
- Regener, V.H., 1964: Measurement of atmospheric ozone with the chemiluminescent method. J. Geophys. Res., 69, 3795-3800.
- Rosen, J.M., 1964: The vertical distribution of dust to 30 kilometers. J. Geophys. Res., 69, 4673-4676.
- Rosen, J.M., 1966: Correlation of dust and ozone in the stratosphere. Nature, 209, 1342.
- Rosenberg, G.V. (Ed.), 1960: Searchlight beam in the atmosphere (in Russian). Moscow, Publishing house of the Acad. of Sciences of the U.S.S.R., 245 pp. Partial translation: AID report 62-126, 28 August 1962, AID work assignment no. 35, OAR no. 2, Task 5.
- Rosenberg, G.V., and V.V. Nikolaeva-Tereshkova, 1965: Stratospheric aerosol measured from space ship. Akademiia nauk SSSR. Izvestiia. Fizika atmosfery i okeana., 1, 386-394.

- Rosenberg, G.V., A.B. Sandomirsky, and V.K. Poldmaa, 1966: Measurements of altitude variation of scattering coefficient in stratosphere. paper presented at the IQSY conference on the investigation of noctilucent clouds, Tallin, Estonia, U.S.S.R.
- Ross, M.D., 1958: High clouds observed in the stratosphere at sunset. Bull. Amer. Meteor. Soc., 39, 624.
- Rössler, F., 1963: Aerosolmessungen mittels des diffusen Himmelslichtes von einer Rakete aus, Ber. Deut. Wetterdienstes, no. 91, 96-98.
- Synge, E.H., 1930: Phil. Mag., 9, 1014-1020.
- Van de Hust, H.C., 1957: "Light scattering by small particles", New York, Wiley, 470 pp.
- Vassey, A., 1965: Atmospheric ozone. In "Advances in Geophysics", 11, New York, Academic Press, 116-173.
- Volz, F.E., 1954: Die Optik und Meteorologie der atmosphärischen Trübung. Ber. Deut. Wetterdienstes, no. 13, Teil 2.
- Volz, F.E., 1964: Twilight phenomena caused by the eruption of Agung Volcano. Science, 144, 1121-1122.
- Volz, F.E., 1965: Note on the global variation of stratospheric turbidity since the eruption of Agung Volcano. Tellus, 17, 513-515.
- Volz, F.E., and R.M. Goody, 1962: The intensity of the twilight and upper atmospheric dust. J. Atmos. Sci., 19, 385-406.
- Wexler, H., 1951: Spread of the Krakatoa dust cloud as related to the high-level circulation. Bull. Am. Meteor. Soc., 32, 48-51.

BIOGRAPHICAL NOTE

The author was born December 7, 1937, at Mankato, Minnesota. Raised on a farm near Janesville, Minnesota, he graduated from Janesville High School in 1956. At Mankato State College he majored in mathematics and physics and received a Bachelor of Science degree in 1960. The following year was spent as a high school teacher in St. Peter, Minnesota where he taught physics and twelfth-grade mathematics at St. Peter High School.

Since fall 1971 he has been a graduate student in the department of Meteorology at the Massachusetts Institute of Technology. He held a Ford Foundation Fellowship from 1961 to 1964. The summer of 1962 was spent at the Air Force Cambridge Research Laboratories as an atmospheric physicist in the Upper Atmosphere Branch of the Meteorology Laboratory of the Geophysics Research Directorate. Since September 1964, he has been a Research Assistant working on the optical radar project of the Geophysics group of the Research Laboratory of Electronics at the Massachusetts Institute of Technology.

Publications include:

- G. Fiocco and G. Grams, 1964: Observation of the Aerosol Layer at 20 km by Optical Radar. J. Atmos. Sci., 21, 323-324.
- G. Grams, G. Fiocco, K. Urbanek, and R. Breeding, 1965: Optical Radar Observations of the Upper Atmosphere in Alaska and Sweden (abstract). Trans. Am. Geophys. Union, 46, 62.

- G. Fiocco and G. Grams; 1966: Observations of the Upper Atmosphere by Optical Radar in Alaska during the Summer 1964. Tellus, 18, 34-38.
- G. Grams and G. Fiocco, 1966: Studies of Stratospheric Aerosols and Correlations with Ozone (abstract). Trans. Am. Geophys. Union, 47, 127.